Novel protein-lipid composite nanoparticles as delivery systems of vitamin B_{12}

by

Guangyu Liu

A thesis submitted in partial fulfillment of the requirements for the degree of

Doctor of Philosophy

in
Food Science and Technology

Department of Agricultural, Food and Nutritional Science
University of Alberta

Abstract

Many protein and lipid based nanoparticles have been developed to encapsulate hydrophilic nature health products (NHPs) with the purpose to improve their oral bioavailability. However, the efficacy of these nanoparticles was usually compromised due to low encapsulation efficiency, low physical stability or poor release behaviour in the gastrointestinal tract. This work aims to combine protein and lipid to develop novel protein-lipid composite nanoparticles for hydrophilic NHP delivery. Specifically, vitamin B_{12} was focused which is essential for human life. The absorption of vitamin B_{12} is an intrinsic factor mediated and cubilin receptor dependent process. Gastrointestinal problems can impair the absorption pathway and lead to vitamin B_{12} deficiency. Thus, in this work the developed protein-lipid composite nanoparticles were applied as vehicles to load vitamin B_{12} and improve its absorption through alternative pathways *in vivo*.

The first part of the thesis introduces the design, preparation and characterization of the protein-lipid composite nanoparticles. The nanoparticles were prepared using a modified double emulsion solvent evaporation method and the transmission electron microscope (TEM) demonstrated their unique three-layer structure (phospholipid layer, α-tocopherol layer and barley protein shell) and inner water compartments for loading of vitamin B_{12}. In addition, the nanoparticles had homogeneous size distribution (size 243 nm, polydispersity index 0.17) and high encapsulation efficiency of vitamin B_{12} (69%). Such nanoparticles could also resist the gastric digestion, with only 10.4% of vitamin B_{12} released into the simulated gastric fluid after 2 h incubation. This is because the mechanical pressure treatment enhanced the formation of intermolecular β-sheets in barley protein, leading to solid interfacial films that could resist the harsh stomach environment. Also, protein hydrophobic groups were “locked” in the compact interfacial network. This greatly

limited the gastric degradation of nanoparticles by pepsin which preferentially attacked the hydrophobic sites of proteins. Whereas in the simulated intestinal fluid, quicker degradation of nanoparticles was observed, with 65.8% vitamin B_{12} found in the release medium after 6 h.

In the second study, the performance of these nanoparticles was improved by modifying the protein shell through succinylation, which significantly increased the particle surface charge, hydrodynamic diameter and decreased the surface hydrophobicity. The modified nanoparticles still maintained the favorable three-layer structure and high vitamin B_{12} encapsulation efficiency. The increased surface charge and spatial extension of succinate chain on nanoparticle surface improved the nanoparticle stability in both physiological buffer and water. The crosslinking by succinate minimized the leakage of vitamin B_{12} to 4.5% during one month of storage. Moreover, succinylation slowed down the pancreatic digestion of protein shell because the succinyl-lysyl-peptide bond was resistant to the tryptic hydrolysis. As a result, the modified nanoparticles demonstrated more sustainable release behavior in the simulated intestinal fluid, with around 62.1% vitamin B_{12} released in 10 h.

In the last study, the biological responses of original and modified nanoparticles were evaluated. Both nanoparticles could enter the Caco-2 cells through non-specific endocytosis (clathrin mediated endocytosis and macropinocytosis) and increased the uptake efficiency of vitamin B_{12} over 20 folds. The original and modified nanoparticles also showed good mucoadhesive capacities (over 29.1%) which potentially prolonged the residence time of vitamin B_{12} in the intestine. A 14-day *in vivo* toxicity study showed no evidence of toxicity in rats. *In vivo* efficacy study showed that the developed vitamin B_{12} loaded nanoparticles could increase the serum vitamin B_{12} level and decrease the methylmalonic acid level more efficiently than the free form in a vitamin B_{12} deficiency rat model.

Overall, this research represented the development of novel protein-lipid composite nanoparticles with elaborated design. Nanoparticles had many desired physicochemical properties (e.g. high encapsulation efficiency, good stability, controlled release behavior) and good biological responses (enhanced mucoadhesive property, increased vitamin B_{12} absorption), which overcame the limitations of sole protein and lipid based nanoparticles. Therefore, such nanoparticles have significant potential to improve the absorption of vitamin B_{12} in humans, especially those suffering from vitamin B_{12} malabsorption. This system could also be applied as a platform to deliver many other hydrophilic NHPs.

Preface

This thesis contains original work done by Guangyu Liu under the supervision of Drs. Lingyun Chen, Afsaneh Lavasanifar and Le Luo Guan. It has been written according to the thesis formatting requirements of the Faculty of Graduate Studies and Research at the University of Alberta.

Chapter 2 and part of Chapter 4 of this thesis have been published as Guangyu Liu, Weijuan Huang, Oksana Babii, Xiaoyu Gong, Zhigang Tian, Jingqi Yang, Yixiang Wang, René L Jacobs, Donna Vine, Afsaneh Lavasanifar, and Lingyun Chen, "Novel protein-lipid composite nanoparticles with an inner aqueous compartment as delivery systems of hydrophilic nutraceutical compounds" in Nanoscale, 2018, 10, 10629-10640. Guangyu Liu was responsible for literature search, experiment design, data collection, result analysis, and manuscript writing. Weijuan Huang, Oksana Babii, Xiaoyu Gong, Zhigang Tian assisted in the *in vivo* animal studies. Drs Jingqi Yang, Yixiang Wang assisted in protein extraction, protein characterization, and nanoparticle morphology studies. Drs Afsaneh Lavasanifar, René L Jacobs, and Donna Vine gave critical reviews on the manuscript. Dr. Lingyun Chen was the corresponding author and contributed to the experimental design, data discussion, manuscript edit and submission.

Another manuscript based on the data in Chapter 3 and part of Chapter 4 was submitted as Guangyu Liu, Jingqi Yang, Yixiang Wang, Xinghai Liu, Le Luo Guan, and Lingyun Chen, "Protein-lipid composite nanoparticles for the oral delivery of vitamin B_{12}: impact of protein succinylation on nanoparticle physicochemical and biological properties". Guangyu Liu was responsible for literature search, experiment design, data collection, result analysis, and manuscript writing. Drs Jingqi Yang, Yixiang Wang, Xinghai Liu assisted in protein extraction, protein characterization, and nanoparticle morphology studies. Dr Le Luo Guan gave a critical review on

the manuscript. Dr. Lingyun Chen was the corresponding author and contributed to experimental design, data discussion, manuscript edit and submission.

Animal studies conducted in Chapter 4 were executed under the guidelines of the Canadian Council on Animal Care (CCAC) and Animal Care and Use Committee (ACUC) at the University of Alberta. All studies were approved by ACUC (Protocol number: AUP1713).

Acknowledgement

Foremost, I would like to express my sincere gratitude to my supervisor, Dr. Lingyun Chen, for giving me the opportunity to start my PhD study in 2012. And in the past six years, she gave me invaluable guidance in the research, academic writing, teaching and presentation skills. Her supervision enabled me to gradually develop critical thinking as an independent researcher during my PhD study. I would also like to thank my supervisory committee members, Dr. Afsaneh Lavasanifar and Dr. Le Luo Guan, for their insightful suggestions for my research projects during committee meetings, as well as constructive comments and critical reviews on my research manuscripts. I would like to express thanks to Dr. Raimar Löbenberg from Department of Pharmacy and Pharmaceutical Sciences for being my arm's length examiner and Dr. Chibuike Udenigwe from Faculty of Health Science, University of Ottawa, for accepting to be my external examiner.

My sincere thanks also go to my labmates in 3-30 and 3-52, Agriculture/Forestry Center, University of Alberta. They are all friendly and helpful. I had a lot of wonderful time with them in the past years. I learned a lot of knowledge and useful experiment skills from them. I cannot finish my PhD program without their help. I would like to extend my thanks to Drs. Yixiang Wang and Jingqi Yang for their help in all respects of my research work.

University of Alberta is always an important source of good advice and collaboration. I appreciated the help from agricultural genomics and proteomics unit for cell culture work. I would also like to thank technical supports from departments of biological science, chemical and material engineering, pharmaceutical science, health science lab animal service, cross cancer institute, and nanoFAB.

Last but not the least, I would like to thank my family for their support and love. I appreciate the trust and patience from my parents and parents-in-law. I also deeply thank my wife, Wujun Zhao, for her unconditional support, timely encouragement and great companion. I am so lucky to have her in my life.

Table of Contents

List of Tables

List of Figures

List of Abbreviations

NHP	Nature health product
ATCC	American Type Culture Collection
DMEM	Dulbecco's modified eagle medium
FBS	Fetal bovine serum
NEAA	Non-essential amino acids
HBSS	Hank's balanced salt solution
DPBS	Dulbecco's phosphate-buffered saline
EDTA	Ethylenediaminetetraacetic acid
MTT	Thiazolyl blue tetrazolium bromide
CPZ	Chlorpromazine hydrochloride
CyD	Cytochalasin D
FLI	Filipin III
CME	Clathrin-mediated endocytosis
CvME	Caveolae-mediated endocytosis
GALT	Gut-associated lymphoid tissues
WGA	Wheat germ agglutinin
DAPI	4',6-diamidino-2-phenylindole
TEM	Transmission electron microscopy
SEM	Scanning electron microscopy
CLSM	Confocal laser scanning microscopy

RI	Refractive index
PdI	Polydispersity index
EE	Encapsulation efficiency
EC	Encapsulation capacity
ANOVA	Analysis of variance
ATR	Attenuated total reflectance
HPLC	High performance liquid chromatography
SGF	Simulated gastric fluid
SIF	Simulated intestinal fluid
BSA	Bovine serum albumin
EGCG	Epigallocatechin gallate
FTIR	Fourier transform infrared
ANS	1-anilinonaphthalene-8-sulfonic acid
VB12	Vitamin B_{12}
NP	Nanoparticle
O-NP	Original nanoparticles
M-NP	Modified nanoparticles
ALT	Alanine transaminase
AST	Aspartate transaminase
BUN	Blood urea nitrogen
Crea	Creatinine

Chapter 1-Introduction

1.1 Brief introduction of NHP delivery

Natural health products (NHPs), by the definition from health Canada [1], are "a class of health products which include: vitamin and mineral supplements, herbal preparations, traditional and homeopathic medicines, probiotics and enzymes". NHPs usually demonstrate physiological benefits and can be used to "restore or maintain good health". However, many of them suffer from low bioavailability due to low solubility, low stability, and/or poor intestinal permeability.

Bioavailability is a pharmacokinetic parameter that measures the percentage of orally administered dose that enter the systemic circulation unchanged [2]. Factors that limit NHP's oral availability are similar to those in pharmaceutical science and can be categorized into three major classes: solubility, permeability and stability (including degradation and metabolism) [3]. The first factor, "solubility", is related to the physical form of NHPs in the intestine. Hydrophilic NHPs could directly dissolve in the intestinal fluid for absorption. But hydrophobic NHPs, like Coenzyme Q10 [4], α-lipoic acid [5], and resveratrol [6], need to solubilize in the micelles formed by bile salts and phospholipids before they can be absorbed. Poor dissolution of hydrophobic NHPs in the intestine could be a bottleneck in absorption. The second factor, "permeability", is related to NHP's capacity in passing through the intestinal epithelium. Intestinal epithelium is the major barrier that controls the absorption of NHPs. NHPs can travel across the epithelial layer *via* transcellular and paracellular pathways [7]. The transcellular pathway allows NHPs to enter epithelial cells through active cellular uptake or passive diffusion and then infuse into the circulation. While in the paracellular pathway, NHPs are directly transported across the space between epithelial cells. Low transepithelial capacity can lead to low bioavailability of NHPs. The third factor, "stability", is related to the degradation and metabolism of NHPs in human body. Many NHPs, like peptides,

enzymes, probiotics, unsaturated fatty acids, could be degraded, denatured or oxidized by low pH and digestive enzymes in the gastrointestinal tract and show reduced bioactivity [8, 9]. Enzymes in the enterocytes and liver can also degrade some NHPs or convert them to metabolites with low bioactivity, which is known as the first-pass effect [10]. For example, decursin, a nature plant extract with cancer prevention property [11], was extensively converted to a much less active metabolite, decursinol [12] after oral administration because of the first-pass effect. Therefore, an oral delivery system is required to help NHPs overcome these limitations and absorption barriers.

1.2 Introduction to vitamin B_{12} (VB12)

1.2.1 Chemical structure of VB12

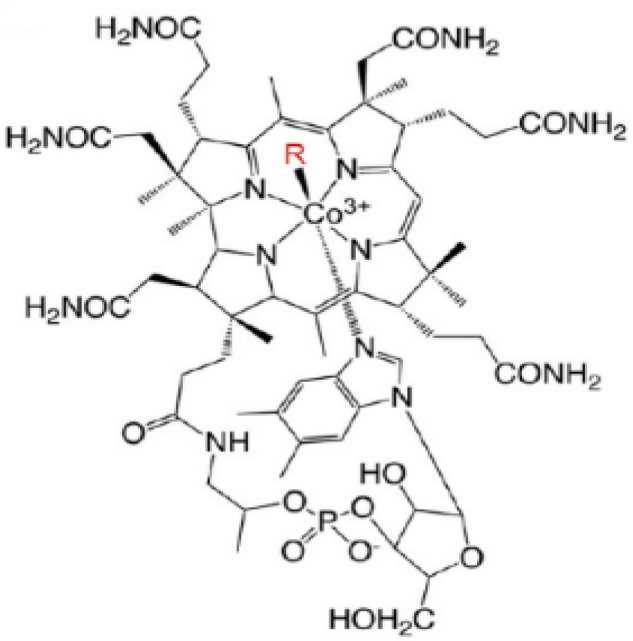

Figure 1.1 Chemical structure of VB12, from Ref [13]. R could be adenosyl group, methyl group, hydroxyl group or cyanide group. The molecular weight of cyanocobalamin is 1355 g/mol.

VB12 is a water-soluble vitamin with low intestinal permeability. Generally, VB12 can be considered in three parts (Fig. 1.1), the upper ligand "R"; the central corrin ring, and the lower

ligand, 5,6-dimethylbenzimidazole. VB12 by definition should be restricted to cyanocobalamin, while in a broad sense, VB12 can also refer to all forms of cobalamin with different upper ligands, like adenosylcobalamin, methylcobalamin, and hydroxocobalamin. Commercial VB12 is exclusively produced by bacteria and archaea. Adenosylcobalamin, methylcobalamin and hydroxocobalamin are main products from these microorganisms, but they are unstable upon exposure to light[14]. To stabilize these cobalamin forms, industry uses cyanide to form a stable molecule of cyanocobalamin. Therefore, cyanocobalamin is widely applied in food and pharmaceutical industry [15].

1.2.2 Source of VB12

Daily recommended VB12 intake is 2.4 μg for adult, and more VB12 is required for pregnant and breastfeeding women [16]. Human cannot get sufficient VB12 supplement from plant based foods. Very small amount of VB12 (<0.1 μg/100 g) can be found in certain vegetables like broccoli, asparagus, Japanese butterbur [17]. Meats, like cooked beef liver (83 μg/100 g), lean meat (3 μg/100 g), and turkey (33 μg/100 g), have high VB12 content. Milk (0.3-0.4 μg/100g), egg (0.9-1.4 μg/100 g), shellfish (10 μg/100 g), fish (3.0 to 8.9 μg/100 g) also contribute to human daily VB12 intake [17]. Although VB12 is produced in human large intestine by gut microbes, it cannot be considered as a resource of VB12 for human [18]. This is mainly because VB12 produced by gut microbes is too low to meet the daily VB12 requirement [19]. Moreover, VB12 from gut microbes is mainly produced in the colon, where microbial numbers are the highest. It cannot reach the VB12 receptors in the distal ileum, which locate in the upstream of colon [19].

1.2.3 VB12 absorption, circulation and excretion in human body

1.2.3.1 Physiology of VB12 absorption

The absorption of VB12 is a multistep process that involves stomach, pancreas and small intestine [13, 20, 21]. After ingestion, dietary VB12 is released from food protein by gastric digestion and binds with haptocorrin (Hc) in stomach. Hc is a glycoprotein that can bind with all VB12 analogs and primarily presents in the saliva and gastric fluid. The Hc-VB12 complex is degraded by pancreatic enzymes in the duodenum and the released VB12 will further bind with intrinsic factor (IF). IF is also a glycoprotein, mainly secreted by the gastric parietal cells in the human gastric mucosa in the fundus and body of the stomach. IF has a weaker binding capacity with VB12 in the acidic environment (stomach) but stronger in the neutral pH (intestine). Meanwhile, the IF is not sensitive to pancreatic enzymes, especially when it is bound with VB12. Afterwards IF-VB12 complex goes through the small intestine to the distal ileum, where the complex is specifically recognized by a cubilin receptor (CUBN) and transported into the intestinal epithelial cell. Upon internalization, IF-VB12 dissociates from CUBN in the early endosome and then reaches the lysosome where the IF is degraded. After lysosomal digestion, free VB12 will be released into cytoplasm, bind with intracellular transcobalamin (TC) and enter the circulation [13, 20]. The absorption of VB12 in infant is a little different. Infant's gastrointestinal tract is not mature therefore the IF secretion is lower than adult. However, IF receptors are expressed along the whole small intestine in infant, not limited in the distal ileum. Hc receptors are also found in infant intestine, suggesting Hc-mediated VB12 absorption may play an critical role in the early stage of human life [20, 22].

1.2.3.2 VB12 circulation and excretion

After going into the blood circulation, VB12 binds with two different proteins [13, 20, 21]. Plasma Hc is the protein that the majority of VB12 (70-80%) binds with. This protein has a long half-life (9-10 days) therefore can maintain the normal circulating level of VB12. The other protein is

plasma TC. It binds with around 10-20% of total VB12 in plasma. Though its half-life time is short (60-90 min), it plays an essential role in VB12 cellular uptake because the TC receptors are expressed on all cells and the transportation of VB12 into cells is dependent on these receptors.

VB12 is excreted through bile duct and kidney at the rate of around 2-5 μg/day, which is corresponding to 0.1–0.2% of total VB12 storage in the body [23]. The biliary excretion of VB12 (0.5-5 μg/day) is reabsorbed in the distal ileum through intrinsic factor mediated active transport. The enterohepatic circulation of VB12 is very effective so that around 65-75% of biliary excretion of VB12 can be re-utilized by human body. VB12 lost from kidney is minimal, around 0.25 μg/day, and this amount of VB12 is thought to be derived from the tubular epithelial cell and lymph.

1.2.4 VB12 Malabsorption and current treatment

VB12 malabsorption can be caused either by gastric or intestinal problems [21]. For example, gastritis or gastrectomy can result in reduced production of stomach acid to digest food protein to have VB12 released, or/and generating less IF that is necessary for VB12 uptake in the small intestine. Since the distal ileum is the site for physiological IF-mediated VB12 absorption, any disease that affects the health of distal ileum will reduce the absorption of VB12. Ileitis, ileal resection or radiation therapy can damage the ileal epithelium which leads to the loss of IF receptors. Under this condition, the absorption of orally administrated VB12 becomes very low. Only around 1% of VB12 can pass the intestinal epithelium and enter the circulation, which finally leads to VB12 deficiency [24].

Nowadays, VB12 deficiency has been a world-wide problem [24, 25]. Notably, high prevalence of VB12 deficiency was found in the aging population [26, 27] and over half of them were associated with food VB12 malabsorption (intrinsic factor deficiency or hypochlorhydria) [26-29].

Severe VB12 deficiency can further result in pernicious anemia and irreversible neurological disorders, which usually requires VB12 intramuscular injection treatment [30]. Oral administration and intranasal spray of VB12 in high dose have been used as an alternative treatment, but the bioavailability of VB12 from both routes is low (<5%) because VB12 has large molecule weight (>1000 Da) which limits its passive diffusion through intestinal/nasal epithelial membrane [31-33]. Nanoparticles can enhance the absorption of encapsulated compounds through non-specific endocytosis in the small intestine [34], thus developing oral nanoencapsulation of VB12 could be a potential strategy to improve VB12 absorption. However, research regarding VB12 nanoencapsulation is still limited (see section 1.4.3).

1.3 Nanoparticles improve the oral bioavailability of encapsulated NHPs

Nanoparticles have great potential to increase the bioavailability of NHPs [35]. Because of their small size and large surface area, nanoparticles can adhere to the surface of digestive tract which prolongs the residence time of encapsulated NHPs [36, 37]. The small size also favors the direct uptake of nanoparticles by endocytosis, which improves the absorption of core ingredients through intestine [34, 38]. Moreover, through specific design and modulation, nanoparticles can release encapsulated compounds to specific location in a desired rate. This property can protect core ingredients from undesired degradation and premature release before reaching the physiological site for absorption [39]. Details of these advantages are reviewed below.

1.3.1 Controlled release behavior

NHPs need to reach a desired range of concentration in the human body to produce health benefits. However, some NHPs have quick eliminating rate in the circulation so frequent dosing is usually required. Nanoparticles enable the delivery of NHPs to human body in a sustainable manor which

potentially avoids repeated administration of NHPs [40]. Nanoparticles have two major release mechanisms: 1) NHP diffusion from nanoparticles and 2) nanoparticle degradation/erosion [41]. In a diffusion-controlled system, NHPs are released from nanoparticles primarily by passive diffusion. While in an erosion-controlled system, NHP release is mainly triggered and accelerated by nanoparticle degradation and erosion. Size is an important factor impacting the release kinetics of the nanoparticles. Generally, nanoparticles with smaller size have a larger surface area to volume ratio, which increased the contact area between particles and the release medium, leading to quicker diffusion of encapsulated compounds and faster degradation of nanoparticles [42, 43]. However, research to understand how particle size may impact the release behavior of food nanoencapsulation in the gastrointestinal environment is still limited. Further investigation in this area is required to optimize the NHP release kinetics.

Material selection and structure design can also modulate the release behavior of nanoparticles by controlling NHP diffusion and/or matrix degradation. For example, Li et al. [44] loaded epigallocatechin gallate (EGCG), a green tea extract with anti-inflammatory and anti-cancer properties, into bovine serum albumin (BSA) nanoparticles. The release of EGCG from BSA nanoparticles reached 53% in the simulated gastric fluid with pepsin after 0.5 h and 69% in the simulated intestinal fluid with pancreatin after 2 h. The diffusion of EGCG from the nanoparticles into release media was a factor determining the release rate. The loss of nanoparticle structural integrity under protease digestion further accelerated the EGCG release. In order to improve the release behavior, poly-lysine was used to coat the surface of nanoparticles. As a barrier, the poly-lysine coating reduced the permeability of water which decreased the diffusion rate of EGCG. It also made the BSA nanoparticles less digestible in the gastrointestinal tract. As a result, the release of EGCG reduced to 33% in the simulated gastric environment after 0.5 h and 45% in the simulated

intestinal environment after 2 h. More sustainable release behavior allows a single-oral-dose administration of EGCG to exert health benefits for a longer period of time.

For protein nanoparticles, the protein conformation can affect the response of nanoparticles to environment factors, like pH and digestive enzymes, resulting in different release behavior in different sections of the digestive tract. This property allows protein nanoparticles to release encapsulated NHPs to the active site of absorption, like intestine, and protect them during transportation, which is especially useful in the delivery of NHPs that are unstable and degradable in the stomach. For example, after high-pressure homogenization and spray drying treatment, both barley protein nanoparticles [45] and casein nanoparticle [46] could reduce the exposure of hydrophobic amino acids. This change made them resistant to the digestion of pepsin which preferably attacks hydrophobic domains of the protein [47]. Meanwhile, their digestibility in intestine was not affected because hydrophilic lysine and/or arginine residues were still readily available on the nanoparticle surface, and trypsin from pancreatin can attack these residues to hydrolyze protein nanoparticles [48]. As a result, both nanoparticles showed minimum release of encapsulated NHPs in the simulated gastric environment and enhanced release in the simulated intestinal fluid.

1.3.2 Mucoadhesive property

Mucoadhesive property is another critical factor for nanoparticles to maximize their benefit effect. Mucoadhesive property allows nanoparticles to resist the self-cleaning mechanisms of mucosal tissues and slow down their transit in the intestine [49], which in turn increases the intestinal residence time of nanoparticles and encapsulated NHPs. Size can substantially influence the mucoadhesive behavior of nanoparticles. It was found that nanoparticles with hydrodynamic diameter no larger than 500 nm could efficiently diffuse into the mucus layer. While beyond this

range, the diffusion of nanoparticles was significantly slowed down due to the steric hindrance, resulting in reduced contact between nanoparticles and the mucosal tissue [50]. Surface properties can also affect the mucoadhesive properties of nanoparticles. Generally, nanoparticles that can generate non-specific interaction(s) (e.g. electric interaction hydrophobic interaction, hydrogen bond) or specific interaction(s) (e.g. ligand binding) with mucosa can enhance nanoparticles' mucoadhesive capacity [51]. Positive charge improves nanoparticle's mucoadhesive capacity. Teng et al. developed polyethyleneimine conjugated β-lactoglobulin nanoparticles for NHP delivery. Different from regular β-lactoglobulin nanoparticles which carried a negative charge (-42.6 mV), the new synthesized nanoparticles had a strong positive charge (+39.9 mV), which facilitated the binding of nanoparticles with negatively charged mucin, resulting in a 40-fold increase in the mucoadhesive capacity. Besides charge, the surface hydrophobicity can also modulate nanoparticle's mucoadhesive property. Arangoa et al. investigated the mucoadhesive property of gliadin based nanoparticles [36]. As gliadin has high amount of nonpolar amino acids(~40%) [52], nanoparticles based on gliadin demonstrated high hydrophobicity and low negative charge. High surface hydrophobicity allowed nanoparticles to bind to intestinal mucosa through hydrophobic interaction, and the low negative charge reduced the repulsive force between nanoparticles and mucosa. In the mucoadhesive study, over 40% of gliadin based nanoparticles adhered to the intestinal mucosa after 0.5 h of incubation. Whereas when gliadin nanoparticles were coated with hydrophilic protein such as bovine serum albumin, the mucoadhesive capacity was reduced by around 60%. This could be explained by the decreased hydrophobicity and increased surface charge of nanoparticles at the physiological pH. Lectins are carbohydrate-binding proteins that can provide specific binding to sugar residues on the surface of epithelial cells [53]. Such specific interaction could also increase the mucoadhesive capacity of

nanoparticles. Arbos et al. found the mean residence time of nanoparticles in the intestine was increased by 35 min after lectin coating compared to those without surface coating [37].

1.3.3 Epithelial membrane translocation

Nanoparticles can enhance the absorption of encapsulated compounds through active endocytic pathways (Fig. 1.2). There are three major endocytic pathways [54]: clathrin-mediated endocytosis (CME), caveolae-mediated endocytosis (CvME), and macropinocytosis. CME is the most extensively investigated endocytosis pathway, which mediates a wide range of cargo transport in all mammalian cells. In this pathway, clathrins are assembled on the cytosolic side of cell membrane and form a pit with extracellular compounds (like nanoparticle) inside. Then the pit becomes invaginated and detached from the membrane. The endocytosed vesicles are trafficked into endosomes and finally merge into lysosomes [55]. Generally, clathrin-mediated endocytosis can internalize nanoparticles with size no larger than 200 nm [56]. However, in certain cell line, like the Caco-2 cell line, it was able to transport nanoparticles over 400 nm in diameter [57]. CvME has similar cargo formation process like CME and also presents in many types of cells. The cargo in CvME is formed by a different structural protein, caveolin. CvME does not contribute to bulk transport across epithelium because of its small cargo size (50-60 nm in diameter). Moreover, CvME has alternative endocytic pathways to the Golgi and endoplasmic reticulum, suggesting the compounds in CvME cargo have a chance to avoid lysosomal degradation [58]. Macropinocytosis mediates the uptake of a large amount of extracellular fluid. Macropinocytosis can transport particles up to several micrometers [59]. In macropinocytosis, actins rearrange at the cell membrane and form ruffles. Ruffles fold back and fuse with cell membrane, leading to the formation of macropinosomes with extracellular fluid entrapped. Similar to CME, the content in macropinosomes will finally merge into lysosome and be digested [60].

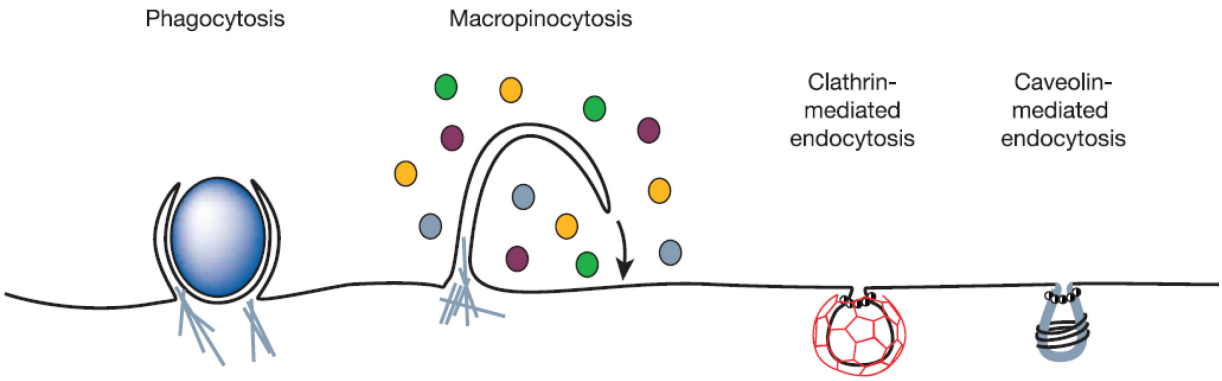

Figure 1.2 Different endocytic pathways that can potentially be used for nanoparticle uptake. From ref. [59]

Nanoparticle's physiochemical properties have significant impact on their cellular uptake efficiency. The effect of size has been extensively investigated. Generally, nanoparticles with diameter at around 50-200 nm are optimal for cellular uptake [61-63]. Surface properties are also critical in modulating the internalization rate of nanoparticles. The properties that enhance the nanoparticle-cell attractive interaction can increase the uptake efficiency. For example, positively charged nanoparticles generally demonstrate higher uptake efficiency than negatively charged ones because of the electrostatic attraction between cationic nanoparticle surface and anionic cell membrane [64]. However, nanoparticles with positive charge could cause perturbation of cell membrane and inhibit the proliferation of cells [65], which may damage the intestine. Nanoparticles conjugated with targeting ligands on the surface can also enhance the uptake efficiency because ligands provide extra binding force between nanoparticles and cell membrane [66]. While nanoparticles with highly negative charged surface normally show lower internalization rate because of the strong repulsion forces between nanoparticles and cells [67]. Decreased negative charge could reduce such repulsion force therefore favor the endocytosis of nanoparticles [68]. The shape of nanoparticle is another factor that affects the cellular uptake of

nanoparticles. However, because most nanoparticles designed for oral delivery are spherical, less attention has been paid to nanoparticle's geometry design and its related interaction with cells. Banerjee et al. reported that rod and disc shaped nanoparticles showed significantly higher uptake efficiency than spherical ones in Caco-2 cells [66]. And no difference was observed between rod and disc shaped nanoparticles. Similarly, Huang et al. found that rod shaped nanoparticles had higher probability to enter cells than spherical shaped ones in A375 cells [69]. But Chithrani et al. suggested that spherical nanoparticles could internalize into Hela cells more efficiently than rod shaped ones [70]. So far, no conclusion can be made regarding the effect of particle shape on their cellular uptake efficiency. This question requires more extensive investigation.

Phagocytosis is a different kind of endocytosis that is primarily conducted by immune cells. During phagocytosis process, immune cells can change their shape and form cup-like extensions to engulf extracellular compounds. This process allows immune cells to uptake large particulates [71]. In the intestine, immune cells form lymphoid follicles which are called gut-associated lymphoid tissue (GALT). GALT is one of the largest lymphoid organs in the human body and primarily locates in the distal ileum [72]. Although it only accounts for 1% of intestinal surface, GALT is considered as an important route for nanoparticle based NHP delivery because compounds delivered to GALT can bypass the liver and be transported to the circulation system directly through lymph node or spleen, which minimizes the first-pass effect on unstable NHPs. Generally, compound loaded in nanoparticles has higher chance to enter GALT than its free form, because cells with phagocytic activity can internalize antigens in particulate form more efficiently than those in soluble form [73]. Aramaki et al. tested the accumulation of Rhodamine with/without nano encapsulation in GALT enriched intestine tissue [74]. They found that after liposome encapsulation, the concentration of Rhodamine in GALT increased for around three folds.

Nanoparticles can also be uptaken through paracellular transport. However, because of very small pore size (radius < 7.5 Å) at the tight junctions [75], most of nanoparticles cannot pass through the space between epithelial cells. Special materials that can temporarily open the tight junctions are required. For example, EDTA can bind with Ca^{2+} involved in tight junctions to open the space between intestine epithelial cells [76]. Thiolated polymers can also expand the tight junctions by inhibiting the function of protein tyrosine phosphatase [77]. As most of the nanoparticles do not process this specific mechanism, it is not discussed here in detail.

1.4 Nano-delivery systems (nanoparticles and liposomes) for hydrophilic NHPs

Recently, many nano-delivery systems have been created to maximize the therapeutic effects and minimize the side effects of drug in the biomedical and pharmaceutical area [51, 78, 79]. However, among the materials that can be used to fabricate nano-delivery systems, only a few can be used for regular food consumption [80]. Nature polymers and lipids are materials that are suitable for food application. In this section, protein and lipid based nano-delivery systems designed for hydrophilic NHP delivery will be reviewed (Fig. 1.3). Discussion primarily focuses on the advantages, challenges as well as preparation methods of these nano-delivery systems.

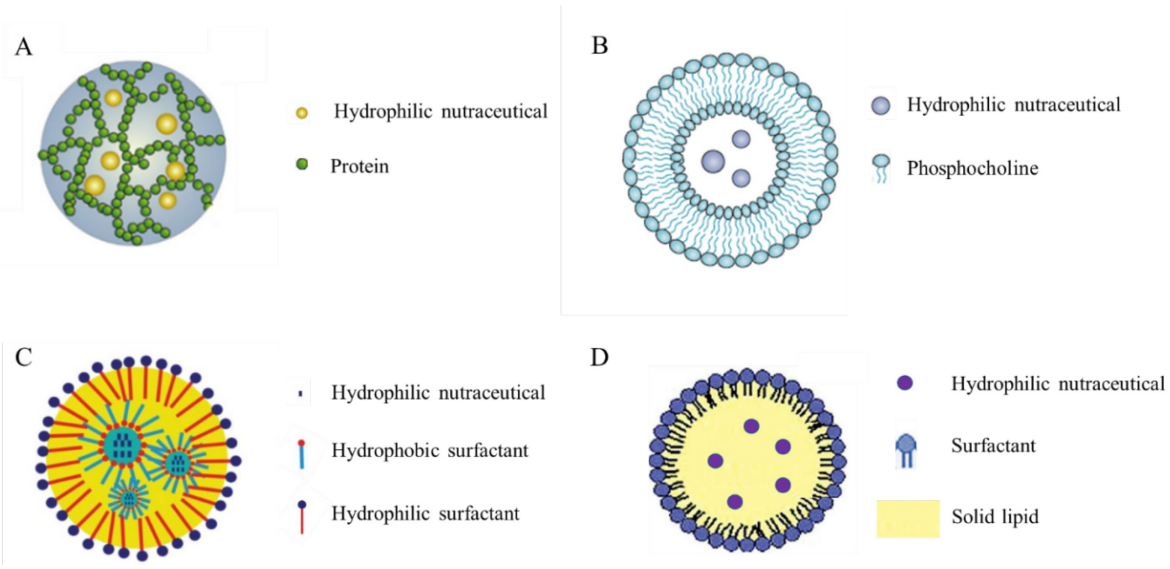

Figure 1.3 Scheme of nanoparticles reviewed in section 2.2. (A) protein nanoparticles; (B) liposomes; (C) multiple emulsion; (D) solid lipid nanoparticle. Reproduced from Ref [81-84].

1.4.1 Protein based nanoparticles

Food proteins are nature polymers and digestible in human gut. They have excellent functional properties such as emulsifying and gelling capacity which allow them to be converted into delivery systems of both hydrophobic and hydrophilic NHPs. Proteins emulsions have been widely used for encapsulation of hydrophobic NHPs, such as β-carotene [45, 85], ω-3 polyunsaturated fatty acids [86], and vitamin D_3 [87]. At the o/w interface, proteins normally undergo unfolding and re-orientation to have hydrophobic sections directed towards the oil phase and hydrophilic sections towards the aqueous phase [88]. This allows proteins to form a viscoelastic network at the oil/water interface which provides a structural barrier to droplets rupture and aggregation/coalescence due to steric and electrostatic effects [89]. Meanwhile, protein gelation allows the formation of three-dimensional networks for the encapsulation and controlled release of both hydrophobic and hydrophilic NHPs [35, 90].

Many methods have been developed to prepare protein nanoparticles for the delivery of hydrophilic NHP compounds. Antisolvent precipitation (desolvation) is one of the most commonly used methods which involves of protein precipitation from original solvent using a desolvating agent. The solubility of protein in solvents is determined by many factors, including solvent polarity, environment pH and ionic strength. Adjusting these factors can control the aggregation and precipitation of protein, leading to the formation of protein nanoparticles with various size (from ~100 to ~900 nm) [91]. Hydrophilic NHPs can be directly mixed with the nanoparticle suspension and then loaded into nanoparticle through electrostatic interaction or hydrophobic interaction [44, 92-95]. For example, bovine serum albumin (BSA) nanoparticles were prepared by adding excessive amount of ethanol into BSA water solution. The precipitated nanoparticles were crosslinked by glutaraldehyde and incubated with epigallocatechin gallate for 0.5 h. The epigallocatechin gallate loaded nanoparticles had a size of 186 nm and encapsulation efficiency of 32.3% [44].

Protein nanoparticles can also be produced by cold gelation method [96-98]. This method involves a thermal treatment to denature the proteins and have their nonpolar amino acids exposed in the aqueous environment, leading to the formation of protein soluble aggregate through hydrophobic interaction. The protein aggregates are then associated by adding calcium to form a three-dimensional network. The NHPs can be added in the soluble protein aggregates suspension at room temperature before gelation. To make the nanoparticles, the gel size should be controlled in nano-range by using a low protein concentration. For example, soy protein nanoparticles were used to encapsulate vitamin B_{12} using a cold gelation method [63]. Protein solution was firstly heated at 85 ^{o}C for 30 min to denature protein molecules. After cooling down to room temperature, VB12 was introduced into the protein solution and left to react overnight, followed by the addition of

$CaCl_2$ to induce the formation of nanoparticles. The obtained nanoparticles had a size of 180 nm and encapsulation efficiency of 13.5%.

Emulsion-templating method (W/O emulsion) is another way to prepare hydrophilic NHP loaded protein nanoparticles [99-101]. A protein aqueous solution is dispersed in oil phase to form a W/O emulsion. The size of W/O emulsion can be further decreased to nanoscale by high speed homogenization or ultrasonication. Then, the proteins in the water droplets will be rigidized by crosslinking reagent to form nanoparticles. Hydrophilic NHPs can be added in protein solution before nanoparticle formation, or loaded into nanoparticles by adsorption after nanoparticle formation. Because hydrophilic NHPs have low solubility in oil, they stay in the aqueous droplets exclusively and can be efficiently entrapped in the nanoparticles. Finally, nanoparticles are collected by centrifugation and the surface oil can be removed by organic solvent. For example, Gupta investigated the potential application of gelatin nanoparticles in the delivery of hydrophilic compounds, using fluorescein isothiocyanate-dextran (FITC-Dex) as a model [99]. Briefly, gelatin aqueous solution (800 μL) was dispersed in hexane (50 mL) and stabilized by sodium bis (2-ethylhexyl sulphosuccinate) (0.03 M). The proteins in the W/O emulsion were crosslinked with glutaraldehyde to form nanoparticles. FITC-Dex in water solution (20 μL) was added into above solution and incubated with nanoparticles overnight to form FITC-Dex loaded nanoparticles. Minimal loss of FITC-Dex (encapsulation efficiency: ~90%) was observed during the preparation process and the obtained nanoparticles had their size around 37 nm.

Electrospraying [102, 103] and nano spray drying [104, 105] are relatively new methods to generate protein nanoparticles which had been prepared only for drug delivery currently. In the electrospraying method, the hydrophilic NHP and proteins are mixed in the same solvent and placed in an electrospinning equipment. The solution is dispensed through a nozzle, passed through

a high-voltage electric field, and finally attached onto a target surface under the effect of electric field. During this process, solvent is evaporated in the air and proteins/hydrophilic compounds aggregate with each other to form nanoparticles. In the electrospraying method, protein concentration should be precisely calculated, as inappropriate concentration can result in the formation of protein nanofibers, rather than nanoparticles [106]. For example, Gulfam et al. prepared cyclophosphamide loaded protein nanoparticles using the electrospraying technology [103] . Gelatin was dissolved in 90% acetic acid and gliadin was dissolved in 70% ethanol. Cyclophosphamide was added into the mixture of these two solutions (1:1) and sprayed into a high voltage electric field (12-14 kV). The sprayed droplets were dried in the air and the formed nanoparticles were collected under the effect of electric field. The obtained nanoparticles (size 218 to 450 nm) had relatively high loading capacity (52.8% to 72.0%).

Nano spray drying needs to be performed on a spray drying machine [104, 105]. Proteins and hydrophilic compounds are dispersed in adequate solvent and sprayed into fine mist (micro/nano scaled droplets). The droplets are dried by a heated airflow and proteins/hydrophilic compounds in the droplets will bind with each other to form nanosized aggregations (nanoparticles). For example, Alfuzosin hydrochloride loaded casein nanoparticles were prepared using a Büchi B-290 spray drier [105]. Alfuzosin hydrochloride was simply mixed with casein in water, spray dried to form nanoparticles, and crosslinked with genipin in ethanol solution. Nanoparticles had small size (110 to 260 nm) and high encapsulation efficiency (>92%).

The most challenging issue for protein nanoparticles as oral NHP delivery systems is their instability in gastrointestinal environment. Fu et al. [107] investigated the digestibility of food proteins in the simulated gastrointestinal tract. They found that the majority of food proteins could be degraded in stomach within 5 min, except very few ones, like β-lactoglobulin, β-conglycinin

(β-subunit) and zein. Therefore, nanoparticles made by food proteins could be highly susceptible to peptic digestion, leading to burst leakage of NHPs in the stomach before reaching the small intestine where most of the NHPs are absorbed. The second challenge existing in protein nanoparticles is related to low encapsulation efficiency of hydrophilic NHPs. The loading capacity of protein nanoparticles is largely dependent on the interaction(s) between NHPs and protein molecules, such as one or combinations of electrostatic or hydrophobic interactions [108]. Unlike lipophilic NHPs which can bind with proteins through strong hydrophobic interaction, many hydrophilic NHPs are small and uncharged molecules which have only weak or no interaction with proteins. The weak interaction can lead to low encapsulation efficiency of hydrophilic NHPs in protein nanoparticles. It also causes rapid diffusion and release of encapsulated NHP in an aqueous environment due to the nanoparticle's large surface to volume ratio.

1.4.2 Lipid based nano-delivery systems

1.4.2.1 Liposomes

Liposomes are phospholipid vesicles consisting of one or more enclosed phospholipid bilayer(s) and an aqueous core. Liposomes enable the encapsulation of both hydrophobic and hydrophilic NHPs. Hydrophobic NHPs are incorporated in liposome's phospholipid bilayer(s), and hydrophilic NHPs are entrapped in the aqueous core. Many methods have been developed to prepare liposome, among which, thin film hydration, ethanol injection, and reverse phase evaporation are the most commonly used methods. In the thin film hydration method [109], phospholipids are first dissolved in the organic solvent (usually chloroform and/or methanol). The solvent is then removed by a rotary evaporator to obtain a dry film, which are formed by stacks of phospholipid bilayer sheets. Afterwards, the lipid film is hydrated with NHP loaded buffer solution under stirring. During this process, the lipid sheets self-close to form multilamellar vesicles with NHP loaded buffer solution

entrapped as aqueous core. The multilamellar vesicles can be extruded through a porous membrane or sonicated to form nanoliposomes. Zhou et al. prepared vitamin C loaded liposomes using the thin film hydration method [110]. Briefly, soybean phosphatidylcholine and cholesterol were dissolved in the ethanol and dried under vacuum to obtain a thin lipid film. This film was hydrated with vitamin C solution to form multilamellar liposomes, which were further processed with a microfluidizer to form nanoliposomes. The nanoliposomes had a small size (67 nm) and good encapsulation efficiency (48%).

In the ethanol injection method [111], phospholipids are dissolved in the ethanol and injected into an aqueous medium where the hydrophilic NHP is dispersed. Because phospholipids have lower solubility in aqueous medium than in ethanol, they associate with each other and spontaneously form bilayer liposomal structure to minimize the exposure of their hydrophobic groups in the aqueous medium. During this process, the NHP loaded aqueous medium is entrapped as aqueous core of liposomes. Finally, ethanol in the system can be removed by a rotary evaporator. Different from the thin film hydration method which requires further process to reduce the size, uniformed single bilayer nanoliposomes can be directly obtained using this method. For example, salidroside was loaded into liposomes using the ethanol injection method [112]. Salidroside was firstly dispersed in phosphate buffer under vigorous stirring and the solution was then heated to 60^{o}C. Egg phosphatidylcholine and cholesterol in ethanol solution was quickly injected into above solution to form salidroside loaded liposomes. After removal of ethanol using a rotary evaporator, the liposomes showed a small size (<102 nm) and the encapsulation efficiency was up to 45%.

The reversed phase evaporation method is specially designed for hydrophilic compounds encapsulation [113]. The phospholipids in organic solvent (usually ether or chloroform) are firstly mixed with a small amount of hydrophilic NHP in water dispersion and sonicated to form reversed

micelles. Then the organic solvent is gradually removed under reduced pressure which leads to the disintegration of some micelles and release of free lipids. These lipids merge to the remaining reversed micelles and finally form liposomes. Liposomes prepared by this method have large internal aqueous space, therefore demonstrate higher encapsulation efficiency for hydrophilic compounds. For example, ferrous sulfate was loaded into liposomes using the reversed phase evaporation method [114]. In this work, ferrous sulfate solution (10 mL) was added into egg phosphatidylcholine in diethyl ether solution (30 mL) and sonicated to form W/O emulsion. The organic solvent was gradually removed using a rotary evaporator and ferrous sulfate loaded liposomes were formed under the reduced pressure. The obtained liposomes had a large size (microns) and the encapsulation efficiency was 67%.

Although the inner aqueous core allows liposomes to entrap hydrophilic NHPs more efficiently than protein nanoparticles, it is still more challenging for liposomes to encapsulate hydrophilic NHPs than hydrophobic ones [115]. Hydrophobic NHPs are generally insoluble in the preparation medium and can tightly bind with phospholipids through hydrophobic interaction, thus can be efficiently loaded in the liposomes. While hydrophilic NHPs are highly soluble in the preparation medium and in many circumstances only weak or none attractive interaction exist between hydrophilic NHPs and phospholipids. During liposome formation, only part of the preparation medium is entrapped as the aqueous core of liposomes. Significant amount of NHPs in the preparation medium will be left outside of liposomes, resulting in a lower encapsulation efficiency [116]. Challenges in natural phospholipids based liposomes are also associated with their low stability in the gastrointestinal environment. Natural phospholipids normally have phase transition temperature lower than 37^{o}C [117]. After ingestion, the physical state of phospholipid bilayers can switch from ordered gel phase to disordered liquid crystalline phase due to the increased

temperature. This change largely increases the permeability of phospholipid layer, leading to the leakage of hydrophilic NHP from liposome's aqueous core. Low pH can further accelerate the leaking process [118]. For example, Liu et al. found that liposome lost over 60% of encapsulated compound in the simulated gastric environment within 5 min[119]. Bile salts can also cause the lysis of phospholipid bilayer structure [120] and studies showed that bile salt could trigger over 80% release of encapsulated contents from liposomes within 0.5 h [118, 121]. Ideally sustainable, rather than burst, release of NHP in the gastrointestinal tract is preferred for oral NHP delivery because this release behavior can help maintain a stable NHP concentration in the body and allow the NHP to produce health benefits for a longer time.

1.4.2.2 Double/multiple emulsions

Double/multiple emulsions for the delivery of hydrophilic compounds normally consist of a large oil-in-water droplet with one or more water-in-oil droplets dispersed inside. Typically, a two-step process is required to make double/multiple emulsions. In the first step, an NHP aqueous solution (inner aqueous phase) is dispersed in the oil phase with hydrophobic surfactant(s) and homogenized to form a W/O emulsion. The W/O emulsion is then mixed with a second water phase (outer water phase) containing hydrophilic surfactant(s) to form the W/O/W emulsion. In order to keep the integrity of W/O droplets, mild emulsifying condition should be used in the second emulsification step. Similar to liposomes, the inner aqueous phase (water-in-oil droplets) of the double/multiple emulsions can load various hydrophilic NHPs. Double/multiple emulsions can encapsulate hydrophilic NHPs more efficiently than liposomes, with encapsulation efficiency reaching as high as 98.4% [122], because almost all the preparation medium with hydrophilic NHPs can be incorporated to form the inner aqueous phase (water-in-oil droplets). Moreover, the intermediate oil phase in the double/multiple emulsions can effectively isolate the internal aqueous

phase from outside environment at body temperature, resulting in minimal diffusion of hydrophilic NHPs from double/multiple emulsions and limited access of gastrointestinal fluid to encapsulated compounds. This property significantly increases the stability of encapsulated NHPs in the gastrointestinal tract [122, 123]. For example, Nayak et al. used a multiple emulsion to encapsulate the catechin [124]. Briefly, catechin solution (25%, v/v) was added into olive oil (75%, v/v) with polyglycerol polyricinoleate as a hydrophobic surfactant. The mixture was processed with a probe sonicator to form a fine O/W emulsion. The O/W emulsion was then added into 1% Tween 80 solution and sonicated in a milder condition to form a W/O/W emulsion. The multiple emulsion had a size of 2.82 μm and high encapsulation efficiency of 97%.

However, there are also drawbacks associated with these delivery systems. Double/multiple emulsions are unstable thermodynamic systems, in which there are two proximal opposite interfaces (inner water phase and oil phase, oil phase and outer water phase) stabilized by different surfactants. Generally, a hydrophobic surfactant is required to stabilize the interface between inner water phase and oil phase; and a hydrophilic surfactant is required to stabilize the interface between oil phase and outer water phase. Because these two interfaces are proximal to each other, surfactants stabilizing these two interfaces can diffuse across the oil layer which finally leads to coalescence[125, 126]. Moreover, most double/multiple emulsions have their size in micron-scale[127], and nano-scaled double/multiple emulsions ($\leqslant$ 200 nm) have been seldomly reported. A cross linker/photo initializer [128] or specifically synthesized copolypeptide [129] was required to stabilize the inner aqueous droplets in the nano-scaled double emulsion. However, it is difficult to remove the undesired compound, such as crosslinker (N, N'-methylene-bisacrylamide) [128], from the inner aqueous phase of double emulsion.

1.4.2.3 Solid lipid nanoparticle/nanostructured lipid carrier

Solid lipid nanoparticles are designed as an alternative to nanoemulsion, in which a solid lipid with melting point higher than body temperature, is used to protect encapsulated compound from photodegradation/oxidation [130] and better control the release of encapsulated compounds in the digestive tract [131]. However, single lipid can form a highly ordered crystal structure, leading to the expulsion of encapsulated compounds from nanoparticles during storage. In order to overcome this problem, blends of solid lipids and liquid lipids are used to produce nanoparticles, which are called nanostructured lipid carriers [131]. The blends of lipids still remain solid at the body temperature, but they can form imperfect crystal structure which reduces the expulsion of encapsulated compound from nanoparticles during storage [132]. Hot and cold homogenization methods can be used to make solid lipid nanoparticles/nanostructured lipid carriers [130]. In the hot homogenization method, NHP and melted lipids are added to a hot surfactant dispersant and mixed by a high-speed homogenizer. The pre-emulsion is then treated by high-pressure homogenization to form nanoemulsion. The obtained nanoemulsion is cooled down to room temperature, and lipids will recrystallize to form solid nanoparticles. In the cool homogenization method, a NHP is firstly dispersed in the melted lipids. Then the mixture is cooled down to room temperature and ground to microparticles. The microparticles are added into cold surfactant solution and broken into nanoparticles by high-pressure homogenization.

Solid lipid nanoparticles/nanostructured lipid carriers are primarily designed for hydrophobic compound delivery. Due to similar polarity, hydrophobic compounds can be well dissolved in the lipid matrix and encapsulated into nanoparticles. However, many hydrophilic NHPs can hardly be entrapped in solid lipid nanoparticles/nanostructured lipid carriers due to their high polarity and low solubility in the hydrophobic lipid matrix. Therefore, organic solvent or assistant surfactant is required to enhance the solubility of hydrophilic compounds in the lipids [133]. For example,

Almeida et. al investigated the feasibility of loading lysozyme into solid lipid nanoparticles[134]. In order to achieve higher solubility in the lipid, lysozyme was premixed with Poloxamer 182 (assistant surfactant) in water and then added into melted lipid matrix at 50 ^{o}C. The mixture was then dried using a rotary evaporator, cooled down to room temperature, grinded into powder, dispersed in a 3% (w/w) aqueous surfactant solution (sodium cholate, Poloxamer 188 or Tween 80) and homogenized to form nanoparticles. It is worth mentioning that despite the use of an assistant surfactant, the quantity of lysozyme solubilized in the lipids was still low. Short of lipids that can dissolve hydrophilic NHP is the major obstacle in developing solid lipid nanoparticles/ nanostructured lipid carriers for hydrophilic NHP delivery. Moreover, the dissolution of NHP in lipid(s) needs to be conducted at a relative high temperature (usually >50^{o}C), which is unfavorable for the temperature sensitive NHPs [34].

1.4.3 Nature polymer and lipid based nanoparticles for VB12 delivery

VB12 have been loaded in microparticles or bulky delivery systems, including yeast glucan microparticles [135], nature (e.g. dextran, alginate) and synthetic polymer (e.g. poly(lactic-co-glycolic acid), Poly(acrylic acid)) microparticles [136-142], double emulsions (>3 μm) [122, 143-148], bulk hydrogels [149, 150] and mini tablets [151]. Less work has been done in preparing nanocarriers for VB12 delivery. Among the limited samples, some are unsuitable for daily oral consumption, such as carbon nanotubes [152] and ion nanoparticles [153], because of the potential adverse effects caused by these materials [154-156]. So far, only a limited number of VB12 loaded nanoparticles that are suitable for oral administration have been developed. These nanoparticles were primarily made from protein, polysaccharide and lipids. The physiochemical properties and biological responses of these nanoparticles are briefly reviewed in this section.

VB12 loaded soy protein nanoparticles were prepared using a cold gelation method [63]. Soy protein was dispersed in an alkaline solution and denatured through heating. After cooling down to room temperature and adjusting pH to neutrality, proteins were mixed with VB12 and then associated to nanoparticles by the addition of $CaCl_2$. Nanoparticles had relatively small size (30 to 180 nm) and good uptake efficiency in the Caco-2 cell model. The transport efficiency of VB12 was increased around 2 to 3 folds after being encapsulated into protein nanoparticles. However, both VB12 and soy protein are water soluble compounds carrying negative charge. In an aqueous environment, VB12 could only bind with soy protein through moderate hydrophobic interaction [157], which led to a low VB12 encapsulation efficiency of soy protein based nanoparticles (up to 13%).

Chitosan and its derivative (N,N,N-trimethyl chitosan) based nanoparticles were developed for VB12 delivery [158-160]. All the formulas had chitosan or its derivatives dissolved in 1% acetic acid and crosslinked with sodium tri-poly phosphate. Obtained nanoparticles had a size of 107 to 335 nm and exclusively carried positive surface charge (+20 to +29 mV). The highest encapsulation efficiency (16%) was obtained at chitosan/VB12 ratio of 100:15, and chitosan based nanoparticles showed higher encapsulation efficiency than N,N,N-trimethyl chitosan based nanoparticles(4.4%) [159]. Low encapsulation efficiency of these nanoparticles was mainly due to lack of interactions between VB12 and chitosan/ chitosan derivatives [159].

VB12 loaded nanoliposomes were prepared by Bochicchio [161], Jung [162], and Ohsawa [163]. The thin film method was adopted by Bochicchio and Jung for liposome preparation. But VB12 was loaded into liposomes in different ways. In Bochicchio's work, the dried phospholipid film was directly hydrated with VB12 loaded buffer solution to form multilamellar liposome vesicles [161]. The multilamellar liposomes were then sonicated to small unilamellar liposomes. Whereas

in Jung's work, citric acid loaded liposomes were firstly prepared [162]. VB12 was then added into the liposome solution and diffused into the aqueous core of liposomes. After entering the aqueous core, VB12 could bind with proton from citric acid and form $VB12H^+$. The $VB12H^+$ complex had reduced permeability to neutral phospholipid bilayers, so it accumulated in the liposomes. Different from Bochicchio and Jung's work, Ohsawa et al mixed VB12 with concentrated phospholipid solution (up to 25%) and used ultrasonication to prepare VB12 loaded nanoliposomes [163]. The obtained liposomes received a freeze-thaw treatment to temporarily disrupt their bilayer structure and allowed more VB12 to diffuse into the aqueous core [164]. All three liposomes had small size (51 to ~300 nm) and high encapsulation efficiency of VB12 (38% to 62%). *In vitro* release study was not conducted in these nanoliposomes. In terms of the biological response, only one study investigated the effect of nanoliposome on animal skin [162]: VB12 in nanoliposomes showed 17 times greater permeability than its free form after 24 h treatment.

Genç et al. prepared VB12 loaded solid lipid nanoparticles using a hot homogenization method [165]. VB12 was added into a melted lipid (Compritol®) and then mixed with Tween 80 solution under high speed homogenization. The obtained emulsion was cooled down to room temperature to form solid lipid nanoparticles. Nanoparticles (size: ~200 nm) had high encapsulation efficiency of VB12 (92%). However, *in vitro* release showed a burst release of VB12 (80% in 30 min) in phosphate buffer solution (pH=6.8) at 37ºC. This could be caused by quick diffusion of VB12 from partly melted lipid matrix (low solubility) to the release medium. Cell studies indicated nanoparticles could internalize into different cell lines (no quantitative data available).

1.5 Novel protein-lipid composite nanoparticles for VB12 delivery

In this study, we aimed to design novel protein-lipid composite nanoparticles with inner water compartments for the delivery of VB12. This system may take advantages of both barley protein and lipid based delivery systems and can potentially overcome their inherent limitations.

Barley protein was selected as the primary wall material because of its favorable property to protect core ingredient in the gastric tract and then subsequently control the release of NHPs in the small intestine for absorption [166]. In previous work, solid barley protein microparticles (1-5 μm) were obtained by processing barley protein coarse emulsion with high-pressure homogenization [167, 168]. Barley protein nanoparticles (90-150 nm) could be further prepared by decreasing protein and oil concentration [45]. The prepared barley protein micro- and nano-particles demonstrated high encapsulation efficiency (> 92.9%) and loading efficiency (46.5-50.1%). Barley protein microparticles were able to protect encapsulated NHPs from environment stress (like oxidation) [167, 169]. C hordein is a major fraction of barley protein with a repetitive domain that could form a helical secondary structure rich in β-turns. The whole C hordein molecule has a rod like conformation (30 nm x 2 nm in dimensions) [170]. This structure may efficiently encapsulate the lipid inside of protein network, and protect it from oxidation. More importantly, both microparticles and nanoparticles could resist harsh gastric environment (low pH and presence of pepsin) and deliver NHPs intact to the small intestine where most of the NHPs are absorbed. The main storage protein in barley are prolamins, which have high content of proline (~21%) [171, 172]. Proline can hardly form hydrogen bonds and the prolyl peptide bond has only limited degree of rotation [171], which reduce protein's non-covalence binding force with the digestive enzyme. Thus, it is difficult for protein high in proline to form geometric complimentary structure to fit the active site of enzyme, resulting in slow enzymatic digestion. Meanwhile, pressure treatment

enhanced the formation of intermolecular β-sheets in barley protein at the oil/water interface, leading to "solid-like" interfacial films that could resist the harsh stomach environment [166]. Also, protein hydrophobic groups are "locked" in the compact interfacial network. This greatly limits the gastric degradation of nanoparticles by pepsin, which preferentially attacks the hydrophobic sites of a protein [47]. Two lipids (α-tocopherol and phospholipid) were used to form the interior structure of the nanoparticles. α-tocopherol could attach underneath the barley protein shell to minimizes the leakage of VB12, thus created greater encapsulation efficiency. As an amphiphilic surfactant, phospholipid could stabilize an inner aqueous compartment, which facilitated the loading of water-soluble VB12.

Meanwhile, the small size of nanoparticles could enhance the endocytosis of nanoparticles, leading to improved bioavailability of encapsulated NHPs. This may also provide an alternative way to absorb VB12 without relying on the intrinsic factor-cubilin mediated active transport. So far, these protein-lipid composite nanoparticles have never been reported in literature.

1.6 Hypotheses and Objectives

The overall objective of this study was to develop novel protein-lipid composite nanoparticles as delivery systems of hydrophilic NHPs for improved oral bioavailability. VB12 was selected as a hydrophilic NHP model with low intestinal permeability.

The research was conducted based on the following hypotheses:

1) Protein-lipid composite nanoparticles with inner aqueous compartments could be prepared to efficiently encapsulate hydrophilic NHPs.

2) Such nanoparticles could still maintain the favorable property of barley protein to resist the harsh gastric environment and release NHPs in the small intestine in a controlled manner.

3) The composite nanoparticles could improve the bioavailability of VB12 and correct VB12 deficiency more efficiently than free VB12 supplement.

The specific objectives were:

Objective 1: to develop and optimize the processing to prepare protein-lipid composite nanoparticles with inner aqueous compartments for efficient encapsulation of hydrophilic NHPs.

Objective 2: to study and improve the stability and the *in vitro* release behavior of nanoparticles in relation to nanoparticle structural characteristics (e.g. surface charge, surface hydrophobicity, hydrodynamic diameter, surface functional groups).

Objective 3: to study the impact of nanoparticle structural parameters (e.g. hydrodynamic diameter, surface charge and hydrophobicity) on the *in vitro* cytotoxicity, uptake mechanism and uptake efficiency of nanoparticles using a Caco-2 cell model.

Objective 4: to evaluate nanoparticles' capacity to improve the bioavailability of VB12 *in vivo*.

Chapter 2-Novel protein-lipid composite nanoparticles with inner aqueous compartments as delivery systems of hydrophilic nature health products

2.1 Introduction

The emergence of functional foods incorporating nature health products (NHPs) provides new opportunities to reduce the risk of chronic diseases. However, the efficacy of these functional foods can be compromised due to NHPs' low stability or bioavailability. Recent advances in nanotechnology has enabled creation of nano-carriers for modulated and selective delivery of drugs to specific areas in the body in order to maximize drug action and minimize side effects in the biomedical and pharmaceutical sectors. However, among the materials that can be used to fabricate a drug nanocarrier, only few are suitable for regular food consumption [80]. Food grade protein and lipid are two such materials that have attracted specific interest in the food industry.

Food proteins are abundant, biodegradable and biocompatible. Many of them have good gelling and emulsifying properties, and therefore can be used to incorporate both hydrophilic and lipophilic NHPs in form of a nano-carrier system. Significant challenges exist though when developing a protein based oral delivery system, where high loading capacity of the delivery system is a desired property. The loading capacity of protein nanoparticles is largely dependent on the interaction between NHPs and protein molecules, such as one or combinations of electrostatic or hydrophobic interactions [108]. The loading capacity for small uncharged hydrophilic NHPs is, however, usually low since such compounds have weak or no interaction with proteins. The weak interaction of the loaded

material with protein nanoparticles can also lead to the rapid diffusion and release of encapsulated NHP in an aqueous environment due to the nanoparticle's large surface to volume ratio. The second challenge is the instability of protein nanoparticles in a gastric environment. The low pH and pepsin of a gastric environment can denature and degrade a protein carrier, leading to leakage of NHPs in the stomach before reaching the small intestine where most NHPs are absorbed. These disadvantages limit protein nanoparticles as a platform for oral delivery of hydrophilic NHP and must be addressed strategically in the carrier design.

Lipid systems, like double or multiple emulsions and liposomes, seems more suitable for loading of hydrophilic NHPs compared with protein carriers, as their inner aqueous compartment(s) is expected to load hydrophilic NHPs of different structure with greater efficiency. However, there are several limitations for them too in food application. For instance, it has been shown that double or multiple emulsions can be thermodynamically unstable since they possess two proximal curved interfaces and surfactants diffusing across the interface can lead to coalescence [125]. At nanoscale (< 200 nm) usually a cross linker/photo initializer [128] or a specifically synthesized copolypeptide [129] is required to stabilize the inner aqueous droplets of the double emulsion, and information documenting the *in vitro* or *in vivo* performance of these nano-delivery systems are limited, which restricts their suitability for application in delivery of NHPs.

Liposomes are successful as oral delivery platforms in pharmaceutical science. But conventional liposomes from natural phosphatidylcholine (soy, egg) and cholesterol, which are considered to be more appropriate for the delivery of NHPs than their synthetic counterparts, are unstable in the gastric environment [74, 119, 173]. Natural

phosphatidylcholine has a low phase transition temperature, and when the temperature increases to 37^{o}C, the lipid physical state changes from ordered gel phase to disordered liquid crystalline phase. Thus liposomes made from natural phosphatidylcholine become "leaky" in the stomach at body temperature [118]. Also, conventional liposomes are susceptible to the actions of bile salts and lipases, and may respond unpredictably to these factors in the intestinal environment [118, 119, 121]. Using a phospholipid that possesses a greater phase transition temperature and/or modifying it in such a way to reduce NHP leakage is necessary for successful adaption of liposomal delivery systems to NHP delivery. In this regards, processing and ingredient costs, safety, and sourcing considerations are other important factors that must be considered [115].

To overcome the shortcomings of lipid and protein based nano-carriers for oral delivery of hydrophilic NHPs, in this research, development of a novel protein-lipid composite nanoparticle with an inner water compartment for hydrophilic NHP encapsulation was explored. This particular strategy takes advantages of a protein's good gelling capacity and uses the lipid to "seal" the inner water compartment. Barley protein was selected as the primary wall material because it can form a "solid-like" film at the interface after mechanical pressure treatment, instead of liquid film for many other proteins [166]. We assumed the solid-like protein shell would serve as a "nano-scaffold" allowing attachment of the lipid layers. Incorporating α-tocopherol into the nanoparticle was our strategy to better isolate the inner water compartment from the outside environment. This was intended to make the nanoparticle less "leaky" compared to conventional liposome systems. Also, a barley protein shell should have the capacity to better resist gastric digestion and protect the incorporated NHPs [45, 168].

Vitamin B_{12} (VB12) and glucose were used as hydrophilic NHP models. VB12 plays vital roles in normal functioning of the nervous and blood systems. The classical symptom of VB12 deficiency is anemia, but a significant deficiency can potentially cause severe and irreversible nerve damage. VB12 deficiency is frequently seen among the elderly due to poor dietary patterns and absorption issues. In North American the major cause of VB12 deficiency is malabsorption rather than an insufficient intake, because VB12 has a complex route for intestinal absorption [29]. Firstly, VB12 is separated from its food matrix by the acidic environment in the stomach and then bound to gastric intrinsic factor. This complex then travels to the small intestine to cubilin receptor located in proximal region of the small intestine. Any disruption of gastric acid, secretion of intrinsic factor, or the functioning of the intestinal receptor can result in malabsorption and subsequent deficiency. Nano-particulate delivery of V12 can bypass some of these requirements and lead to better bio-availability of this NHP through oral route.

2.2 Material and method

2.2.1 Material

Barley protein was extracted by alkaline method as previously described [172]. Protein content in the extract (86.7±2.6%, w/w) was determined by combustion with a nitrogen analyzer (CN-628, Leco Corporation, St. Joseph, MI) with a protein calculation factor of 5.83 [174]. High purity soy phosphatidylcholine (95%) was purchased from Avanti Polar Lipid (Alabaster, AL, USA). Food grade soy lecithin was a gift from CIRANDA (Hudson, WI, USA). Cell culture reagents including Dulbecco's Modified Eagle's Medium (DMEM), fetal bovine serum (FBS), nonessential amino acids (NEAA), HEPES solution, trypsin–EDTA and Hank's balanced salt solution (HBSS) were purchased from GIBCO

(Burlington, ON, Canada). Human colorectal adenocarcinoma cell line Caco-2 was purchased from the American Type Culture Collection (ATCC) (Manassas, VA, USA). The rest of the chemicals were all of reagent grade and from Sigma-Aldrich Canada Ltd (Oakville, ON, Canada).

2.2.2 Preparation of protein nanoparticles with inner aqueous compartments

2.2.2.1 Inner organic phase: 200 mg soy phosphatidylcholine, 50 mg cholesterol, 35 mg soy lecithin, 300 mg α-tocopherol were dissolved in 15 mL ethanol. For VB12 loading, it was dissolved in ethanol and added into the solution above. Since glucose is insoluble in ethanol, it was dissolved in water and mixed in the ethanol solution. The ratio of water and ethanol was adjusted to prevent compound precipitation. The mixture was then vortexed together with approximately 15 mL of solid-glass beads (borosilicate, diam. 3 mm) for 1 min, and dried under a stream of nitrogen gas. A thin film of the mixture was formed on the glass beads and interior wall of the centrifuge tube. The film was dissolved in 10 mL of diethyl ether and dried again under nitrogen flow. The solvent was further removed in a vacuum oven for 2 h at room temperature. The residual was re-dissolved in 1.2 mL of diethyl ether and 0.4 mL of chloroform and mixed with a 0.35 mL of distilled water in a 5 mL centrifuge tube. The mixture was sonicated (sonic dismembrator, Model 500, fisher scientific) for 4 min in ice-water bath to form a homogeneous water in oil dispersant.

2.2.2.2 Nanoparticle preparation: 1g barley protein was dispersed in 20 mL distilled water and the suspension was then stirred at 1000 rpm for 0.5 h in ice bath. Immediately after inner organic phase was prepared, it was added into the ice-cold barley protein dispersant (pH=8) and mixed by high speed homogenization (24,000 rpm, T18 ULTRA-TURRAX, IKA work Inc., NC, USA) to make a coarse emulsion. The pre-mixed emulsion was then

passed through a high-pressure homogenizer (10000 psi, 2 cycles, Nano DeBEE, Bee International, Inc., MA, USA) to form nanoparticles. Organic solvent in nanoparticle was removed in a rotary evaporator with a water bath at 25 ^{o}C for 2 h and further eliminated by gentle agitation of the suspension in a fume hood overnight. On the second day, the nanoparticle suspension was centrifuged at 3200 g for 10 min (Avanti J-E, Beckman Coulter Centrifuge, CA) to remove a small portion of solid aggregates and the supernatant was used for further study. When necessary, the nanoparticle suspension could be ultra-filtered to remove un-encapsulated VB12 (300 kDa T-Series Membrane, Pall cooperation).

2.2.3 Characterization of nanoparticles

2.2.3.1 Particle size measurements

The size and polydispersity index (PdI) of the nanoparticles were measured at room temperature (22 ^{o}C) by dynamic light scattering using a Zetasizer Nano S (model ZEN 1600, Malvern Instruments Ltd). The refractive index (RI) was set at 1.45 and dispersion medium RI was 1.33. The samples were properly diluted before measurement.

2.2.3.2 Encapsulation efficiency

The encapsulation efficiency (EE) and encapsulation capacity (EC) was determined by the equation below. To separate and quantify the un-encapsulated NHP, 1 mL nanoparticle suspension was diluted to 25 mL in a volumetric flask using phosphate buffer solution (PBS, 0.1 M, pH=5.5). The solution was centrifuged (3200 g for 10 min, Avanti J-E, Beckman Coulter Centrifuge, CA), filtered (220 nm pore size nylon filter, Millipore) and used for free NHP quantification. For total NHP quantification, 1 mL nanoparticle suspension was mixed with 3 mL ethanol, vortexed for 1 min, and then sonicated for 15 min. The solution was further diluted to 50 mL in volumetric flask with distilled water. The

dilution was collected, centrifuged, filtered as described above and used for analysis (see section 2.2.7).

$$\text{EE} = (1 - \frac{\text{Free NHP}}{\text{Total NHP}}) \times 100\%$$

$$\text{EC} = \frac{\text{mass of NHP in nanoparticle}}{\text{mass of nanoparticle}} \times 100\%$$

2.2.4 Electron microscopy

Transmission electrical microscopy (TEM, Morgagni 268, Philips-FEI, Hillsboro, USA) at an accelerating voltage of 80 kV was employed to study the morphology and interior structure of the nanoparticles. For general morphology study, the nanoparticles were negatively stained with 2% (w/v) sodium phosphotungstate and observed directly on a carbon coated grid. For interior structure observation, nanoparticles were imbedded in 4% agarose gel, fixed with 2.5% glutaraldehyde and 2% paraformaldehyde, rinsed with PBS, stained with 1% OsO_4, rinsed again with water, dehydrated, infiltrated with embedding medium (spurr kit), and finally polymerized. Sections (~100 nm) were cut by ultramicrotome (EM UC6, Leica) and finally stained with 2% uranyl acetate and 1% lead citrate for observation. To demonstrate individual layers of nanoparticles, α-tocopherol and phospholipids (phosphatidylcholine and food grade lecithin) were stained with OsO_4 vapor (1 mL of 1% OsO_4) in 35mm glass petri-dishes for 3 h. Afterwards, OsO_4 solution was removed and petri-dishes were left open in the fume hood overnight to remove unreacted OsO_4. The OsO_4 stained α-tocopherol and phospholipid were used to prepare nanoparticles separately. Ultrathin sectioning for these nanoparticles followed the protocol described above with all staining procedure skipped.

2.2.5 *In vitro* release

For *in vitro* release study, nanoparticles (5 mL) were mixed with pre-warmed release medium (95 mL, 37ºC) in a 150 mL plastic container with screw caps to prevent water evaporation. Experiment was conducted at 37ºC in an incubator (Isotemp, Fisher Scientific) and all samples were continuously shaken at 100 rpm by an orbital shaker. Release profiles of the nanoparticles in the simulated gastrointestinal environment were studied by incubating them in different release media [168]: 1) Simulated gastric fluid (SGF): HCl-saline solution, pH 2.0; 2) simulated gastric fluid with pepsin (SGF-E): SGF with 0.1% pepsin (w/v); 3) simulated intestinal fluid (SIF): phosphate buffer, pH=7.4; 4) simulated intestinal fluid with pancreatin (SIF-E): SIF with 1.0% pancreatin (w/v). To further understand the roles of different layers in nanoparticle release profile, more release media were used: 5) SIF with 0.61% trypsin; 6) SIF with 0.61% chymotrypsin;7) SIF with 0.12% lipase (type II lipase); and 8) SIF with mixed enzyme (0.61% trypsin and 0.12% lipase). The amount of protease or lipase added is based on their proportion in pancreatin [175]. The experiment was conducted at 37ºC and all samples were continuously shaken at 100 rpm. Three batches were tested for each medium. At different time intervals, samples were withdrawn and the same amount of fresh medium was added. Samples were filtered (220 nm pore size nylon filter, Millipore) and injected into HPLC for analysis.

2.2.6 *In vitro* cell evaluations

Caco-2 cell line (passage 19-30) was used for *in vitro* evaluation. Cells were cultured in DMEM, supplemented with 20% FBS, 1% nonessential amino acids, 1% antibiotic-antimycotic and 25 mM HEPES. Cells were cultured in a humidified atmosphere containing 5% CO_2 at 37°C.

The cytotoxicity of nanoparticles was examined by MTT (3-(4,5-dimethylthiazol-2-yl)-2,5-diphenyltetrazolium bromide) assay. Caco-2 cells were transferred to 96-well plate at a density of 5000 cells per well in 100 uL of culture medium. Cells were allowed to grow overnight before experiment. Various concentrations of nanoparticles were dispersed in culture medium and incubated with cells for 20 h. Upon removal of nanoparticles, 10 uL of MTT solution (5 mg/mL in PBS) was added into each well and incubated with cells for another 4 h. The medium was then replaced by 100 uL of DMSO to dissolve the formed formazan. OD value was measured at 570 nm using a microplate reader (SpectraMax, Molecular Devices, USA). The viability was expressed by the percentage of living cells with respect to the control cells.

To evaluate the uptake of nanoparticles in cells, Nile red was incorporated into the inner organic phase during nanoparticle preparation. Cells were seeded onto 6-well plate at a density of 1 x 10^5 cells per dish and cultured for 5-7 days until full confluency. On the day of experiment, the culture medium was replaced with HBSS and equilibrate at 37ºC for 0.5 h. Then HBSS was replaced by Nile red stained nanoparticles in HBSS suspension. After 1, 3, 6 h, cells were harvested, washed with cold PBS, fixed using 4% paraformaldehyde (w/v in PBS, pH=7.2) and recorded by flow cytometer (BD Fortessa-SORP, USA). Cells without treatment were used as negative control.

The uptake of the nanoparticles by Caco-2 cells was also investigated by confocal laser scanning microscopy (CLSM, 510 Meta Carl Zeiss, Jena, Germany). Caco-2 cells were seeded onto glass bottom microwell dishes (P35G-1.5-14-C, MatTek Corp., USA) at a density of 10^5 cells per dish and cultured for 5-7 days until full confluency. On the day of experiment, the culture medium was replaced with HBSS and equilibrate at 37ºC for 0.5 h. Then HBSS was replaced by Nile red stained nanoparticles in HBSS suspension. After 1, 3, 6 h, cells were gently washed with PBS 3 times and fixed with 4% paraformaldehyde at 37ºC for 15 min. The cell membrane was stained with wheat

germ agglutinin (WGA) Alexa Fluor 488 conjugate (5 μg/mL in HBSS, 15 min) and cell nuclei were stained by DAPI (4',6-diamidino-2-phenylindole) (0.1 μg/mL in PBS, 10 min) before CLSM observation.

2.2.7 Quantitative analysis

2.2.7.1 VB12 determination:

VB12 concentration between 1 μg/mL and 20 μg/mL were measured by high performance liquid chromatography (HPLC, 1200 Series, Agilent Technologies) with diode array detector (G1315D, Agilent Technologies) at 360 nm. Eclipse XDB-C18 column (4.6×150 mm, 5 μm, Agilent Technologies) was used and the elution gradient was water/acetonitrile with 0.1% formic acid at a flow rate of 1 mL/min [151]. VB12 was quantified employing an external calibration.

2.2.7.2 Glucose determination

Phenol-sulfuric acid method was adopted to determine the glucose concentration [176]. Briefly, 2 mL of diluted analyte solution or standard solution was put in a test tube. 1 mL of 5% phenol solution and 5 mL of sulfuric acid were added into each tube and mixed by general vortex. After 15 min, 200 μL of sample were transferred onto microplate and read at 492 nm. Glucose was quantified employing an external calibration.

2.2.8 Statistic analysis

Experiments were performed in three independent batches unless otherwise stated. Data were represented as the mean of three batches with standard deviation. t-test was used in statistical comparison between two groups. One-way Analysis of Variance (ANOVA) with Tukey's honest significant difference test were used in multiple-comparisons (three or more

groups). Statistical differences between samples were performed with a level of significance as $p < 0.05$.

2.3 Result and discussion

2.3.1 Nanoparticles design

The original idea of this nanoparticle design was based on previous research by Szoka and Cui [113, 177]. We have used this idea and extended it to create a nanoparticle with both novel structure and performance. The process of nanoparticle formation is illustrated in Fig. 2.1. The inner organic phase was designed to entrap hydrophilic NHPs and served as a sacrificial core (step 1). Soy phosphatidylcholine served as primary emulsifier and a small amount of food grade lecithin was used as co-emulsifier to increase the stability of this reversed phase emulsion. The addition of the cholesterol at a cholesterol-to-phosphatidylcholine ratio of 1:2 (molar ratio) was intended to increase the rigidity of the phosphatidylcholine layer to better tolerate shear stress during sonication or homogenization [178]. Finally, large α-tocopherol to phosphatidylcholine molar ratio was used in the system with the purpose of preventing phosphatidylcholine from forming a liposome [179] so that the desired structure could be developed in the subsequent steps.

A pre-emulsion was formed by mixing the inner organic phase with barley protein solution (step 2), followed by high-pressure homogenization processing. It was expected that barley protein would adsorb onto the surface of the inner organic phase droplets and then form a solid shell by the effects of the high-pressure homogenization treatment (step 3). Our previous work demonstrated that under mechanical pressure barley protein's secondary structure is re-organized at the interface [166]. Here, we discovered a large amount of intermolecular β-sheet was developed which enhanced the interaction between barley

proteins. This change further led to the switch of interfacial network from an expanded liquid phase to solid-like film with good rheological elasticity and compressibility. The compressed barley protein finally formed a solidified shell served to better stabilize the organic phase droplets loaded with NHPs.

Finally, the organic solvent was removed under reduced pressure in step 4. As a consequence, it was expected that water could penetrate into the particle shell to replace the organic solvent and mix with the small water droplets in reverse emulsion to form one large inner water compartment. Meanwhile, α-tocopherol was speculated to move outwards together with organic solvent due to its hydrophobic nature and bound with the barley protein solid coating *via* hydrophobic interaction. It was also expected that an α-tocopherol layer could be formed to isolate inner water compartment from the outside environment, so that the hydrophilic NHP was better trapped and protected in the inside aqueous compartment of the nanoparticles.

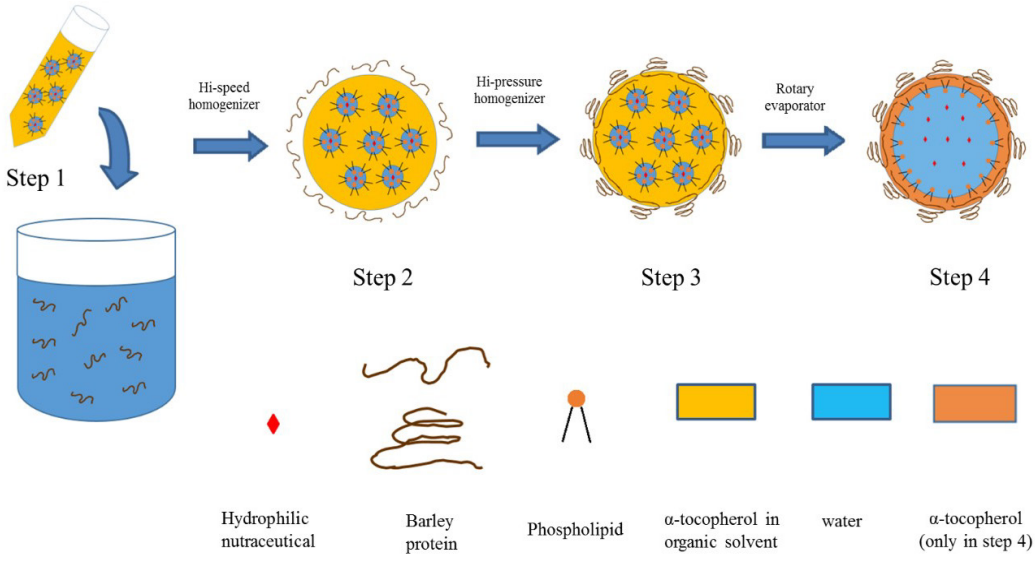

Figure 2.1 Scheme of nanoparticles preparation and the proposed structure of nanoparticles

2.3.2 Structure characterizations

In order to elucidate the nanoparticle structure, transmission electron microscope (TEM) was used to observe the particle surface and interior morphology. Fig. 2.2A demonstrates that nanoparticles were spherical in shape with a diameter between 200 and 300 nm. This is in accordance with dynamic light scattering analysis (Fig. 2.2A inset; average size 243 ± 5 nm, PdI 0.17±0.03). Since all the compounds in nanoparticles are primarily composed of C, H, N, O, the interior structure of nanoparticle could not be identified based on contrast. Thus, positive staining of different compound(s) was applied. As shown in Fig. 2.2B, all compounds together formed the black ring structure and the blank inner area confirms the existence of inner water compartment. Fig. 2.2C and 2.2D demonstrate the positive staining of α-tocopherol and phospholipids (soy phosphatidylcholine and food grade lecithin), respectively. Both compounds formed a circular structure with their size similar to that of the nanoparticles. These two figures prove the existence of α-tocopherol layer and phospholipid layer. Since barley protein is the coating material to stabilize the nanoparticle, the three-layer structure (barley protein layer, α-tocopherol layer and phospholipid layer) proposed in previous section (Fig. 2.1 step 4) was confirmed based on these TEM images. It was challenging to identify which layer (α-tocopherol layer or phospholipid layer) stabilized the inner water compartment by TEM, however, it is reasonable to assume that the interior interface exposed to water to be filled with phospholipid due to the amphiphilic nature of this material. Fig. 2.2E shows the structure of nanoparticle after step 3. Without

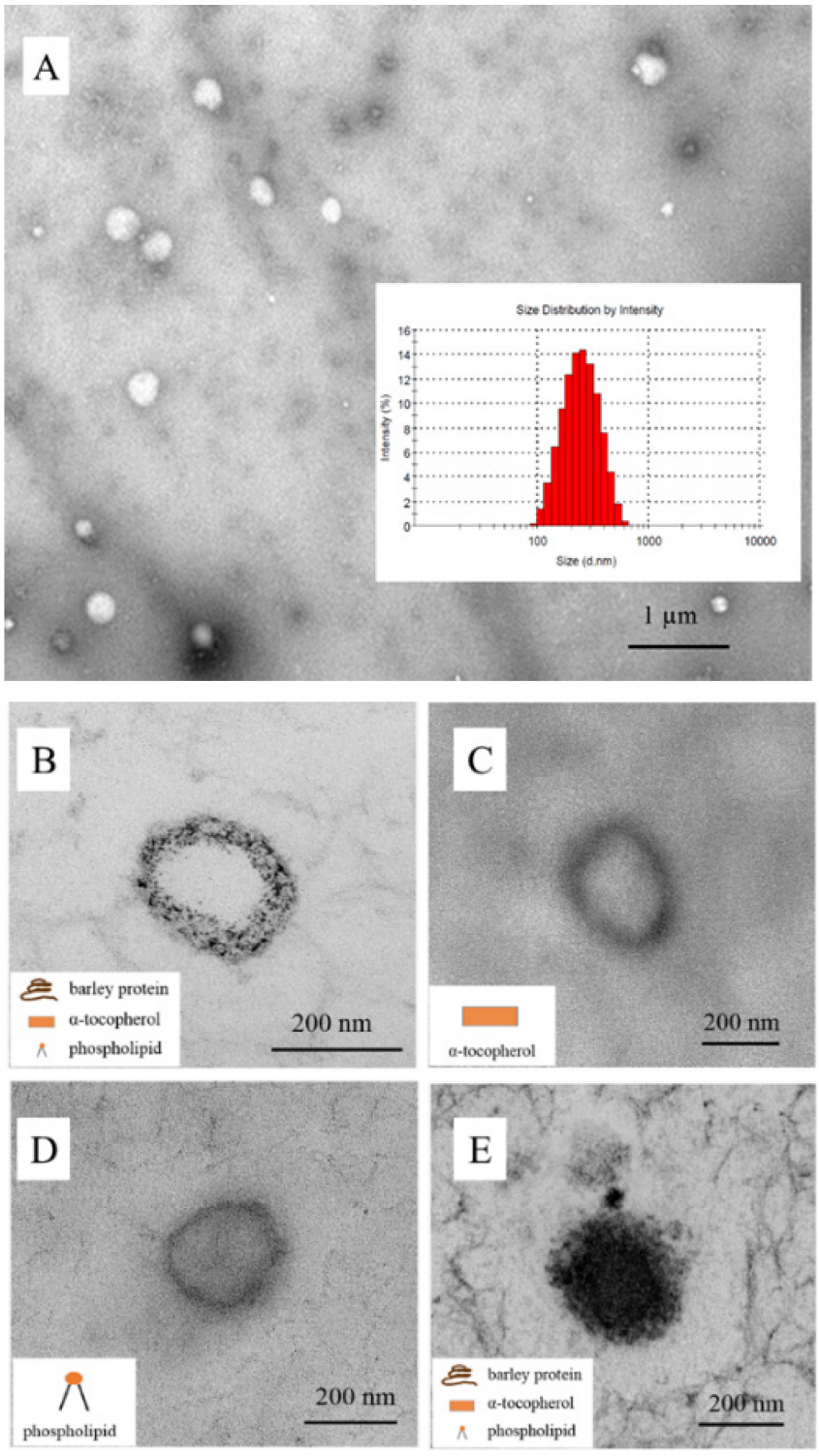

Figure 2.2 TEM imagine of nanoparticles A: overview of nanoparticles (negative staining); B, C, D: interior structure of nanoparticle at step 4; E: structure of nanoparticles at step 3. Inset graph in A shows the result form dynamic light scattering. Inset graphs in B, C, D, E demonstrate compound(s) with positive staining.

removing the organic solvent, the nanoparticle could not form the desired inner aqueous compartment, therefore TEM image of the nanoparticle had a dark solid core. The solid core is unfavourable for the incorporation of hydrophilic NHPs. Moreover, based on the literature [113] and our observations, the reverse emulsion stabilized by phosphocholine could not be kept stable for a long time. The leakage of compounds from nanoparticles was usually observed over night as an oil layer on the solution.

2.3.3 Encapsulation efficiency study

The influence of formulation variables and procedure on the encapsulation efficiency (EE) and encapsulation capacity (EC) of VB12 and Glucose is summarized in Table 2.1. Relatively high encapsulation efficiency (69%) could be achieved when 5 mg VB12 was added in the system (20 mL). This is superior to soy protein nano-carrier (EE~13%) [63] and nanoliposomes (EE 39-62%) [161-163]. Double emulsions have high encapsulation efficiency normally (EE as high as over 95% for VB12), but they have much larger size (> 3 μm) [122, 143-148]. A further increase of the VB12 concentration resulted in a decreased encapsulation efficiency, but the amount of VB12 that encapsulated in the nanoparticle (EC) kept increasing. Removal of α-tocopherol decreased the encapsulation efficiency by > 13 folds. This was attributed to the key role of α-tocopherol in isolating the inner water

Table 2.1 Impact of preparation variable and procedure on encapsulation efficiency (EE) and encapsulation capacity (EC)

Sample (20 mL)	**Nutraceutical**	**EE (%)**	**EC (%)**
Standard procedure	5 mg VB12	69 ± 1	0.218 ± 0.003
Standard procedure	20 mg VB12	55 ± 6	0.694 ± 0.076
Standard procedure	50 mg VB12	33 ± 2	1.041 ± 0.063
No α-tocopherol	5 mg VB12	5 ± 1	0.016 ± 0.003
Standard procedure	50 mg Glucose	31 ± 4	0.978 ± 0.126

compartment from the outside environment and minimizing the leakage of encapsulated NHPs. Decent encapsulation efficiency (31%) was also observed for glucose as a small molecule (~180 Da) with high hydrophilicity. The encapsulation efficiency result suggests that the protein-lipid nanoparticle has potential to be used as a platform technology to achieve good encapsulation efficiency of hydrophilic NHPs.

2.3.4 *In vitro* release

The first barrier for oral NHP delivery is the low pH and the pepsin protease in the stomach. The stomach environment can degrade nanoparticle matrix, leading to premature release of NHP before reaching the intestine, which may in turn result in the reduced bioavailability of the encapsulated NHP. The cumulative release curves of VB12 from nanoparticles developed here in SGF and SGF-E were shown in Fig. 2.3A. The release of VB12 was low in SGF and reached only 13.1% after 6 h of test. Adding pepsin into release medium did not significantly increase the release of VB12 at 6 h ($p > 0.05$), indicating that the protein-lipid composite nanoparticles were stable and able to protect hydrophilic NHP in a gastric environment. According to our previous work [166], pressure treatment enhanced the formation of intermolecular β-sheets in barley protein, leading to solid interfacial films that could resist the harsh stomach environment. Also, protein hydrophobic groups are "locked" in the compact interfacial network. This greatly limits gastric degradation of nanoparticles by pepsin, which preferentially attacks the peptide bonds formed by phenylalanine, tyrosine and leucine [180]. This property allows nanoparticles to better protect encapsulated ingredients than nanoliposomes. For example, it was shown that around 70% of encapsulated bovine serum albumin was lost from soy phospholipid based nanoliposomes in the simulated gastric environment within 10 min [119].

In the simulated intestinal environment, different release profiles were observed. In SIF without digestive enzymes, the release was slow. When pancreatin (1%) was added in SIF, a biphasic release behaviour was observed. A burst release of VB12 (41.5%) occurred in the first half hour and then release rate gradually slowed down. After 2 h, nanoparticles started releasing VB12 at a constant rate (R^2=96.8% for zero-order model) and 65.8% VB12 was found in the release medium after 6 h. To further explore the degradation mechanism of the nanoparticle in a simulated intestinal environment, the release profiles in the presence of protease (trypsin, chymotrypsin) and lipase were investigated (Fig. 2.3B). As protease and lipase account for 61% and 12% in pancreatin, respectively [175], the total protease and lipase used in simulated intestinal fluid were fixed at 0.61% and 0.12%. The release of VB12 in the presence of chymotrypsin did not show significant increase compared to the release of VB12 in SIF (Fig. 2.3A). This could be explained by the fact that chymotrypsin, similar to pepsin, prefers to act on bulky hydrophobic amino acids [181]. Since protein hydrophobic groups are hidden in the compact interfacial network, the nanoparticles were less vulnerable to chymotrypsin digestion. In the medium with chymotrypsin and trypsin (1:1), the release of VB12 significantly increased with 47.4 ± 4.6% VB12 found in release medium at 6 h (data not shown). However, this value was lower than VB12 release (69.4±1.9%) in the medium with trypsin at 6 h, suggesting trypsin played a major role in the digestion of the protein layer. In the presence of lipase, an increased VB12 release (47.9±4.2%) was found after 6 h, suggesting the digestion of lipid layer also contributed to VB12 release from the nanoparticles. These results confirmed our previous assumption regarding the function of different layers in VB12 entrapment. However, the initial burst release of VB12 did not happen in either protease or lipase

medium. It recurred only when nanoparticles were incubated in the mixed enzyme solution (trypsin + lipase), suggesting the synergistic effect of protease and lipase hydrolysis contributed to the burst release. After burst release, nanoparticles in all three media (trypsin, lipase and mixed enzyme) exhibited decreased release rate and a controlled release stage (2-6 h) was observed again in mixed enzyme medium. Lipase triggered release had the slowest rate during this period. This could be because the majority of lipids were protected under barley protein coating, so lipase had limited contact with the lipids. In trypsin medium, the release of VB12, although slower than early time points, kept increasing and reached 69.4% at 6 h, suggesting the tryptic degradation of protein coating was the determining factor in the second release phase. Existence of hordein in barley protein shell may be a reason for the decreased protein degradation rate. Hordein is a major barley protein fraction and has very low lysine (~0%) and arginine (~2.7%) content [172, 182]. As lysine and arginine are the exclusive target amino acids for trypsin [183], the tryptic digestion of hordein could be inefficient. Moreover, high proline (~21%) in hordein limited rotation of the prolyl peptide bond, making the formation of geometric complimentary structure in protein that can fit the active site of trypsin more difficult [171, 172]. This effect was to our advantage as it allowed controlled release of VB12 at the second stage of release profile.

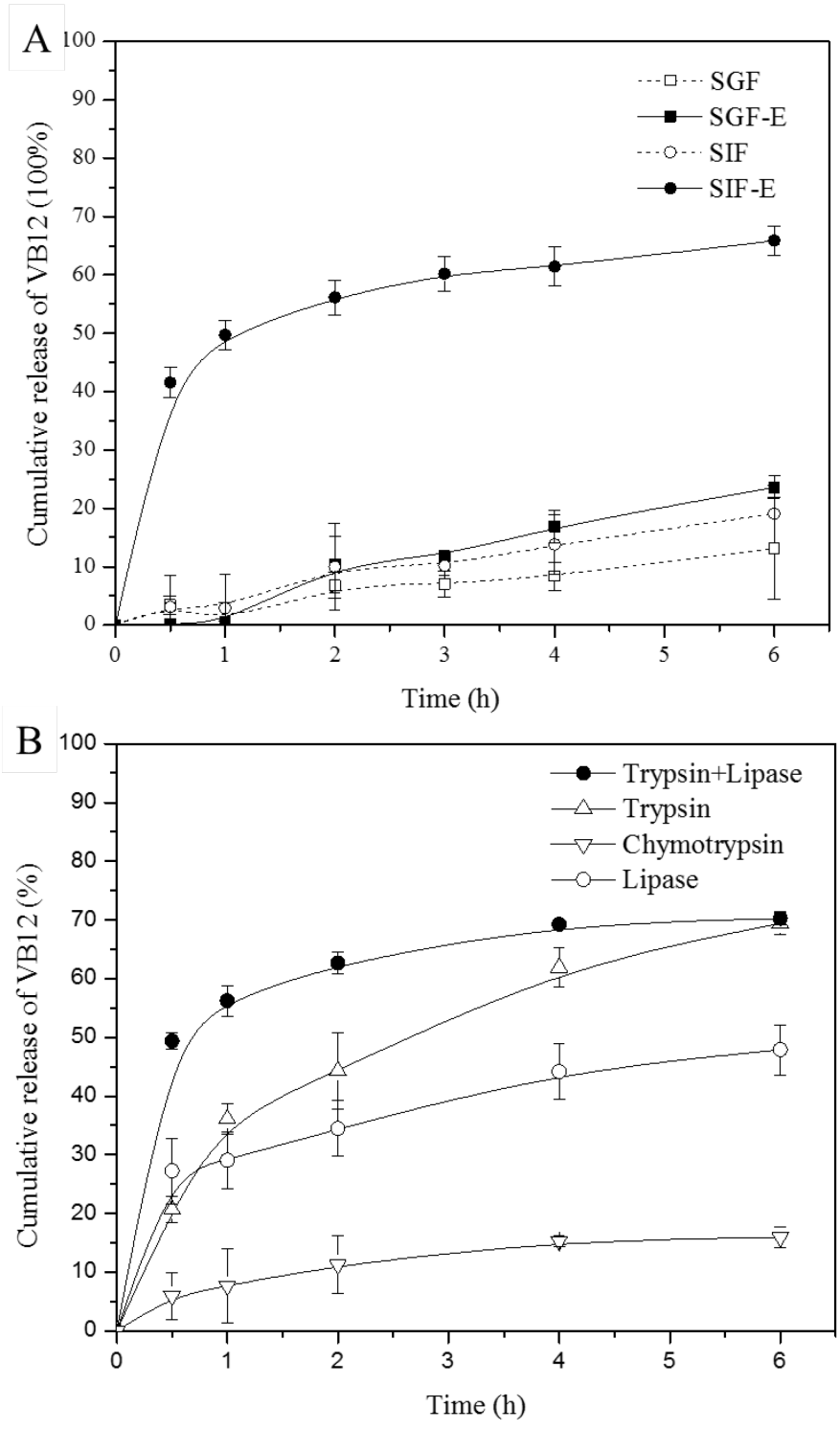

Figure 2.3 VB12 release profile of nanoparticles in SGF, SGF-E, SIF, SIF-E (A), and SIF-trypsin/chymotrypsin /Lipase/trypsin+lipase; (B). SGF: HCl-saline solution, pH 2.0; SGF-E: SGF with pepsin; SIF: phosphate buffer, pH= 7.4; SIF-E: SIF with pancreatin.

2.3.5 *in vitro* cytotoxicity and uptake study

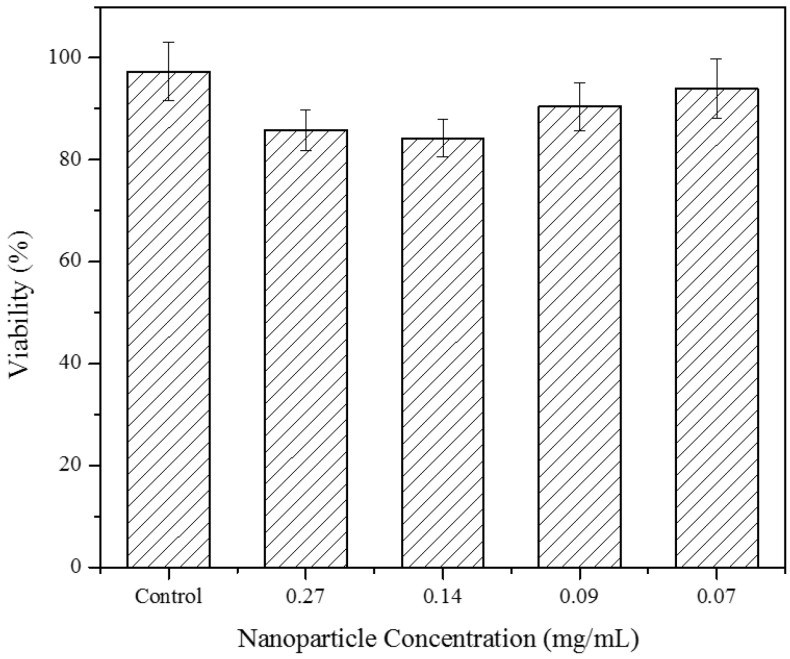

Figure 2.4 Percentage of cell viability evaluated by MTT assay on Caco-2 cells treated with nanoparticles for 20 h.

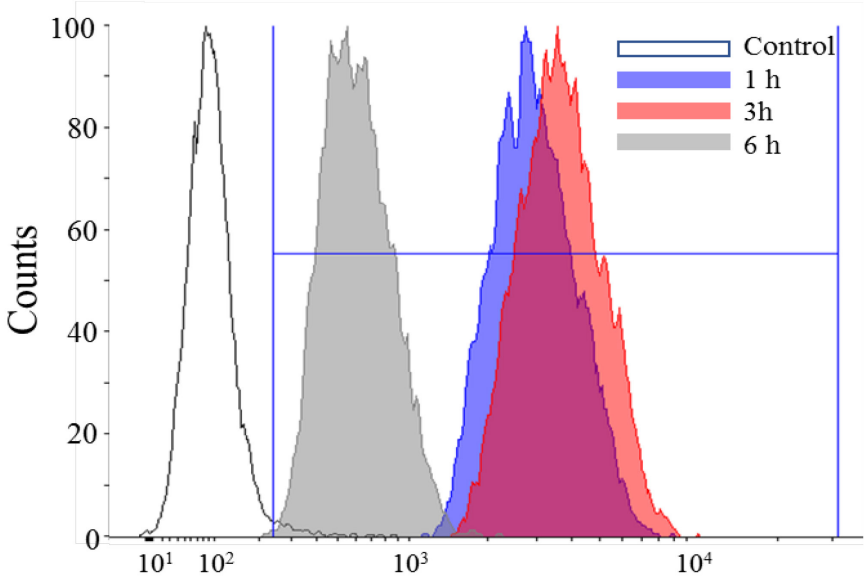

Figure 2.5 fluorescent intensity in cell at different time points.

Both cytotoxicity and cell uptake of nanoparticles were evaluated by Caco-2 cells. Small size gives nanoparticles unique properties, but unexpected toxicity or side effects may occur, so that the

safety level of nanoparticles was firstly determined by MTT assay. As shown in Fig. 2.4, the viability of Caco-2 cells was high (90.3%) when the concentration of nanoparticles was at about 0.1 mg/mL. Therefore, this concentration was used in the following cell experiments.

When Caco-2 cells grow upon full confluency, they will generate tight junctions with each other to form a monolayer which can be used to mimic the epithelium of human small intestine. This allows us to better understand the behavior of nanoparticles in intestinal cells. The internalization of nanoparticles was firstly evaluated using flowcytometry. As shown in Fig. 2.5, the fluorescent intensity increased at 1 h and 3 h, followed by a significant decrease at 6 h. The results from CLSM further confirmed these changes (Fig. 2.6). The increase in fluorescent intensity at 1 and 3 h suggested that nanoparticles were able to gradually internalize and accumulate in Caco-2 cell cytoplasm, while the decrease could possibly be explained by the degradation of nanoparticle in cells. Generally, nanoparticles entering the cell through endocytosis pathway could merge to a lysosome [184]. Protein and lipid could be digested by lysosomal enzymes which cause the release of Nile red from nanoparticles. Nile red is a highly hydrophobic dye and its fluorescent intensity drops sharply in polar environment like intracellular fluids [185]. Quick degradation of nanoparticles in lysosome may be responsible for the decrease in the fluorescent intensity of Nile red at 6 h. These phenomena required further investigation, thus more in-depth cell uptake efficiency and mechanism studies were conducted in chapter 4.

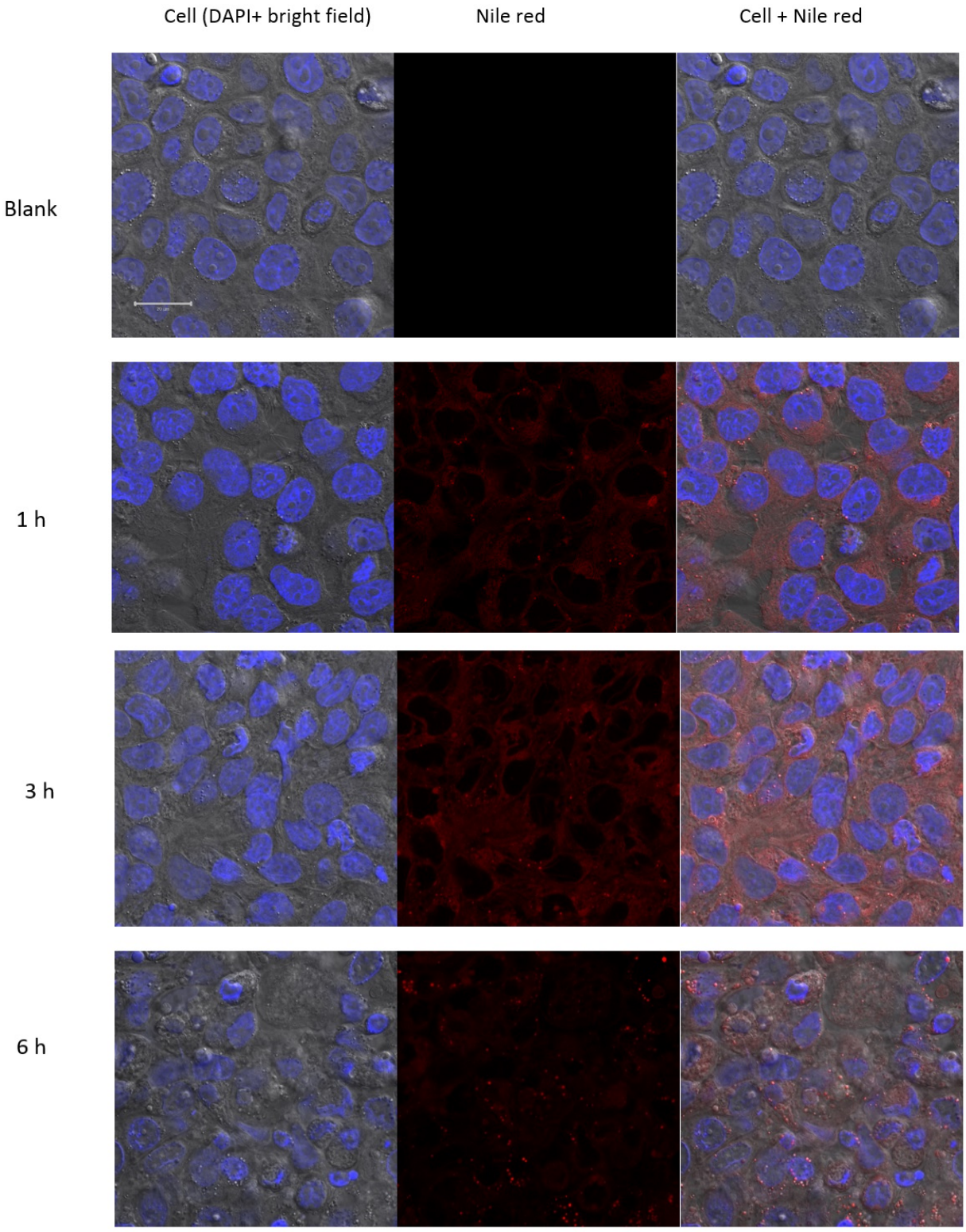

Figure 2.6 Change of fluorescent intensity (Nile red) at 1, 3, and 6 h. Blank: no nanoparticle was added. Scale bar= 20 μm

2.4 Conclusion

This is the first report of a protein-lipid nanoparticle featuring three-layer coating (protein layer, α-tocopherol layer and phospholipid layer) and an inner water compartment. The barley protein layer serving as a "scaffold" to which the α-tocopherol and phospholipid layers are attached. The phospholipid and α-tocopherol layers stabilize the inner aqueous compartment and separate it from the outer water phase, creating greater encapsulation efficiency for the contained hydrophilic compounds (69% for VB12). In addition, the protein shell could resist the harsh gastric environment with low pH and the presence of pepsin, and then subsequently control the VB12 release in the intestinal juice. Nanoparticles exhibited low cytotoxicity through an *in vitro* study using the Caco-2 cell model. Cell uptake study further suggested nanoparticles could efficiently internalize into the cytoplasm of Caco-2 cells. The decreased fluorescent intensity at 6 h indicated the quick degradation of nanoparticles in cells. Overall, the protein-lipid composite nanoparticles have strong potential to be used as delivery systems of hydrophilic bioactive compounds for food, pharmaceutical and cosmetic applications.

Chapter 3-Protein-lipid composite nanoparticles for the oral delivery of vitamin B_{12}: protein succinylation improve the physicochemical properties of nanoparticles.

3.1 Introduction

In chapter 2, we developed protein-lipid composite nanoparticles for delivering hydrophilic nature health products (NHPs) to the intestinal environment. These nanoparticles had a three-layer structure (protein layer, α-tocopherol layer and phospholipid layer) and an inner water compartment. The barley protein layer served as a "scaffold" to which the α-tocopherol and phospholipid layers were attached. The phospholipid and α-tocopherol layers stabilized an inner aqueous compartment which could be loaded with hydrophilic NHPs. This unique structure overcomes many shortcomings of liposome and double emulsion based nano-delivery systems such as instability [125] and leaking in the gastric environment [74, 119, 173]. Furthermore, it can encapsulate hydrophilic NHPs more efficiently (69% for vitamin B_{12}) than many other natural polymer-based delivery systems [63, 159] since no interaction is required between the NHP and the carrier materials. In addition, the nanoparticles can effectively resist the harsh gastric environment to deliver VB12 intact to the small intestine for absorption. Regardless, these protein-lipid composite nanoparticles have shortcomings. Firstly, they are unstable in the present of salt due to a relatively low surface charge, leading to the aggregation of nanoparticles bridged by hydrophobic and other interactions between protein molecules of adjacent nanoparticles. Secondly, leakage of the core ingredients can occur during storage, thus reinforcement of the coating is still required. Thirdly, the nanoparticles degrade fast in a simulated intestinal environment in the presence of pancreatic enzymes, resulting in a quick burst release of VB12

(49.6%) within one hour. This significantly impacts the absorption efficiency of the formulation since VB12 has a low intestinal permeability [186]. VB12 from such a burst release cannot be efficiently utilized; a formulation with improved stability and sustainable intestinal release profile is needed.

Succinylation primarily involves derivatization of ε-amino groups (lysine and arginine) in proteins with succinate [187, 188], which increases the protein surface charge, leading to improved water solubility [189-192]. Succinylation can reduce protein tryptic digestibility, due to the resistance of the succinyl-lysyl-peptide bond to tryptic hydrolysis [193, 194]. Therefore, succinylation may potentially resolve problems associated with the protein-lipid composite nanoparticles. We chose to modify surface after protein-lipid composite nanoparticle formation, allowing the nanoparticle to maintain the favorable three-layer structure. Systematic evaluation on surface succinylation of protein based nanoparticles for oral NHP delivery has not been reported yet. In this chapter, the nanoparticle size, morphology and surface properties were characterized after surface protein succinylation modification, and the impact of structural changes on the nanoparticle physiochemical and biological properties were investigated.

3.2 Material and method

3.2.1 Material

Whole barley protein (over 85%, w/w) was extracted from regular barley grains (Falcon) by alkaline as previously described [172]. Soy phosphatidylcholine (95%) was purchased from Avanti Polar Lipid (Alabaster, AL, USA). Soy lecithin was from CIRANDA (Hudson, WI, USA). Cell culture reagents including fetal bovine serum (FBS), HEPES solution, Dulbecco's Modified Eagle's Medium (DMEM), nonessential amino acids (NEAA), trypsin-EDTA and Hank's balanced salt solution (HBSS) were purchased from GIBCO (Burlington, ON, Canada). Human colorectal

adenocarcinoma cell line Caco-2 was purchased from the American Type Culture Collection (ATCC) (Manassas, VA, USA). Rest of the chemicals were all of reagent grade and from Sigma-Aldrich Canada Ltd (Oakville, ON, Canada).

3.2.2 Nanoparticle preparation

3.2.2.1 Nanoparticle preparation

The protein-lipid composite nanoparticles were prepared according to the method established in chapter 2. Briefly, 200 mg soy phosphatidylcholine, 50 mg cholesterol, 35mg soy lecithin, 300 mg α-tocopherol and 5 mg VB12 were dissolved in 20 mL ethanol. The mixture was vortexed with around 15 mL of solid glass beads (diam. 3 mm) in a 50 mL centrifuge tube and dried under nitrogen. The thin film was dissolved in diethyl ether and dried again under vacuum. Afterwards, 1.2 mL of diethyl ether and 0.4 mL of chloroform were added to fully dissolve the thin film. The solution was sonicated (sonic dismembrator, Model 500, fisher scientific) with 0.35 mL distill water for 4 min in ice-water bath to form inner organic phase. Immediately after inner organic phase was prepared, it was added into 20 mL ice-old barley protein dispersant (5% w/w, pH=8) and mixed by high speed homogenization (24,000 rpm, T18 ULTRA-TURRAX, IKA work Inc., NC, USA). The pre-mixed emulsion was then passed through a high-pressure homogenizer (10000 psi, 2 circles, Nano DeBEE, Bee International, Inc., MA, USA) to form nanoparticles. The final particle dispersant was put in a rotary evaporator to remove the organic solvent. The residual of organic solvent was further removed by leaving dispersant in the fume hood overnight under gentle agitation. On the second day, the nanoparticle dispersant was briefly centrifuged (3200 g, 10 min, Avanti J-E, Beckman Coulter Centrifuge, CA) to remove solid aggregates and stored at 4 ^{o}C in dark until use.

3.2.2.2 Preparation of nanoparticles with succinic anhydride modification

Method for protein outer layer modification was adopted from Thompson and Reyes [189]. Briefly, excessive succinic anhydride (succinic anhydride to protein ratio 1:1, w/w) was added very slowly into the nanoparticle dispersant with agitate stirring at room temperature. The pH was controlled at around 8 with sodium hydroxide after each addition. The reaction was allowed to proceed for 4 h after the last addition. Free VB12 and excessive succinic acid in solution was removed using ultrafiltration equipment with a peristaltic pump (Masterflex console drive Model 77200-62, Cole Parmer Instrument Company, QC, Canada) and a membrane with molecular weight cutoff of 300 kDa (T-Series, Pall Life Sciences, ON, Canada). After ultrafiltration, nanoparticles were stored at 4ºC in dark until use. In this chapter, nanoparticles obtained from 3.2.2.1 were referred as original nanoparticles (O-NPs), and nanoparticles obtained from 3.2.2.2 were referred as modified nanoparticles (M-NPs).

3.2.3 Nanoparticle characterizations

TNBS (2,4,6-Trinitrobenzene Sulfonic Acid) method was adopted to quantify free amino groups (primary and ε-amino group) on nanoparticle surface [195, 196]. Nanoparticles (200 μg/mL, 0.5 mL) were mixed with TNBS (0.01%, w/v, 0.25 mL) and incubated at 37ºC for 2 h. Reaction was then terminated by SDS (sodium dodecyl sulfate, 10% w/v, 0.25 mL) and HCl (1 M, 0.125 mL). The final solution was measure at 340 nm using a SpectraMax M3(Molecular Devices, USA). The amino group content was determined using an external standard curve generated by glycine in a series of known concentrations.

Attenuated total reflectance-Fourier transform infrared spectroscopy (ATR-FTIR) was applied to further study the nanoparticle matrix after succinylation. The spectroscopic data was collected by

a Nicolet 6700 spectrometer (Thermo Fisher Scientific, USA). Freeze dried nanoparticles were directly placed on an ATR accessory with a Ge crystal. All samples were measured at a resolution of 4 cm^{-1} and a total of 128 scans.

The morphology of M-NPs was observed by both scanning electron microscope (SEM, Philips XL-30) and transmission electrical microscopy (TEM, JEM 2100, JEOL). For SEM, diluted M-NPs were frozen in liquid nitrogen and then freeze-dried. The cross-sectional fracture surface of the aggregation was coated by a thin layer (8-10 nm) of sputtered gold under vacuum, and then used directly for photograph. For TEM observation, one drop of diluted M-NP dispersant (5 μL) was added directly to a carbon coated grid and dried at room temperature overnight before observation. For inner structure observation, samples were imbedded in 4% agarose gel, fixed with 2.5% glutaraldehyde and 2% paraformaldehyde, rinsed with PBS, stained with OsO_4, rinsed again with water, dehydrated, infiltrated with embedding medium (spurr kit), and finally polymerized. Sections (100 nm in thickness) were cut by ultramicrotome (EM UC6, Leica) and stained by 2% Uranyl acetate and 1% lead citrate for observation.

The size, size distribution (PdI), and zeta potential of nanoparticles were measured at room temperature (22 ^{o}C) using a Zetasizer Nano S (model ZEN 1600, Malvern Instruments Ltd). The protein refractive index (RI) was set at 1.45 and dispersion medium RI was 1.33. For size determination, samples were diluted to an appropriate concentration using distill water to avoid multiple scattering. For zeta potential determination, nanoparticles were diluted with buffer solution (0.05 M) before measurement (pH adjusted by sodium phosphate monobasic, sodium phosphate dibasic, phosphoric acid).

The surface hydrophobicity of nanoparticles was determined using the method from Kaito and Nankai [197]. Nanoparticle suspension (4 mL) with concentration from 0.002% to 0.01% was mixed with 20 μL 1-anilinonaphthalene-8-sulfonic acid (ANS) solution (8 mM in 0.01 M phosphate buffer, pH=7.4). Fluorescent intensity was measured using SpectraMax M3(Molecular Devices, USA). Excitation and emission wavelengths were 390 and 470 nm. The initial slope of the relative fluorescence intensity versus protein concentration plot was calculated by linear regression analysis and used as an index of the nanoparticle surface hydrophobicity.

The encapsulation efficiency (EE) was determined by the equation below. For total VB12 quantification, 1 mL nanoparticle dispersant was mixed with 3 mL ethanol and sonicated for 15 min. The solution was further diluted in a 50 mL volumetric flask. The dilution was collected, centrifuged (3200 g, 10 min, Avanti J-E, Beckman Coulter Centrifuge, CA), filtered (220 nm pore size nylon filter, Millipore), and then used for analysis. To separate and quantify un-encapsulated VB12, nanoparticle dispersant was diluted to 25 mL in volumetric flask using phosphate buffer solution (PBS, 0.1 M, pH=5.5). The dilution was centrifuged and filtered using the same methods described before quantification. The method for VB12 quantification was described in the section 3.2.6.

$$EE= \left(1- \frac{\text{Free VB12}}{\text{Total VB12}}\right) \text{x } 100\%$$

For storage stability test, nanoparticle dispersants were stored at 4ºC in the dark. The size, PdI and EE of O-NPs and M-NPs were monitored at different time intervals during 30 days of storage.

3.2.4 *In vitro* release

The *in vitro* release behavior of M-NPs was investigated using the same method described previously (section 2.2.5). Nanoparticles were incubated in one of four different release media: 1)

Simulated Gastric Fluid (SGF): HCl-saline solution, pH 1.2; 2) Simulated Gastric Fluid with pepsin (SGF-E): SGF with 0.1% pepsin (w/v); 3) Simulated Intestinal Fluid (SIF): phosphate buffer, pH=7.4; 4) Simulated Intestinal Fluid with pancreatin (SIF-E): SIF with 1.0% pancreatin (w/v). The experiment was conducted at 37^{o}C and all samples were continually shaken at 100 rpm. Samples (0.5 mL) were withdrawn at determined time intervals. An equal volume of fresh medium was added to keep volume constant. Samples were filtered (220 nm pore size nylon filter, Millipore) before injection to HPLC for VB12 quantification (see section 3.2.6).

3.2.5 *In vitro* cell evaluation

The Caco-2 cell line (passage 19-30) was used to investigate the cytotoxicity and uptake of M-NPs. Cells were cultured in DMEM, supplemented with 20% FBS, 1% nonessential amino acids, 1% antibiotic-antimycotic and 25 mM HEPES. Cells were cultured and sub-cultured as described in the chapter 2.

3.2.5.1 Cytotoxicity evaluation

The cytotoxicity of M-NPs was examined by MTT (3-(4,5-Dimethylthiazol-2-yl)-2,5-diphenyltetrazolium bromide) assay. Caco-2 cells were transferred to 96-well plate at a density of 5000 cells per well in 100 μL culture medium. Cells were allowed to grow overnight before experiment. Various concentrations of M-NPs were dispersed in culture medium and incubated with cells for 20 h. After incubation, cells were washed by PBS for three times. MTT solution (20 μL, 5 mg/mL in PBS) was added into each well and incubated with cells for another 4 h. Then MTT solution was removed and the formed formazan crystals were dissolved in 100 μL of DMSO. The absorbance was measured at 570 nm using a microplate reader (SpectraMax, Molecular

Devices, USA). The viability was expressed by the percentage of living cells with respect to the control cells.

3.2.5.2 Cell uptake of M-NPs

Confocal laser scanning microscopy (CLSM, 510 Meta Carl Zeiss, Jena, Germany) was used to preliminary evaluate the cell uptake of M-NPs. Nile red was dissolved in ethanol during M-NPs preparation (section 3.2.2). Caco-2 cells were seeded onto glass bottom microwell dishes (P35G-1.5-14-C, MatTek Corp., USA) at a density of 10^5 cells per dish and cultured for 5-7 days until full confluency. Before experiment, the culture medium was replaced by HBSS (with Ca^{2+}, Mg^{2+}, without phenol red) and pre-incubated at 37°C for 30 min. After equilibration, 2mL of Nile red labeled M-NPs dispersant (0.1 mg/ml nanoparticles in HBSS) was added and incubated with the cells for 1, 3, and 6 h. The cells were then gently washed with PBS 3 times and fixed with 4% paraformaldehyde (w/v in PBS pH=7.2) at 37ºC for 15 min. The cell membrane and nuclei were stained with wheat germ agglutinin (WGA) Alexa Fluor 488 conjugate and DAPI as described in the section 2.2.6 before observation.

3.2.6 VB12 quantification

VB12 concentration between 1 μg/mL and 20 μg/mL was determined by high performance liquid chromatography (HPLC, 1200 Series, Agilent Technologies) with diode array detector at 360 nm. Agilent Eclipse XDB-C18 column (4.6×150 mm, packed with 5 μm particles) was used for chromatographic separation. Gradient elution was performed with water and acetonitrile with 0.1% formic acid and the flow rate was 1 mL/min [151].

3.2.7 Statistic analysis

All data were represented as the mean ± standard deviation (n=3) unless otherwise stated. Student's t-test was used for comparison of two groups. One-way analysis of variance (ANOVA) with Tukey's HSD test was applied when there were more than two groups. p value < 0.05 was considered as significantly different.

3.3 Results and discussion

3.3.1 Nanoparticle preparation and characterization

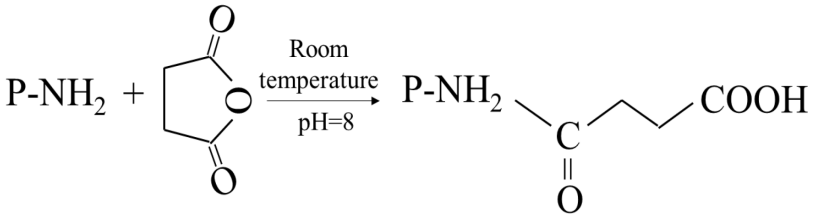

Figure 3.1. Scheme of protein succinylation. P-NH_2: the ε-amino group on the surface of barley protein out layer.

In this work, the prepared protein-lipid composite nanoparticles were modified at their surface by reacting with succinic anhydride (Fig. 3.1). As succinylation primarily takes place at free ε-amino groups in lysine and arginine residues, the analysis of the free amino group content in nanoparticles gives useful information. Nanoparticles with surface succinylation modification (M-NPs) showed greatly reduced free amino group content (10.6±8.5 μmol/g nanoparticle) compared to the original protein-lipid composite nanoparticles (O-NPs) (87.2±1.4 μmol/g nanoparticle) (Fig. 3.2), suggesting the succinylation modification of protein outer layer was successful. The ATR-FTIR spectra (Fig. 3.3) of O-NPs and M-NPs further confirmed the success of succinylation. Amide II (1510-1580 cm^{-1}) is a characteristic band in protein. It originates from N-H and C-N vibration and is more sensitive to the change of N-H group [198, 199]. After succinylation, the amide II band shifted from 1535 cm^{-1} to 1540 cm^{-1} with increased intensity and broader peak width. These

changes implied the formation of new covalent bond between protein and anhydride [200]. A new

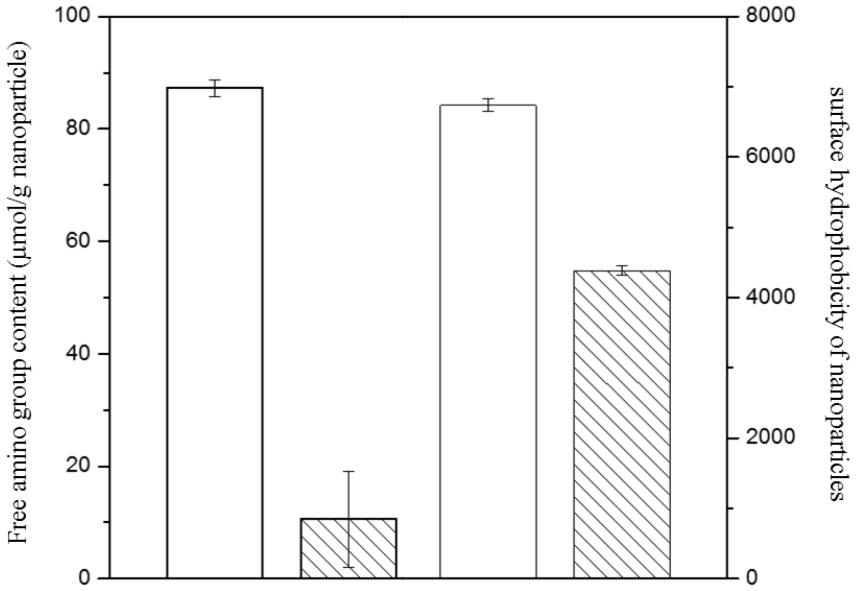

Figure 3.2 Free amino group content (left) and surface hydrophobicity (right) of nanoparticles. Blank column: O-NPs; Patterned column: M-NPs.

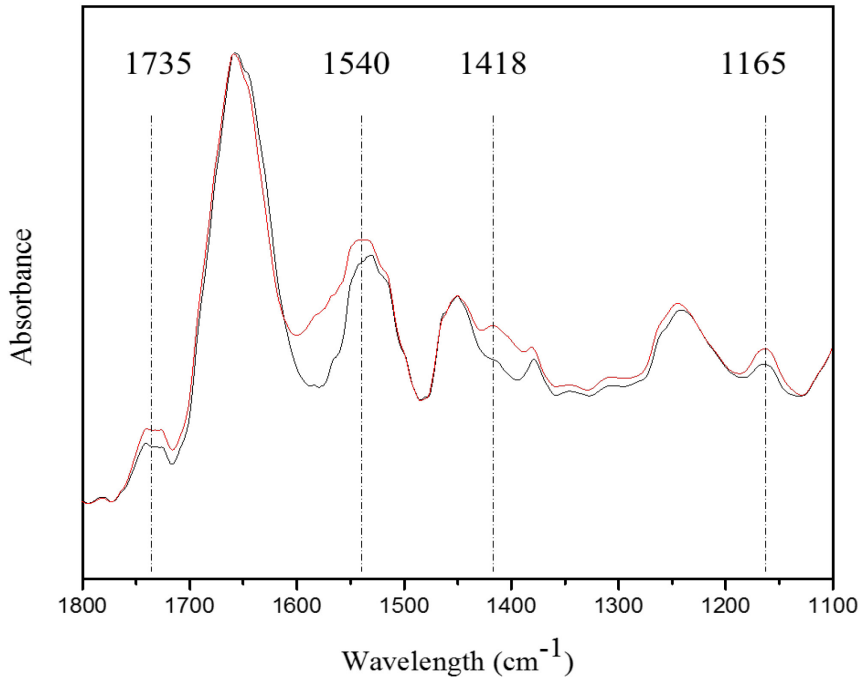

Figure 3.3 ATR spectra of O-NPs (black line) and M-NPs (red line).

band at 1418 cm^{-1} in M-NPs was assigned to the coupled vibration of C-O stretching and O-H bending from succinate [201]. Besides the changes mentioned above, two bands with increased intensity were observed: one was at ~1735 cm^{-1} and the other at 1165 cm^{-1}. The band at 1735 cm^{-1} corresponds to the C=O stretching of the ester and the band at 1165 cm^{-1} accounts for C-O asymmetrical stretching of the ester [202, 203]. The increased intensity in these two bands suggests a new ester bond formation between protein's hydroxyl group and succinate [204].

The introduction of succinate was also confirmed by measuring the nanoparticle's surface charge (Fig. 3.4). The zeta potential of M-NPs (-19.9±1.1 mV) was almost twice as much as O-NPs (-10.2±0.9 mV) at pH 7 because of the conjugation of succinate group on ε-amino groups. Moreover, succinylation decreased the surface hydrophobicity of nanoparticles from 6733±98 for O-NPs to 4385±69 for M-NPs (Fig. 3.2). This is because the addition of succinate groups increased the

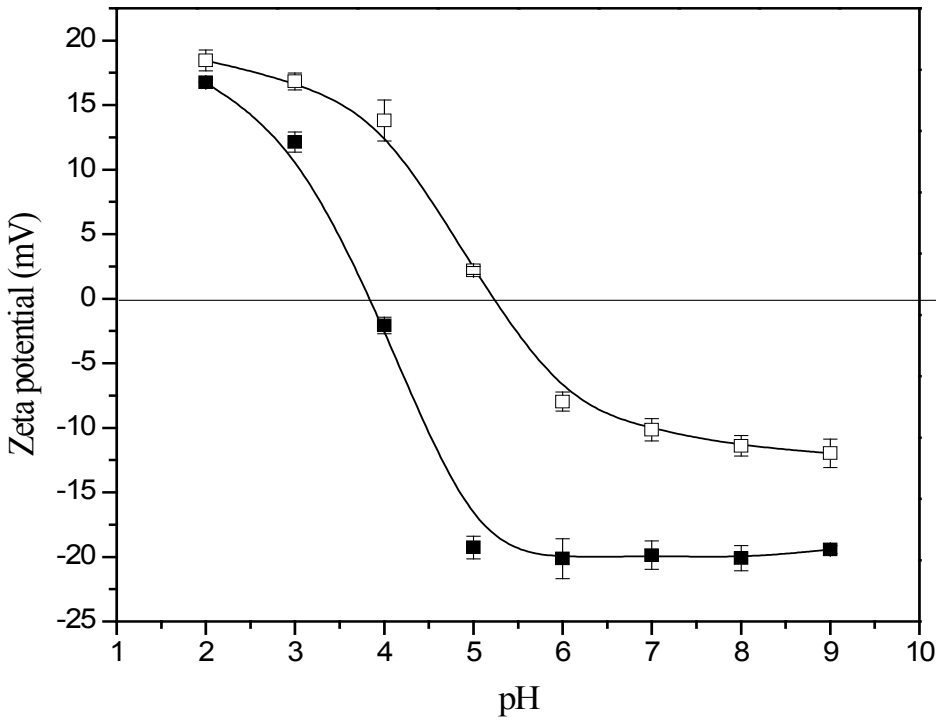

Figure 3.4 the zeta potential of O-NPs (blank square) and M-NPs (filled square)

frequency of hydrophilic groups on nanoparticle surface. The increased negative charge could also partly inhibit ANS from approaching and bind to the hydrophobic area on the nanoparticle [205].

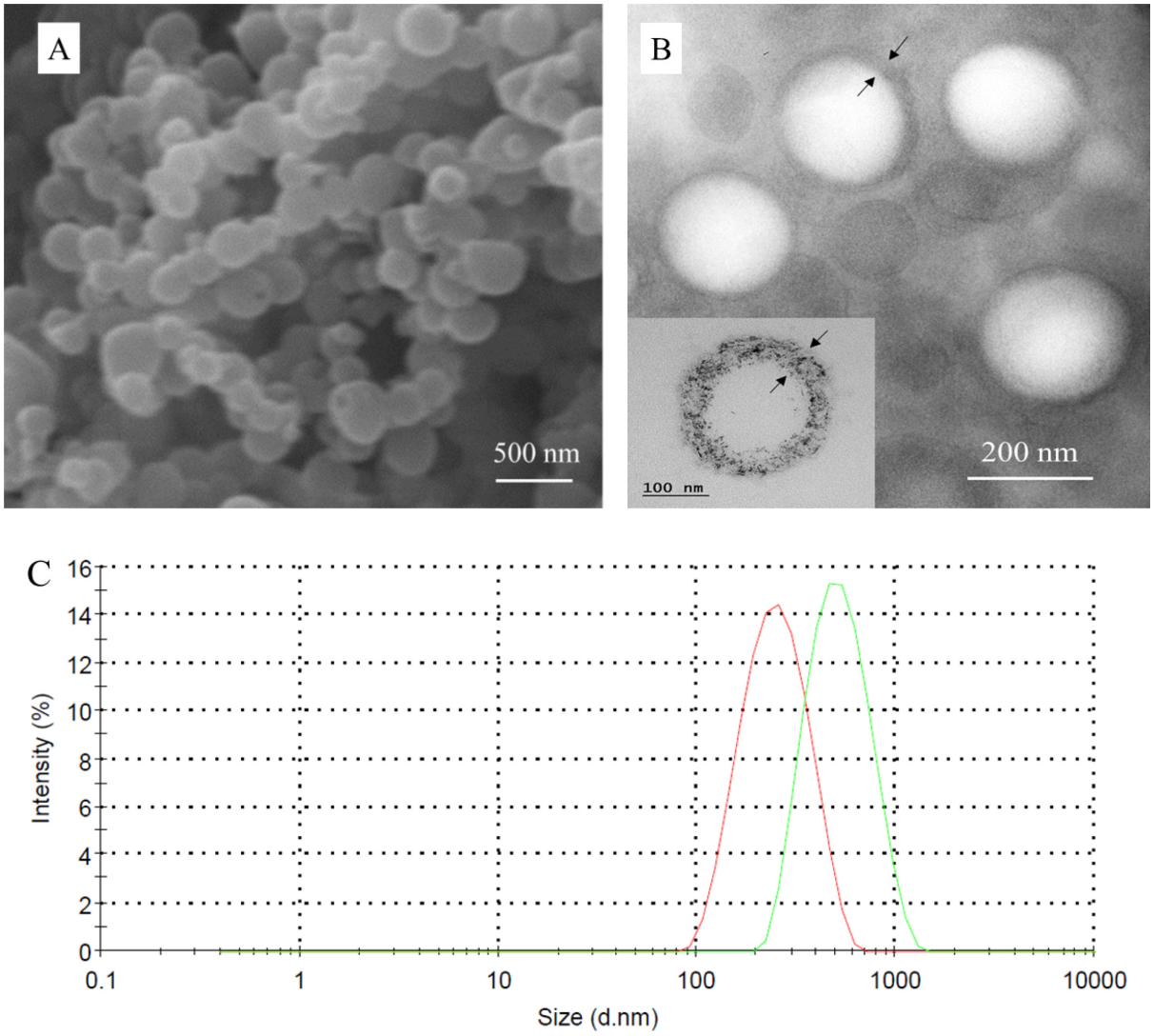

Figure 3.5 SEM image of M-NPs. B: TEM image of M-NPs (unstained). Inset in fig. 3.5 B: TEM image of M-NP with positive staining. The blank inner area confirms the existence of inner water compartment. Arrows demonstrated the wall of hollow nanoparticle. C: hydrodynamic diameter of O-NPs (red) and M-NPs (green);

The morphology of M-NPs was characterized using SEM. As shown in Fig. 3.5A, M-NPs are spherical with around 200 to 300 nm in diameter. This is similar to the electronic microscope image observed in O-NPs (Fig. 2.2). In TEM image (Fig. 3.5B), nanoparticles demonstrate darker ring shade with blank inner area, suggesting the existence of inner water compartment. Positive

staining was used to better illustrate this structure as heavy metals can bind with lipid and protein to enhance the contrast of nanoparticle in TEM image. The positive staining of nanoparticle (Fig 3.5B inset) shows all compounds (protein and lipids) together form a black ring structure with a blank inner area. In our previous work, it has been demonstrated the black ring is composed of three layers (protein layer, α-tocopherol layer and phospholipid layer) and the blank inner area represents an inner aqueous compartment. All electronic microscope images indicate succinylation did not cause notable changes in nanoparticle's geometric structure. The encapsulation efficiency of VB12 was not affected either with 69 ± 1% for O-NPs and 71 ± 6% for M-NPs. However, a difference was found in dynamic light scattering measurement (Fig. 3.5C). Although both nanoparticles showed relatively uniform distribution, the M-NPs showed an increased hydrodynamic diameter (466±15 nm, PdI 0.18±0.02) after succinylation (O-NPs: 243 ± 5 nm, PdI 0.17±0.03). Since nanoparticles with larger average size were not observed in SEM and TEM images, the increased hydrodynamic diameter could probably be explained by the spatial extension of succinate chain on nanoparticle surface and a larger hydration shell introduced by carboxyl groups [206].

3.3.2 Stability test

Stability is essential for nanoparticle applications. Any sedimentation, agglomeration or leakage of core ingredients from nanoparticles can compromise their beneficial effect. The stability of nanoparticle in physiological environment was tested first. As shown in Fig. 3.6A, no apparent sediment was found when M-NPs were dispersed in 0.9% saline for 20 h. In contrast, O-NPs had notable precipitation in the same medium. The improved dissolution allows M-NPs to maintain a small size and a large surface area-to-volume ratio in a physiological environment, like intestinal fluid, and potentially have a more efficient intestinal absorption than aggregated O-NPs. The

stability of the nanoparticle in water during a 30-day storage was also compared between M-NPs and O-NPs. As shown in Fig. 3.6B, M-NPs showed no obvious change in size during the first 15 days. A decrease of nanoparticle size to 287 nm was found towards the end of the test (30th day). As spatial extension of succinate chain on the nanoparticle surface is attributed to the increased hydrodynamic diameter, the decreased size may be explained by the hydrolysis of the amide/ester bond between succinate and barley protein outer layer during storage. However, PdI remained almost unchanged during the whole period, suggesting no major aggregation of nanoparticles. In addition, the VB12 leakage in M-NPs was minimum (4.5±0.5%) during 30 days of storage (Fig. 3.6 D), indicating very little deformation of the nanoparticle occurred during storage. The O-NPs showed comparable stability in the first 7 days (Fig. 3.6 C and D), however, the leakage of VB12 increased to 16.9±5.0% on the 14^{th} day. At the end of study (30^{th} day), PdI of O-NPs increased to 0.4 (in supernatant) and precipitation was observed at the bottom of container. Over half of the VB12 (55.3±14.3%) was released from O-NPs, implying an impaired nanoparticle structure after long-term storage.

Results from these two studies indicate that succinylation largely improved the stability of the protein-lipid composite nanoparticles. Succinylation increased nanoparticle surface charge, leading to stronger electrostatic repulsion force which decreased the chance of colliding and agglomerating among M-NPs. The spatial extension of succinate chain on nanoparticle surface further prevented nanoparticle aggregation owing to the steric hindrance effect. Furthermore, succinate's crosslinking effect should not be ignored. Succinate has one of its carboxyl group conjugated with amino group or hydroxyl group in protein molecule through succinylation. Meanwhile, the other carboxyl group from succinate can bind with free amino group in protein

through non-covalent interactions [207-209], contributing to a more rigid protein outer layer that was resistant to erosion during storage in aqueous medium.

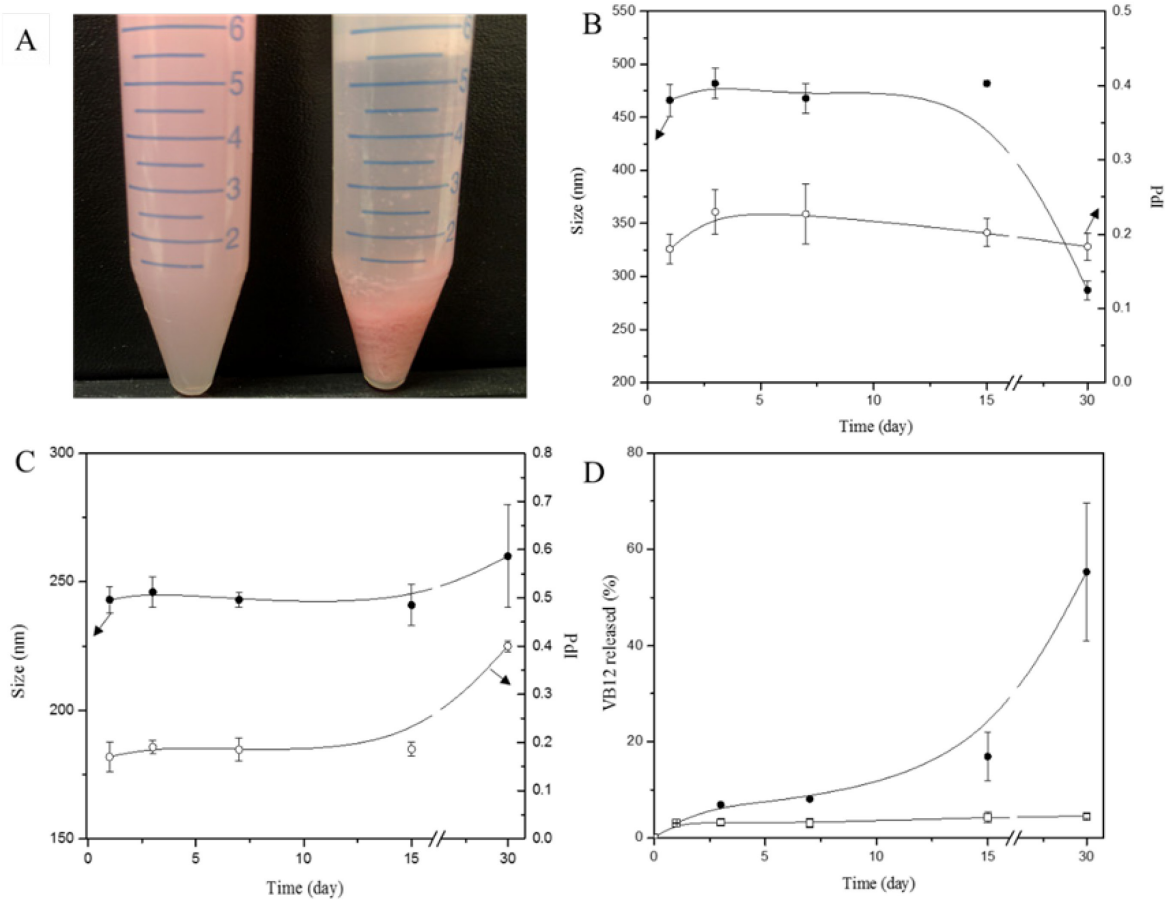

Figure 3.6 A: M-NPs (left) and O-NPs (right) dispersed in 0.9% saline after 20 h at room temperature. B: Change of size (Solid circle) and PdI (blank circle) in M-NPs during 30-day storage; C: Change of size (Solid circle) and PdI (blank circle) in O-NPs during 30-day storage. D: release of VB12 from M-NPs (blank square) and O-NPs (solid circle) during 30-day storage.

3.3.3 *In vitro* release

Poor stability in gastrointestinal tract represents one of the major challenges in developing protein based nanoparticles for oral NHP delivery. The release behavior and mechanism of O-NPs has been elucidated in chapter 2. The release of VB12 was low in SGF with pepsin and reached only 10.4±4.8% after 2 h of testing, indicating that the protein-lipid composite nanoparticles were stable

and able to protect hydrophilic NHP in gastric juice. Our previous study [166] demonstrated that pressure treatment enhanced the intermolecular β-sheets formation in barley protein, resulting in solid interfacial films that could resist the harsh stomach environment. Also, hydrophobic groups in protein were buried in the compact interfacial network, which greatly limited the gastric degradation of nanoparticles by pepsin. In SIF without digestive enzymes, the release was slow. When pancreatin was added in SIF, a burst release of VB12 occurred, with 49.6% of VB12 found in the release medium after one hour. This indicated that the original protein-lipid composite nanoparticles (O-NPs) were vulnerable under pancreatic digestion. Further investigation found that the burst release was related to both protease and lipase hydrolysis with the trypsin digestion of the protein outer layer playing a more important role in VB12 release.

After succinylation, nanoparticles still showed low VB12 release (11.3±3.1%) after 2 h in SGF with pepsin (Fig. 3.7 A), suggesting surface modification did not alter the nanoparticle's capacity to resist the harsh gastric environment. Whereas in SIF with pancreatin, a biphasic release was observed (Fig. 3.7 B). Compared with O-NPs, the burst release in M-NPs was significantly reduced (~50%) and reached only 22.5 ± 4.1% VB12 in the first hour. In the second stage (1-10 h), VB12 was sustainably released from the M-NPs, with around 62.1% VB12 found in the medium after 10 h. The substrate-bind pocket in trypsin is composed of Asp194, Gly217 and Gly277 [48]. The hydrolysis process requires Asp194 to form electrostatic interaction with lysine and arginine residues of substrate. Succinylation on ε-amino acid shielded the positive charge of these amino acid residues so the degradation of surface protein layer was greatly diminished. This work demonstrated the succinylation of protein outer layer could modulate the release behavior of protein-lipid composite nanoparticles in small intestine. This technology may also be applied to other protein based nanoparticles for controlled release in the digestive tract.

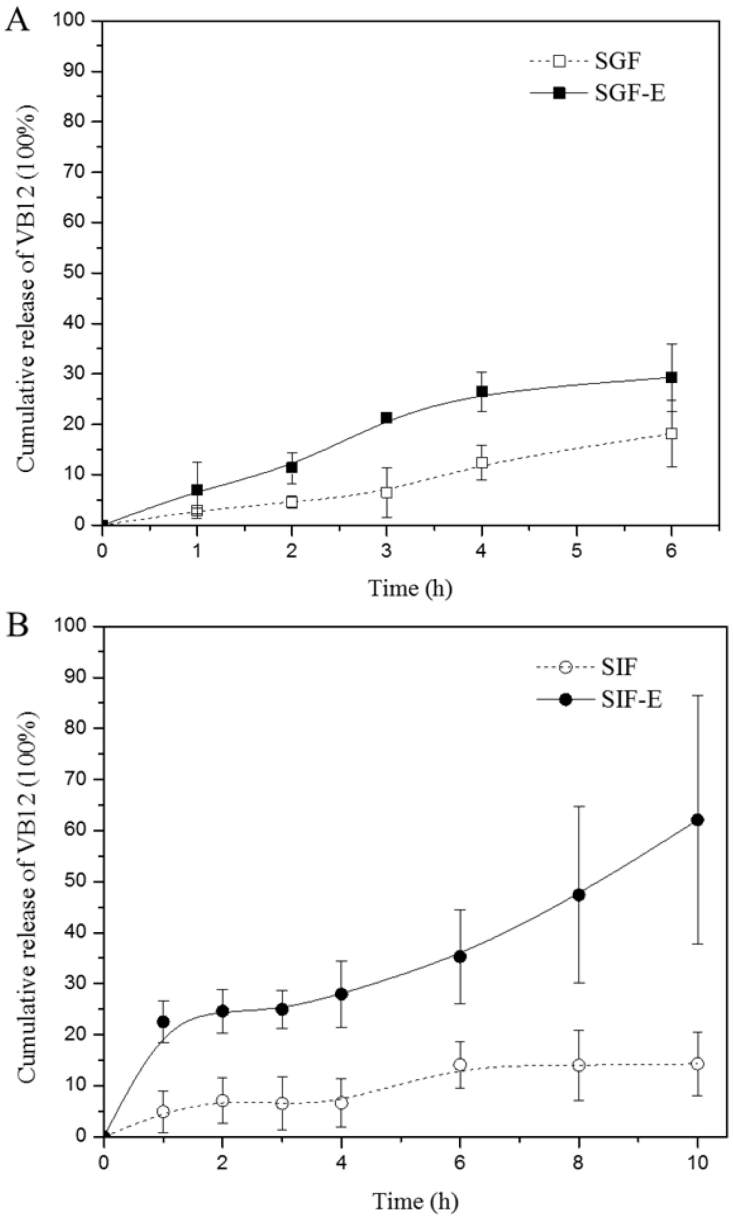

Figure 3.7 *In vitro* release of VB12 from M-NPs in simulated gastric fluid (A) and simulated intestinal fluid (B). SGF: HCl-saline solution, pH 2.0; SGF-E: SGF with pepsin; SIF: phosphate buffer, pH=7.4; SIF-E: SIF with pancreatin

3.3.4 *In vitro* cell evaluation

Both cytotoxicity and cell uptake of M-NPs were evaluated by a Caco-2 cell model. The cell

viability was firstly determined by the MTT assay after incubation with M-NPs for 20 h. As shown in Fig. 3.8, the viability of Caco-2 cells was 86.2% at the nanoparticle concentration of 0.27 mg/mL and around 100% viability was observed at the concentration of about 0.1 mg/mL. Therefore, M-NP concentration of 0.1 mg/mL or lower was used in the following cell experiments.

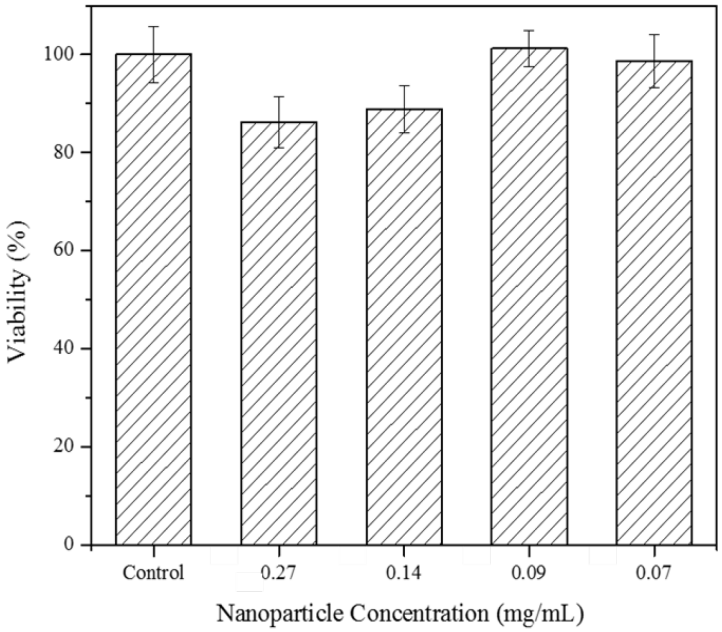

Figure 3.8 Percentage of cell viability evaluated by MTT assay on Caco-2 cells treated with M-NPs for 20 h

Nile red labeled M-NPs were used in the preliminary cell uptake evaluation (Fig. 3.9). Red fluorescence was observed in cells with M-NPs treatment, indicating M-NPs could enter Caco-2 cells and accumulate mostly in the cytoplasm. Similar to O-NPs (chapter 2), the fluorescent intensity increased at 1 h and 3 h, and decreased at 6 h, suggesting the degradation of nanoparticles in the lysosome [184]. However, the fluorescent intensity in cells with M-NPs treatment was not as strong as that with O-NPs treatment, indicating lower uptake efficiency of M-NPs. The increased hydrodynamic diameter in M-NPs could be an important reason, as larger size reduced the interfacial interaction between nanoparticles and cell membrane, resulting in lower uptake efficiency [61, 62]. Moreover, the higher surface charge of M-NPs produced stronger electrostatic

repulsion with anionic cell membrane, leading to less contact between cells and nanoparticles. This assumption was confirmed by more in-depth cell uptake efficiency and mechanism studies in chapter 4.

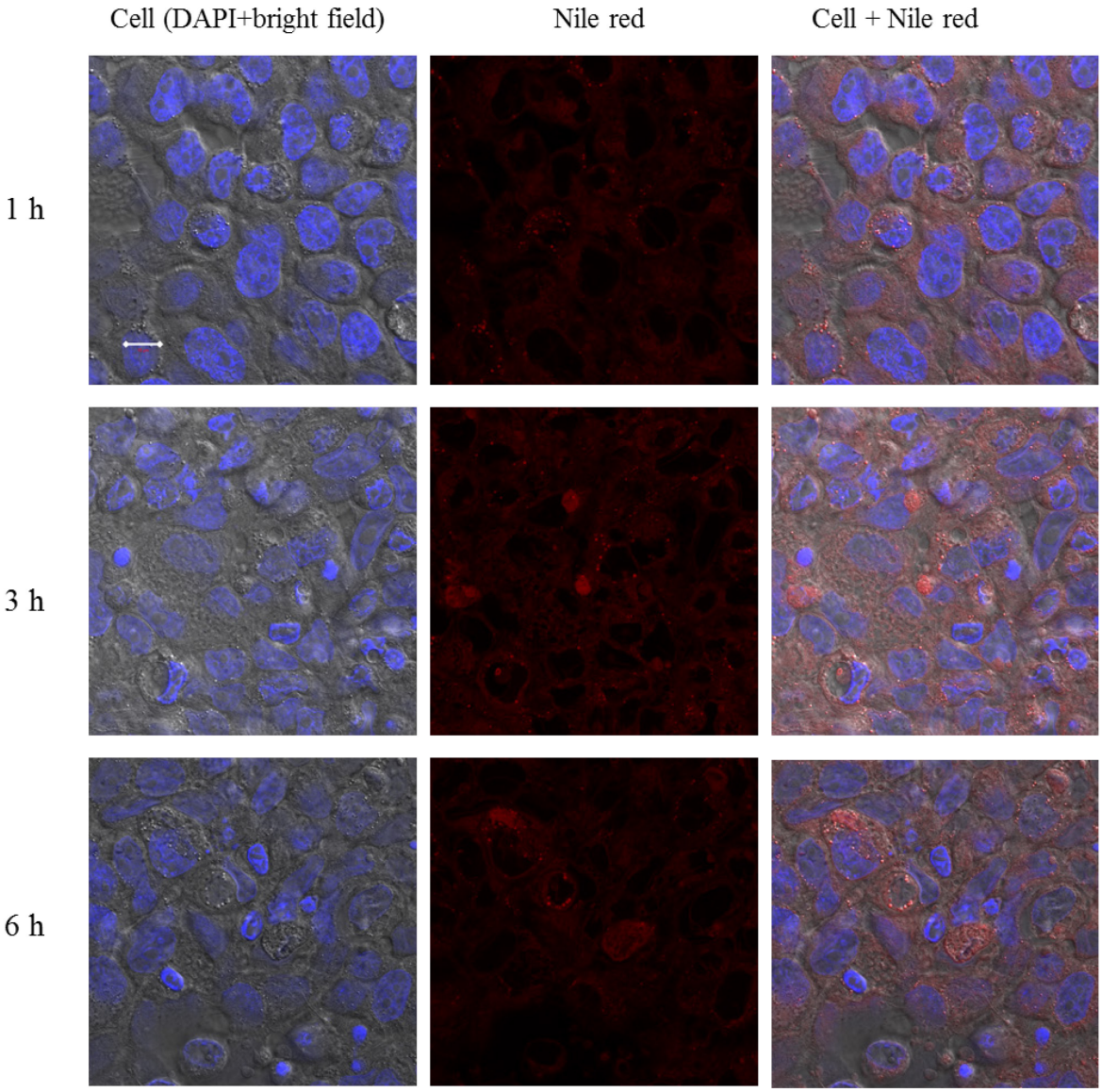

Figure 3.9 Change of fluorescent intensity (Nile red) at 1, 3, and 6 h. Blank: no nanoparticle was added. Scale bar= 10 µm

3.4 Conclusion

This research has demonstrated that the protein-lipid composite nanoparticles with surface succinylation modification had significantly improved stability in physiological buffer. This is due to an increased surface charge and spatial extension of succinate chain on nanoparticle surface. In addition, succinate's crosslinking effect resulted in a stronger coating that maintained the integrity of nanoparticles and minimized VB12 leakage (4.5±0.5%) during a long-term storage experiment of 30 days. The modified nanoparticles resisted a harsh gastric environment and delivered VB12 intact to the small intestine, where they were sustainably released over a reasonable time to promote absorption. An *in vitro* cell evaluation demonstrated the nanoparticles had low cytotoxicity and could internalize into the cytoplasm of Caco-2 cells. Overall, the results of this study show the great potential of modified nanoparticles in increasing the absorption of VB12 upon oral administration.

Chapter 4-*In vitro* and *in vivo* evaluation of protein-lipid composite nanoparticles for oral delivery of vitamin B_{12}

4.1 Introduction

The emergence of nature health products (NHPs) into the market, such as vitamins and phenolic compounds, has provided opportunities to lower the risk of chronic diseases and promote human health [1]. However, the oral bioavailability of many NHPs is low either because of a short residence time in the gastrointestinal tract or low intestinal permeability, both of which have significantly limited their potential health benefits. Vitamin B_{12} (VB12) is one of such examples due to its complex route for absorption [13, 20, 21]. Firstly, VB12 is separated from its food matrix by the acidic environment of the stomach and then it binds to gastric intrinsic factor. This complex then travels to the small intestine and is absorbed by cubilin receptors located in the proximal region of the small intestine. Any disruption in the secretion of gastric acid, digestive enzymes or intrinsic factor, or decreased expression of intestinal receptors can result in VB12 malabsorption and subsequent deficiency. Nowadays, VB12 deficiency has become a world-wide problem [24, 25]. It occurs more frequently in the elderly population (5-20%) [26-28] due to food-cobalamin malabsorption [29]. For these people, particularly with pernicious anemia or neurological disorders, VB12 intramuscular injections are usually required [30].

Nanoparticle based oral delivery systems have the potential to increase the bioavailability of NHPs. This is because nanoparticles are small and therefore have a large surface area-to-volume ratio which favors core ingredient absorption through the intestine [210]; however, there are still several physiological barriers that could diminish this beneficial effect [211]. For example, the harsh gastric environment of low pH and pepsin enzyme can decompose nanoparticles or inactivate

NHPs before they reach the target site. The mucosal layer, a steric barrier in the small intestine, may reduce the interaction between nanoparticles and the intestinal epithelial surface. The physiochemical stability of nanoparticles during storage is another concern. Due to their small size and large surface area, they are more likely to be affected by environmental stressors, like temperature, pH and ionic strength[212-215]. Nanoparticle aggregation and degradation, or premature release of the core ingredients during storage can further reduce the nanoparticles' physiological performance. The careful and deliberate design of the nanoparticles is required to achieve their optimal performance.

In chapter 2, we represented the development of novel protein-lipid composite nanoparticles for hydrophilic NHP delivery, using edible protein and lipids. Nanoparticles had three-layer structure (protein layer, α-tocopherol layer and phospholipid layer) and inner water compartments. This unique structure enables the incorporation of hydrophilic NHPs efficiently (69% for VB12) and can resist the harsh gastric environment to deliver VB12 intact to the small intestine for absorption. Nevertheless, these composite nanoparticles exhibited some shortcomings, such as low solubility in saline buffer, relatively short storage stability and high burst release in the intestinal environment. The performance of these nanoparticles was further improved by modifying their protein outer layer through succinylation (chapter 3), which significantly increased the particle surface charge, hydrodynamic diameter and decreased the surface hydrophobicity. The increased surface charge and spatial extension of succinate chain on nanoparticle surface improved the nanoparticle stability in both physiological buffer and water. The crosslinking by succinate minimized the leakage of VB12 (4.5±0.5 %) during long-term storage. Moreover, succinylation decreased pancreatic digestion of the protein shell because the succinyl-lysyl-peptide bond was resistant to tryptic hydrolysis. This effectively reduced the burst release, leading to a more

sustainable release behavior in the simulated intestinal fluid, with 62.1% vitamin B_{12} released after 10 h of incubation. However, it is still unclear whether these nanoparticles can improve the absorption of VB12. In this chapter, a systemic evaluation of nanoparticles was conducted using *in vitro* and in *vivo* models. The findings provide justification for further research efforts to develop an oral delivery system of VB12 for people who suffer from VB12 malabsorption.

4.2 Material and methods

4.2.1 Material

Whole barley protein (over 85%, w/w) was extracted from regular barley grains (Falcon) by alkaline as previously described [172]. Soy phosphatidylcholine (95%) was purchased from Avanti Polar Lipid (Alabaster, AL, USA). Soy lecithin was from CIRANDA (Hudson, WI, USA). Cell culture reagents including fetal bovine serum (FBS), HEPES solution, Dulbecco's Modified Eagle's Medium (DMEM), nonessential amino acids (NEAA), trypsin-EDTA and Hank's balanced salt solution (HBSS) were purchased from GIBCO (Burlington, ON, Canada). Human colorectal adenocarcinoma cell line Caco-2 was purchased from the American Type Culture Collection (ATCC) (Manassas, VA, USA). Rest of the chemicals were all of reagent grade and from Sigma-Aldrich Canada Ltd (Oakville, ON, Canada).

4.2.2 Nanoparticle preparation and characterization

4.2.2.1 Nanoparticle preparation

The original and modified protein-lipid composite nanoparticles (O-NPs and M-NPs) were prepared according to the established methods in sections 2.2.2 and 3.2.2.

4.2.2.3 Nanoparticle characterization

The size, polydispersity index (PdI), zeta potential of nanoparticles, and encapsulation efficiency (EE) were measured based on the methods described in sections 2.2.3 and 2.2.3.

4.2.3 *In vitro* cell evaluations

Caco-2 cell line (passage 19-30) was used for *in vitro* evaluation. Cells were cultured in DMEM, supplemented with 20% FBS, 1% nonessential amino acids, 1% antibiotic-antimycotic and 25 mM HEPES. Cells were cultured in a humidified atmosphere containing 5% CO_2 at 37°C.

4.2.3.1 Cell uptake study

Cells were seeded onto 6-well plate at a density of 1 x 10^5 cells per dish. Cells were cultured for 5-7 days until full confluency. On the day of experiment, the culture medium was replaced with HBSS (with Ca^{2+}, Mg^{2+}, without phenol red) to equilibrate at 37ºC for 0.5 h. Then HBSS was replaced by 2 mL of VB12 loaded nanoparticle (2 µg/mL VB12) in HBSS suspension. The same amount of free VB12 in 2 mL HBSS was used as control. After 1, 3, 6 h, cells were washed with cold PBS for three times, lysed, sonicated, and centrifuged to pellet the cell debris. The supernatant was collected for VB12 determination. The uptake rate was determined by the equation below.

$$\text{VB12 uptake rate } = \frac{\text{VB12 in cell}}{\text{Total VB12 added in HBSS}} \times 100\%$$

4.2.3.2 Uptake mechanism study

Different uptake pathway inhibitors, chlorpromazine hydrochloride (CPZ), filipin III (FLI) and cytochalasin D (CyD) were used [63]. CPZ and FLI were 5 µg/ml in HBSS, and CyD was 10 µg/ml in HBSS. Cells were incubated with different inhibitors for 30 min. Warm PBS was used to wash cells for three times to remove the inhibitor. VB12 loaded nanoparticle suspension (2 mL) was incubated with cells for 6 h. Changes in uptake rate provide information about the nanoparticle uptake mechanisms.

$$\text{VB12 uptake rate } (\%, \text{normalized}) = \frac{\text{VB12 in cell after inhibitor treatment}}{\text{VB12 in cell without inhibitor treatment}} \times 100\%$$

4.2.4 *Ex vivo* mucoadhesive study

Cadavers of female Sprague Dawley rats (~350 g) were kindly provided by Health Science Lab Animal Service (HSLAS) from University of Alberta. The small intestine was collected within 1 h after euthanization and cleaned with 0.9% saline using the procedure described by Dhawan et al [216]. Intestine was cut into segment of 12 cm and filled with 2 mL of VB12 loaded nanoparticles (5 mg/mL nanoparticle, w/v) in PBS (0.02 mol/L, with 0.85% NaCl, pH=7.2). Nanoparticles in water were used as control. The percentage of nanoparticles adhered to intestine was calculated by the equation below.

$$\text{Adhered nanoparticle} = \frac{\text{VB12 concentration before incubation - VB12 concentration after incubation}}{\text{VB12 concentration before incubation}} \text{ x } 100\%$$

4.2.5 *In vivo* evaluations

All animal studies were executed under the guidelines of the Canadian Council on Animal Care (CCAC) and Animal Care and Use Committee (ACUC) at the University of Alberta. All studies were approved by ACUC (Protocol number: AUP1713). Animals were housed in standard cages and maintained on a 12 h:12 h light-dark cycle in University of Alberta Health Science Lab Animal Service (HSLAS) animal facility. Animals had free access to food and water except otherwise specified.

4.2.5.1 *In vivo* toxicity evaluation

The concentration of nanoparticles was determined using equation (mass (mg) /volume (ml)). Nanoparticle suspension (2 mL) was transferred to a small aluminum tray with known weight using a single channel pipette (1000 µL, Eppendorf Canada). The suspension was dried under a

heat lamp until constant weight was reached. Then the change in the weight of the tray was measured by a digital balance with an accuracy of 0.1 mg for calculation the mass of nanoparticles. The toxicity of the protein-lipid composite nanoparticles was evaluated in Sprague Dawley (SD) rats (strain code 001, Charles river). After seven days of acclimatization, 15 five-week old male rats were randomly divided into three groups (O-NP, M-NP and control groups, n=5/group). Nanoparticles (O-NPs or M-NPs) were pasteurized and dispersed in drinking water. Rats received a daily dose of 200 mg nanoparticles/kg per day (without VB12). In the control group, rats did not receive any treatment. This experiment lasted for 14 days. Body weight gain, food and water intake, and general health were monitored daily. At the 15th day, rats were anesthetized with isoflurane oxygen mix (3.5%) and euthanized by exsanguination under anesthesia. Organ coefficient was determined by the equation below. Heart, liver, spleen, and kidney specimens were fixed in 10% phosphate buffered formalin, embedded in paraffin, cross-sectioned at 5 μm thickness and then stained with hematoxylin and eosin (H&E). Alanine aminotransferase (ALT), aspartate aminotransferase (AST), blood urea nitrogen (BUN), creatinine (Cre) in serum were determined by Sigma assay kits following the standard procedure.

$$\text{Organ coefficient} = \frac{\text{Weight of the respective organ}}{\text{Weight of the individual rat}}$$

4.2.5.2 *In vivo* efficacy evaluation

After 7 days of acclimatization, 15 five-week old male SD rats were fed a VB12 deficient diet (Teklad) that was patterned after the AIN-93M formula with 5% pectin and VB12 omitted [217]. After 10 weeks, animals were randomly divided into three groups (n=5/group): (i) VB12 loaded O-NPs, (ii) VB12 loaded M-NPs, and (iii) VB12 in water. In all groups, the VB12 was 1.25 μg/day and administrated through oral gavage for two weeks. During VB12 treatment, animals still had

the same VB12 deficient diet and free access to water. Food was removed 8 h before oral gavage and given back to animals 1 h after gavage. Blood samples before and after VB12 supplement were collected for VB12 and methylmalonic acid analysis (see section 5.2.6).

4.2.6 Quantitative analysis

4.2.6.1 VB12 determination:

VB12 concentration between 1 μg/mL and 20 μg/mL were measured by high performance liquid chromatography (HPLC, 1200 Series, Agilent Technologies) with diode array detector (G1315D, Agilent Technologies) at 360 nm. Eclipse XDB-C18 column (4.6×150 mm, 5 μm, Agilent Technologies) was used and the elution gradient was water/acetonitrile with 0.1% formic acid at a flow rate of 1 mL/min [151]. VB12 was quantified employing an external calibration.

VB12 concentration between 3 ng/mL and 1 μg/mL were determined by high performance liquid chromatography (HPLC, 1200 Series, Agilent Technologies) and ABI 4000 QTrap mass spectrometer (AB SCIEX). The flow rate was 0.2 mL/min on an Ascentis® Express C18 column (2.1x150 mm, 2.7 μm, SUPELCO). Mobile phase consisted of water (A) and acetonitrile (B) containing 0.1% formic acid. A mixture of A and B (90:10) was run for 2 min, and a gradient phase from 90:10 to 40:60 was eluted for 10 min. Afterward, solvent A and B were brought back to 90 :10 and balanced for 15 min. Ginsenoside Re was used as internal standard [218]. The monitored transitions were m/z 679 → 147 for VB12 [218-220] and 969 → 789 for Ginsenoside Re.

VB12 in serum were determined by Rat Vitamin B12 ELISA Kit (0-2500 pg/mL, MyBioSource, CA, USA). Measurement procedure strictly followed user's manual.

4.2.6.2 Methylmalonic acid (MMA) determination

MMA was determined by high performance liquid chromatography (HPLC, 1200 Series, Agilent Technologies) and fluorescence detector (G1321A, Agilent Technologies) with excitation at 228 nm and emission at 534 nm [221]. Briefly, MMA was extracted from acidified serum with ethylmalonic acid as the internal standard. The extract was dried and derivatized with monodansylcadaverine and dicyclohexylcarbodiimide. The mobile phase consisted of acetonitrile/tetrahydrofuran/water (39/12/49) with 0.25% dibutylamine. The pH of the solution was adjusted to 3 with 20% phosphoric acid. The separation was carried out using eclipse XDB-C18 column (4.6×150 mm, 5 μm, Agilent Technologies) with isocratic elusion at 1 mL/min.

4.2.7 Statistic analysis

Experiments were performed in three independent batches unless otherwise stated. Data were represented as the mean of three batches with standard deviation. Student's *t*-test was used in statistical comparison between two groups. One-way Analysis of Variance (ANOVA) with Tukey's honest significant difference test were used in multiple-comparisons (three or more groups). Statistical differences between samples were performed with a level of significance as $p < 0.05$.

4.3 Result and discussion

4.3.1 Preparation and Characterization of VB12-loaded nanoparticles

The basic information of O-NPs and M-NPs, including size, size distribution, zeta potential and encapsulation efficiency (EE), was summarized in table 4.1 (data from chapter 2 and 3). O-NPs showed a smaller size (243 ± 5 nm) and lower surface charge (-10.2 ± 0.9 mV) than M-NPs (size: 466 ± 15 nm, zeta potential: -19.9 ± 1.1 mV). Both nanoparticles had uniform size distribution (PdI: 0.17±0.03 for O-NPs and 0.18±0.02 for M-NPs). No significant difference in encapsulation efficiency was found between these two nanoparticles.

Table 4.1 Characteristics of VB12-loaded nanoparticles (summarized data from chapter 2 and 3)

Sample	Size (nm)	PdI	Zeta potential (mV)	EE (%)
O-NPs	243 ± 5	0.17±0.03	-10.2±0.9	69 ± 1
M-NPs	466±15	0.18±0.02	-19.9±1.1	71 ± 6

4.3.2 *In vitro* cell evaluation

The intestinal epithelium serves as a barrier to oral NHP delivery, as many NHPs suffer from low intestinal permeability. Nanoparticles may overcome the intestinal barrier because they can transport the encapsulated ingredient across the intestinal epithelium through transcellular or paracellular pathways [222]. Here the potential of nanoparticle to increase the bioavailability of VB12 was investigated using a Caco-2 cell model. Fig. 4.1 shows the uptake rate of VB12 in O-NP group reached 2.8%, 7.2% and 10.9% at 1, 3 and 6 h, respectively. The uptake rate in M-NP

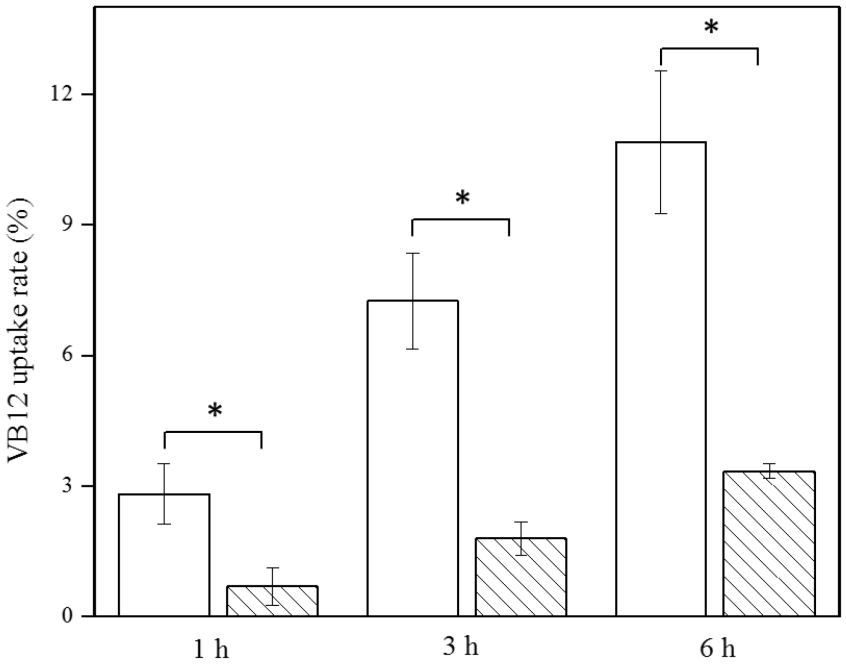

Figure 4.1 uptake efficiency of nanoparticle at different time points. Blank column: O-NPs, Patterned column: M-NPs. "*" shows significance of difference at $p < 0.05$.

group was lower than that in O-NP group, with 0.7%, 1.8%, 3.3% VB12 found at 1, 3, and 6 h. As a general rule, smaller nanoparticles have a greater uptake rate due to their more efficient interfacial interaction with cell membrane [61, 62]. In addition, a lower negative charge generates a weaker electrostatic repulsion with anionic cell membrane, thus increasing the contact between cells and nanoparticles. Succinylation increased both nanoparticle's hydrodynamic diameter and zeta potential, which may explain the reduced cell uptake of M-NPs. However, the uptake rate in both O-NP and M-NP groups were higher than that in the free VB12 group (0.2%) at 6 h ($p<0.05$). The internalization of free VB12 is primarily receptor dependent, so the absence of intrinsic factor in cell culture environment led to very low uptake rate. A large intracellular uptake of VB12 in nanoparticle groups suggested a different endocytosis mechanism. In order to understand the mechanism, three endocytic inhibitors were utilized. CPZ inhibits clathrin mediated endocytosis by preventing clathrin assembly on the cell membrane; CyD inhibits the macropinocytosis by depolymerize actin filaments; FLI inhibits caveolae-mediated transcytosis by depletion of the cholesterol from the cell membrane [223]. When cells were treated with CPZ, the uptake of O-NPs decreased to 14.2%, compared to that of the cells without any pre-treatment with the inhibitors (at 100%). The inhibition effect (63.7% inhibition of uptake) was also observed in CyD treatment, whereas FLI did not show significant inhibition (Fig. 4.2 A). Similarly, for M-NPs, the uptake rate in both CPZ and CyD groups had significant decrease, while that in the FLI group was not affected (Fig. 4.2B). Thus, both macropinocytosis and clathrin-mediated endocytosis were responsible for the internalization of O-NPs and M-NPs. As mentioned previously, the absorption of VB12 is intrinsic factor mediated and a receptor dependent process that occurs only in the distal ileum. However, after encapsulation VB12 absorption is not limited by those factors. It can enter intestinal epithelial cells directly through non-specific endocytosis. This encapsulation technology

provides an alternative pathway for VB12 absorption.

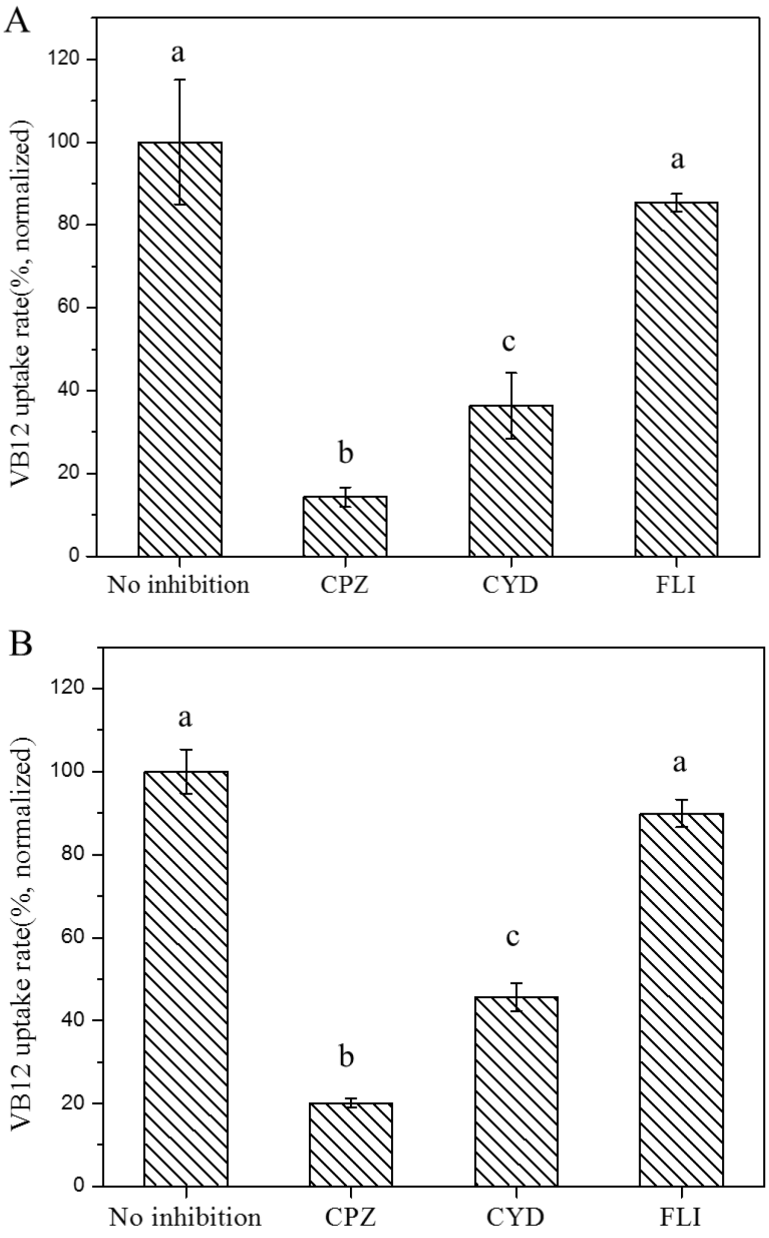

Figure 4.2 endocytosis inhibition effect of different chemicals on VB12 loaded O-NPs (A) and M-NPs (B) at 6 h: chlorpromazine hydrochloride (CPZ), flipin III (FLI) and cytochalasin D (CyD); Different letters (expressed as a, b, c, d) show significance of difference at $p < 0.05$.

4.3.3 Mucoadhesive study.

Mucoadhesion is one of the desired features for an oral delivery system as it prolongs the residence time of encapsulated compounds in the intestine and reduces their diffusion pathway [49]. Polymer based nanoparticles can interact with the mucosa by ionic bonds, hydrogen bonds, hydrophobic bonds, Van-der-Waals bonds and covalent bonds [51]. When the binding force overcomes the repelling force, nanoparticles show mucoadhesiveness. The adhesive capacity of nanoparticles in the small intestine is shown in Fig. 4.3. Nanoparticles suspended in the distilled water show a minimal mucoadhesive capacity (around 10%) because the electrostatic repulsion between the negatively charged nanoparticle surface and the mucosal surface outweighed their attractive interactions in low ionic strength environment. In PBS solution, which represents a physiological buffer, a large adhesion percentage (48.6±5.8%) was found for O-NPs. When the surface charge

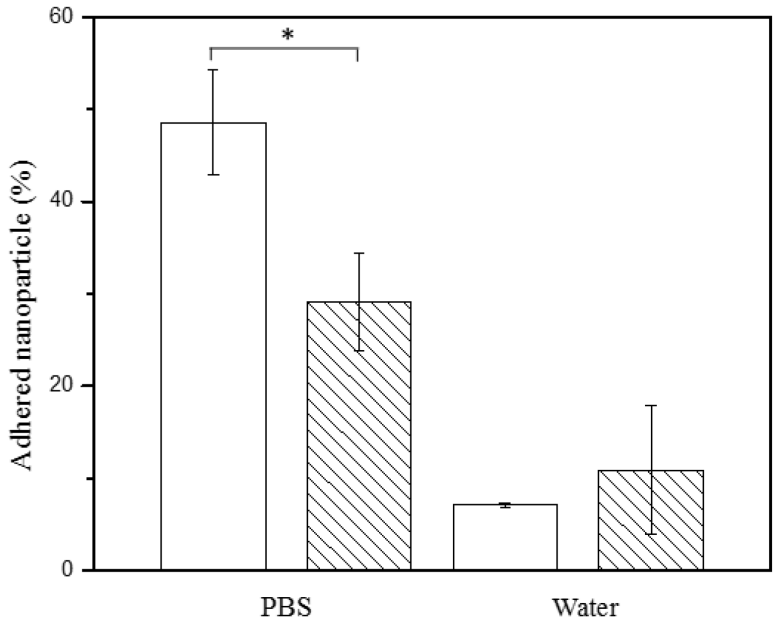

Figure 4.3 Adhesive interaction of nanoparticle with rat small intestine in different media (left: PBS, right: water). Blank column: O-NPs; patterned column: M-NPs. "*" indicates $p < 0.05$.

was suppressed by environmental ionic strength, O-NPs could diffuse into mucus and develop hydrogen bonding and hydrophobic interaction with the network [36]. For M-NPs, a significant increase (29.1±5.2%) in mucoadhesive capacity was also observed in PBS compared to water dispersant, suggesting M-NPs could also prolong the residence time of encapsulated NHPs in the intestine. However, the increase of the mucoadhesive capacity in M-NPs was not as large as that in O-NPs. Possible explanations could be: 1) a stronger electrostatic repulsion introduced by succinate cannot be fully suppressed by the PBS solution; 2) a larger hydrodynamic diameter made the diffusion of nanoparticles into mucus network more difficult.

4.3.4 *In vivo* toxicity

The safety of nanoparticles is very important for their application in food systems, since food is general recognized as safe, and as such does not have the same oversight and regulatory controls as pharmaceutical systems. We have conducted a preliminary toxicity study to investigate whether nanoparticles cause any adverse effects during daily oral administration to rats. The amount of nanoparticles used in toxicity studies can take > 0.5 mg VB12, which is 200 times greater than the recommended daily allowance (2.4 μg/day for adult) [16]. As shown in Table 4.2, the body weight and organ coefficients of rats in O-NP and M-NP groups did not show any difference from untreated control group. To further investigate the toxicity, histological section analysis was

Table 4.2 Organ coefficients and biochemistry results from rats after exposure to 200 mg nanoparticles/kg per day (without VB12) for 14 days. Data represent mean ± S.D. (n=5). ALT: alanine aminotransferase; AST: aspartate aminotransferase; Crea: creatinine; BUN: blood urea nitrogen. No significant difference was observed.

Group	Weight (g)	Heart/BW (mg/g)	Lung/BW (mg/g)	Liver/BW (mg/g)	Spleen/BW (mg/g)	Kidney/BW (mg/g)	ALT (U/L)	AST (U/L)	Crea (μmol/L)	BUN (mmol/L)
O-NPs	433±20	3.62±0.25	4.90±0.97	50.05±6.37	2.03±0.27	9.26±0.93	37.2±4.4	91.1±5.6	36.4±5.4	2.3±0.2
M-NPs	419±23	3.47±0.45	5.14±1.11	49.06±2.72	1.88±0.21	8.82±1.57	37.9±5.4	91.5±9.6	34.4±6.2	2.2±0.2
Control	414±17	3.30±0.34	5.26±0.99	50.31±5.29	2.05±0.40	9.02±0.23	37.0±3.5	99.6±2.8	35.5±4.9	2.1±0.2

conducted, and representative histological specimens are shown in Fig. 4.4. No obvious tissue damage was found in major organs (heart, liver, kidney, spleen). Four biochemical parameters, alanine transaminase (ALT), aspartate transaminase (AST), blood urea nitrogen (BUN) and creatinine (Crea) were assayed to further to evaluate the liver and kidney function. As shown in Table 5.2, there were no obvious changes for serum biochemical parameters in rats after nanoparticle exposure. Overall no adverse effects were found following a 14-day nanoparticle (O-NPs and M-NPs) treatment.

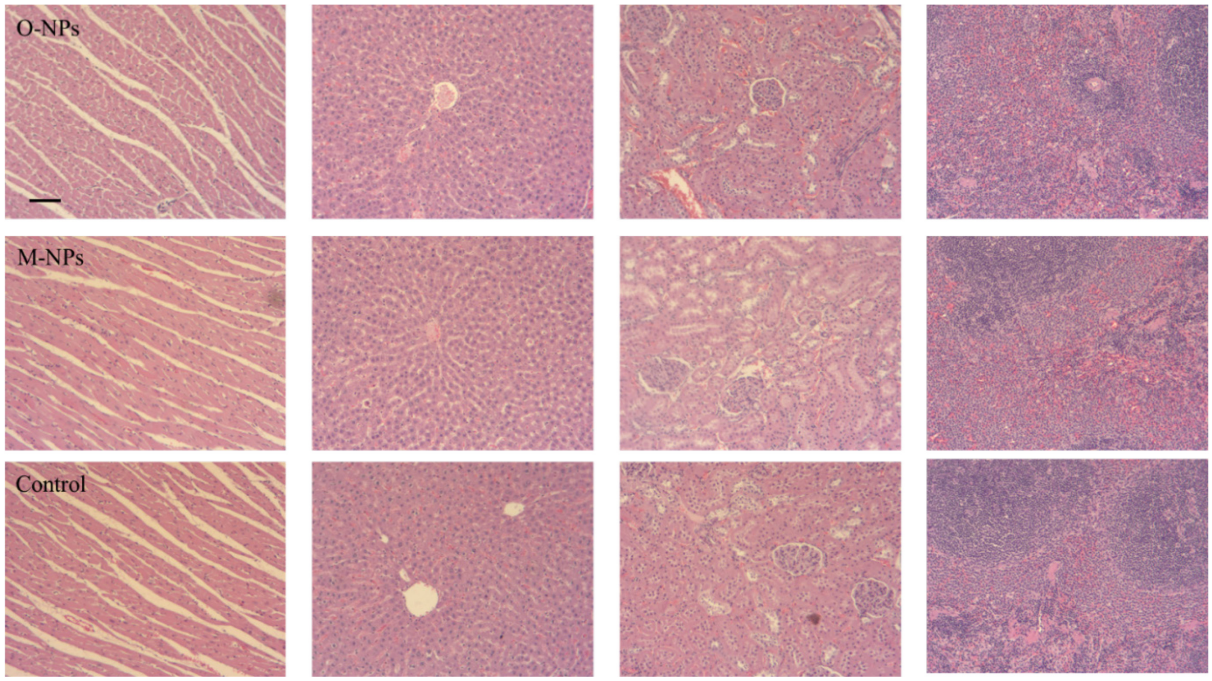

Figure 4.4 The representative histological photomicrographs of the heart, liver, kidney, spleen (from left to right) after exposure to nanoparticles for 14 days (objective: 20x). scale bar: 50 μm

4.3.5 *In vivo* efficacy evaluation

Finally, we tried to understand whether the nanoparticle can enhance the absorption of VB12 at recommended daily allowance level and correct VB12 deficiency *in vivo*. The rat is a model suitable for VB12 absorption study because, similar to human, it also has a intrinsic factor mediated VB12 absorption mechanism [224]. A VB12 deficiency model was developed by

removing VB12 from animal food and adding 5% pectin. Pectin can bind with VB12 and interfere with its normal absorption [217]. This model was intended to mimic the VB12 malabsorption condition in people with gastrointestinal disorder. The serum VB12 level alone is not adequate to evaluate the therapeutic effect, because the clinical and analytical parameters in determining VB12 deficiency is complex [225]. Furthermore, cyanocobalamin, the most common form of oral VB12 supplement, does not have any biological activity. It needs to go through a decynation process and be converted to methyl or adenosyl cobalamin, the two biologically active VB12 forms [226]. The VB12 assay kit is not able to identify the difference among these VB12 analogs, so the VB12 assay cannot reflect the concentration of bioactive VB12. Therefore, the determination of MMA, a metabolite that accumulates when VB12 dependent enzymatic reactions are impaired, was used together with VB12 to better understand the therapeutic effect of our NHP delivery system in rats. A decrease in VB12 and an increase in MMA levels in rat serum at the 10th week confirmed the model was successful (Fig. 4.5). Then 1.25 μg VB12 with and without nanoparticle encapsulation was given to rats through oral gavage. This daily allowance dosage was calculated based on National Research Council (U.S.) recommendation (50 μg/kg VB12 in diet) [227] and 25 g food per day for each animal. After two-week treatment, the serum VB12 level in the O-NP group (602 ± 218 pg/mL) was found significantly greater than that of the free VB12 group (251±103 pg/mL), indicating the O-NPs efficiently improved VB12 absorption (Fig. 4.5A). Meanwhile, a much lower MMA level was found in the O-NP group (5.1±3.1 μmol/L) than in the free VB12 group (15.5±3.8 μmol/L), which further indicated that the O-NPs effectively delivered VB12 in this animal model (Fig. 4.5B).

The M-NP group also had higher serum VB12 level (490 ± 168 pg/mL) than the free VB12 group (251±103 pg/mL), but the difference was not significant (p>0.05, Fig. 4.5A). The insignificance

could be partly explained by the decreased cell uptake rate and mucoadhesive capacity of M-NPs, as well as the pectin in animal diet which kept diminishing the storage of VB12 in rats. In this condition, the MMA level should be used as the major evaluation criteria because it reflects the concentration of bioactive VB12 (methyl or adenosyl cobalamin) that was converted from cyanocobalamin and involved in the metabolism. As shown in Fig. 4.5B, a significantly lower MMA quantity ($p < 0.01$) was found in the M-NP group (4.2±2.4 μmol/L) than in the free VB12 group (15.5±3.8 μmol/L), suggesting the VB12 loaded M-NPs treatment generated a significantly higher amount of bioactive VB12 in rats to proceed the VB12 dependent enzymatic reactions which decreased the MMA level. Therefore, considering the higher VB12 level and significantly lower MMA level in the M-NP group, it could be concluded that VB12 delivered in M-NPs had a greater *in vivo* efficacy than its free form in the rat model.

On the other hand, no significant difference in VB12 and MMA levels was found between M-NPs and O-NPs. Although an increased hydrodynamic size and zeta potential resulted in less cell uptake rate and mucoadhesive capacity, M-NPs showed a slow and sustainable release profile in the simulated intestinal environment (chapter 3), which may facilitate the absorption of VB12 *via* the intrinsic factor dependent route. Moreover, an improved stability in the gastrointestinal environment might allow more M-NPs to be absorbed in the small intestine through non-specific endocytosis, which enhances the absorption of encapsulated VB12 without relying on intrinsic factors. Although it is ideal for a nanoparticle to have superior characteristics of both physiochemical properties (e.g. high encapsulation efficiency, good stability and controlled release) and biological responses (e.g. high cell uptake rate and mucoadhesive property), it is difficult to achieve all optimal parameters. In this study, the protein-lipid composite nanoparticles modified

by succinylation showed a good balance in both physiochemical and biological properties, therefore it also shows promise to be used as a VB12 oral delivery system.

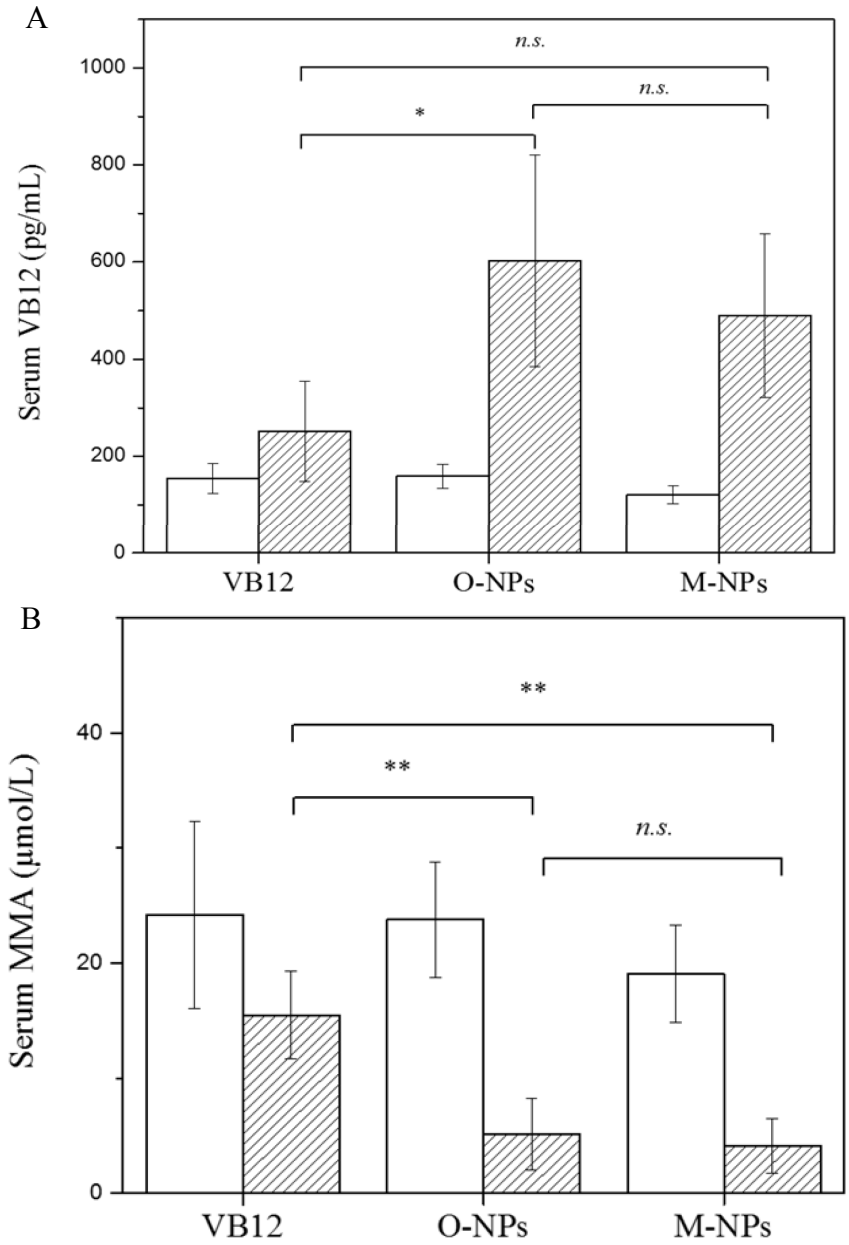

Figure 4.5 Change of serum VB12 (A) and MMA(B) before and after treatment. Blank column: before treatment; Patterned column: after treatment. Data represent mean ± S.D. (n=5). Statistic analysis was performed with one-way ANOVA with Tukey's honest significant difference test. "n.s." indicates the difference is not significant; "*" shows significance of difference at $p< 0.05$; "**" shows significance of difference at $p<0.01$.

4.4 Conclusion

In this chapter, the biological responses of newly developed nanoparticles (O-NPs and M-NPs) were systematically investigated. The nanoparticles could internalize into Caco-2 cells *via* macropinocytosis and clathrin-mediated endocytosis, which increased the uptake rate of VB12 by over 68 folds (O-NPs) and 20 folds (M-NPs). Both nanoparticles demonstrated good mucoadhesive capacity in the physiological buffer solution (48.6% for O-NPs and 29.1% for M-NPs). Animals receiving nanoparticles for 14 days showed no signs of toxicity. Furthermore, both O-NPs and M-NPs were shown to correct a VB12 deficiency state more efficiently than free VB12 supplementation using a VB12 deficiency rat model. Overall, this encapsulation technology shows promise to benefit people who suffer from VB12 malabsorption.

Chapter 5-Conclusion and recommendations

5.1 Summary and conclusion

Food protein and lipid based nanoparticles have attracted recent interest as a means of delivering nature health products (NHPs). Nanoparticle encapsulation of NHPs faces challenges to overcome for it to be readily applied in the food industry, such as low encapsulation efficiency for hydrophilic compounds and poor stability once in the gastrointestinal tract. This research introduced a new protein-lipid composite nanoparticle with three-layer structure (a barely protein layer, α-tocopherol layer and phospholipid layer) and an inner aqueous compartment to load hydrophilic NHPs (e.g. vitamin B_{12}). The barley protein layer served as a "scaffold" to which the α-tocopherol and phospholipid layers were attached. The phospholipid and α-tocopherol layers stabilized the inner aqueous compartment and separated it from the outer water phase, creating greater encapsulation efficiency for the contained hydrophilic compounds (69% for vitamin B_{12}). In addition, nanoparticle could resist a simulated low pH, pepsin gastric environment and release NHPs in the intestine in a controlled manner.

In spite of many advantages, the protein-lipid composite nanoparticle still faced challenges, such as low solubility in saline buffer, relatively short storage stability and high burst release in the intestinal environment. Protein succinylation was then applied to tackle these problems. Succinylation of nanoparticle was primarily achieved by modifying ε-amino acids with succinate. The formation of ester bonds between hydroxyl group and succinate might also be involved in the succinylation. Such modification decreased nanoparticle surface hydrophobicity (from 6733 to 4385) and amino group content (from 87.2 to 10.6 μmol/g nanoparticle), and increased nanoparticle surface charge (from -10.2 to -19.9 mV, pH=7) and hydrodynamic diameter (from 243 to 466 nm). The increased surface charge and decreased surface hydrophobicity resulted in

enhanced nanoparticle solubility in the physiological buffer. The increased surface charge and crosslinking effect of succinate improved the storage stability of nanoparticles. During 30-day storage, the leakage of vitamin B_{12} from modified nanoparticles was 4.3%, which was over 10 folds lower than that of original nanoparticles (55.3%). *In vitro* release study showed succinylation could keep the release behavior in simulated gastric environment unchanged, while largely reduced the initial burst release of vitamin B_{12} in simulated intestinal environment (from 49.6% to 22.5%) due to the resistance of succinyl-lysyl-peptide bond to tryptic hydrolysis. In this study, succinylation was proved an effective way to improve the physiochemical stability of protein-lipid composite nanoparticles.

Both original and modified nanoparticles underwent *in vitro* evaluations using Caco-2 cells. *In vitro* toxicity study showed that cells reached high viability (over 90%) when nanoparticle concentration was at around 0.1 mg/mL. Confocal microscope study found that nanoparticles primarily accumulated in the cytoplasm but not nucleus of Caco-2 cells. After 6 h incubation, the uptake efficiency of vitamin B_{12} were 10.9% and 3.3% in the original and modified nanoparticle groups, respectively, which were much higher than that in the free vitamin B_{12} group (0.16%). Uptake mechanism study revealed that both original and modified nanoparticles could internalize into Caco-2 cells *via* macropinocytosis and clathrin-mediated endocytosis, which was the major reason for the increased vitamin B_{12} uptake efficiency. Modified nanoparticles had lower cell uptake efficiency than original nanoparticles because of their larger hydrodynamic diameter and surface charge. Larger nanoparticles had less efficient interfacial interaction with cell membrane and higher negative charge generated stronger electrostatic repulsion with anionic cell membrane.

In an *ex vivo* mucoadhesive study using small intestine from Sprague-Dawley rats, both nanoparticles showed good mucoadhesive capacity (48.6% for original nanoparticle and 29.1%

for modified nanoparticle). The lower mucoadhesive capacity in modified nanoparticles can also be explained by increased hydrodynamic size and surface charge.

A 14-day *in vivo* toxicity study was conducted to investigate whether nanoparticles could cause any adverse effects. In experiment groups, Sprague-Dawley rats received oral exposure of original or modified nanoparticle at 200 mg nanoparticle/kg body weight per day (without vitamin B_{12}) for 14 days. In the control group, rats did not receive any treatment. Body weight, organ mass, organ histology, and biochemical parameters (alanine transaminase, aspartate transaminase, blood urea nitrogen and creatinine) were examined. No notable change was found in original and modified nanoparticle groups, comparing with the control group.

The *in vivo* efficacy was also evaluated using Sprague-Dawley rats. The vitamin B_{12} deficiency models were developed by treating rats with vitamin B_{12} free food supplemented with 5% pectin for 10 weeks. Then vitamin B_{12} with and without nanoparticle encapsulation was given to rats through oral gavage. After two-week treatment, rats had their serum vitamin B_{12} levels increased to 602 ± 218 pg/mL and 490 ± 168 pg/mL in the original and modified nanoparticle groups, respectively, which were higher than that in the free vitamin B_{12} group (251±103 pg/mL). Meanwhile, much lower MMA levels were found in the original and modified nanoparticle groups (5.1±3.1 μmol/L and 4.2±2.4 μmol/L, respectively) than the free vitamin B_{12} group (15.5±3.8 μmol/L). This could be primarily attributed to the nanoparticle encapsulation which provide alternative pathway (macropinocytosis and clathrin-mediated endocytosis) for vitamin B_{12} absorption *in vivo*. Overall, the results of the whole study show the great potential of developed nanoparticles in increasing the absorption of vitamin B_{12} upon oral administration.

5.2 Significance of research

1) This research represents novel protein-lipid composite nanoparticles for hydrophilic NHPs delivery. Nanoparticles have three-layer structure (protein layer, α-tocopherol layer and phospholipid layer) and inner water compartments. This unique structure overcomes the shortcomings of double/multiple emulsion and liposome based delivery systems (e.g. unstable during storage and leaky in gastric environment). And the existence of inner water compartment allows nanoparticles to load hydrophilic NHPs more efficiently than nature polymer (protein/polysaccharide) based delivery systems because no attractive interaction is required between the NHP and carrier. The developed nanoparticle could serve as a basic platform for the delivery of many different hydrophilic NHPs.

2) This study demonstrated that after encapsulation, vitamin B_{12} could actively internalize into enterocytes without relying on the intrinsic factor-cubilin based active transport. *In vivo* efficacy study also showed that vitamin B_{12} loaded nanoparticles could correct vitamin B_{12} deficiency in a rat model more efficiently than the free form. These results suggested that nanoparticles provided an alternative route for efficient vitamin B_{12} oral absorption, which could potentially benefit people suffering from vitamin B_{12} malabsorption and prevent the occurrence of disease related to vitamin B_{12} deficiency.

3) Although succinylation has been used to improve protein's functionality in food research, information regarding the impact of succinylation on the biological responses of protein based nanoparticles is limited. This research generated new knowledge regarding *in vitro* release behavior, cell uptake efficiency and mucoadhesive capacity in relation to the change of nanoparticle structural parameters caused by succinylation. The outcome of this study facilitates

the development and modulation of protein based nanoparticles with optimized biological performance.

4) Canada is one of the largest barley producers in the world and Alberta produces around 50% of barley in Canada. In 2017, the barley production in Alberta is 4.68 million tones (7.89 million tones in Canada). However, more barley was used for feed and forage (48.4%) than food (1.3%). This may be partly because the utilization of barley is still not fully explored. This work presents a value-added product of barley protein which will commercially benefit Alberta barley farmers.

5.3 Limitations of current work

5.3.1 Organic solvent used in the protein-lipid composite nanoparticles preparation

Chloroform and diethyl ether are good solvents for phospholipids and have been widely used in liposome preparation [228]. In this research, these two solvents were selected to dissolve phospholipids and make the inner organic phase during nanoparticle preparation. However, the residuals in nanoparticles may cause certain adverse effect after long-term oral administration.

5.3.2 The effects of bile salts on the release behavior of nanoparticles

Bile salts can unfold the protein molecules [229] and compete with proteins at the oil/water interface [230], thus can potentially destabilize the nanoparticles in the gastrointestinal environment. In the *in vitro* release study, the impacts of pH and digestive enzymes on nanoparticle degradation and release properties were systematically investigated based on the methods from the United States Pharmacopeia (USP). As USP does not recommend adding bile salts in the simulated intestinal environment, the nanoparticle release property was not studied in the presence of bile acid, however, their effects should not be ignored.

5.3.3 Caco-2 cell model for *in vitro* evaluation

Caco-2 cells have been widely used to evaluate NHP absorption because their morphology and functionality are similar to those of the enterocytes. However, they still represent several limitations [231]. For example, the research model based on Caco-2 cells contains only one cell type, while normal small intestinal epithelium has several cell types. Also, Caco-2 cells do not produce mucus. The absent of protective mucus layer on cell surface might lead to higher cellular uptake rate of nanoparticles.

Furthermore, incorporating intrinsic factor in cell study has allowed us to better evaluate the *in vitro* uptake rate of free vitamin B_{12}. But it is not the best option to conduct this study using Caco-2 cells. It was found that the intrinsic factor mediated vitamin B_{12} uptake/transport was not efficient in Caco-2 cells, as they only expressed very few intrinsic factor receptors according to previous study [232]. These receptors were saturated at very low vitamin B_{12}-intrinsic factor concentration (6 nM) and it took 24 h to reach the maximum uptake efficiency [232]. Moreover, high variation was observed between cell passages in the uptake and transport study of vitamin B_{12}-intrnsic factor by Caco-2 cells, which might lead to biased experiment result [233].

5.3.4 Degree of succinylation

Succinylation on barley protein layer improved the nanoparticle stability and allowed more sustainable vitamin B_{12} release in the simulated intestinal environment. However, the nanoparticle cellular uptake and mucoadhesive capacities were decreased due to the surface succinylation. The optimal degree of protein succinylation is yet to be established to balance the *in vitro* release behavior and biological responses.

5.4 Future direction

5.4.1 Formula optimization and further nanoparticle development for delivery of other water-soluble NHPs

Chloroform and diethyl ether are not favorable in food applications, thus in formula improvement, more efforts are required to find alternative solvents that have better biocompatibility. Research is also required to optimize the nanoparticle succinylation degree to achieve improved overall properties. Also, the impact of bile salts on the nanoparticle release properties should be addressed in future study. Furthermore, it is worthy of investigation where the vitamin B_{12} was located in the nanoparticles. Vitamin B_{12} could be loaded in the water compartment as proposed in the research, or entrapped within the lipid layers of the nanoparticles. Identifying the vitamin B_{12} location will help formula optimization and the incorporation of vitamin B_{12} in the water compartment can reduce its leakage during storage. There are opportunities to expand the nanoparticle applications for many other water-soluble NHPs (e.g. quercetin, anthocyanins and catechin) which also suffer from low intestinal permeability [80].

5.4.2 In-depth *in vivo* test.

Although *in vivo* study has proved that the protein-lipid composite nanoparticles could improve vitamin B_{12} absorption, more in-depth research is still required to understand the nanoparticle behavior *in vivo*. For example, it will be interesting to feed animal with fluorescent dye labeled nanoparticles and conduct histological examination to understand where the nanoparticles are accumulated, how they are metabolized, and what is the final destination. Some microorganisms residing in the small intestine [234] are potential vitamin suppliers (including vitamin B_{12}) to their host [235]. Protein and lipids play a key role in shaping microbial ecology in gut [236], therefore the oral administration of the protein-lipid composite nanoparticles might change the

microorganism composition and affect vitamin B_{12} production. Further investigation will be required to elucidate the possible effects.

A vitamin B_{12} deficiency model was built in this research; however, the animals can still secrete the intrinsic factor and the normal vitamin B_{12} absorption pathway was not fully blocked. Such an animal model cannot perfectly mimic the condition in patients with vitamin B_{12} malabsorption. It is suggested that genetically modified rats that cannot produce intrinsic factor can be further used to study the nanoparticle *in vivo* efficacy.

Although no toxic effect was found in the short-term toxicity evaluation in this study, the effect of long-term administration of nanoparticles is unknown. Therefore, a long-term toxicity study is recommended to better understand the nanoparticles safety to support their food applications [237].

5.4.3 Application development in food area

The protein-lipid composite nanoparticles have been successfully prepared at the lab scale. Pilot study in the next step will allow us to understand if it is feasible to scale up the technique towards food applications. Meanwhile, the impact of food processing (e.g. thermal processing, freezing, dehydration) on the nanoparticle integrity and the NHP stability should be investigated.

In addition, food prototypes (e.g. yogurt, milk, beverage) incorporating the encapsulated NHPs should be developed and the quality (e.g. shelf-life, flavor) of the final products should be evaluated. A cost-benefit analysis should also be conducted to understand whether the profit of these nanoparticles outweighs their cost. Finally, it is important to understand the advantages of the developed protein-lipid composite nanoparticles compared to the commercial products, such as vitamin B_{12} nasal spray, to better estimate their commercialization potential.

Reference:

[1] Natural and Non-prescription Health Products Directorate. Health canada, https://www.Canada.Ca/en/health-canada/services/drugs-health-products/natural-non-prescription.Html.

[2] Flynn E. Pharmacokinetic parameters. Xpharm: The comprehensive pharmacology reference. New York: Elsevier; 2007. p. 1-3.

[3] McClements DJ, Li F, Xiao H. The nutraceutical bioavailability classification scheme: Classifying nutraceuticals according to factors limiting their oral bioavailability. Annual Review of Food Science and Technology. 2015;6:299-327.

[4] Bank G, Kagan D, Madhavi D. Coenzyme q10: Clinical update and bioavailability. Journal of Evidence-Based Complementary & Alternative Medicine. 2011;16:129-37.

[5] Carlson DA, Smith AR, Fischer SJ, Young KL, Packer L. The plasma pharmacokinetics of r-(+)-lipoic acid administered as sodium r-(+)-lipoate to healthy human subjects. Alternative Medicine Review. 2007;12:343.

[6] Pangeni R, Sahni JK, Ali J, Sharma S, Baboota S. Resveratrol: Review on therapeutic potential and recent advances in drug delivery. Expert Opinion on Drug Delivery. 2014;11:1285-98.

[7] Groschwitz KR, Hogan SP. Intestinal barrier function: Molecular regulation and disease pathogenesis. The Journal of allergy and clinical immunology. 2009;124:3-22.

[8] Yang C, Wang Y, Lu L, Unsworth L, Guan LL, Chen L. Oat protein-shellac beads: Superior protection and delivery carriers for sensitive bioactive compounds. Food Hydrocolloids. 2018;77:754-63.

[9] Kenmogne-Domguia HB, Moisan S, Viau M, Genot C, Meynier A. The initial characteristics of marine oil emulsions and the composition of the media inflect lipid oxidation during in vitro gastrointestinal digestion. Food Chemistry. 2014;152:146-54.

[10] Tam YK. Individual variation in first-pass metabolism. Clinical Pharmacokinetics. 1993;25:300-28.

[11] Zhang JH, Li L, Jiang C, Xing CG, Kim SH, Lu JX. Anti-cancer and other bioactivities of korean angelica gigas nakai (agn) and its major pyranocoumarin compounds. Anti-Cancer Agents in Medicinal Chemistry. 2012;12:1239-54.

[12] Zhang J, Li L, Hale TW, Chee W, Xing C, Jiang C, et al. Single oral dose pharmacokinetics of decursin and decursinol angelate in healthy adult men and women. PLoS ONE. 2015;10:e0114992.

[13] Gherasim C, Lofgren M, Banerjee R. Navigating the b12 road: Assimilation, delivery, and disorders of cobalamin. Journal of Biological Chemistry. 2013;288:13186-93.

[14] Martens JH, Barg H, Warren M, Jahn D. Microbial production of vitamin b12. Applied Microbiology and Biotechnology. 2002;58:275-85.

[15] Kumudha A, Kumar SS, Thakur MS, Ravishankar GA, Sarada R. Purification, identification, and characterization of methylcobalamin from spirulina platensis. Journal of Agricultural and Food Chemistry. 2010;58:9925-30.

[16] Institute of Medicine (US). Dietary reference intakes for thiamin, riboflavin, niacin, vitamin b6, folate, vitamin b12, pantothenic acid, biotin, and choline. Washington, DC: The National Academies Press; 1998.

[17] Watanabe F. Vitamin b12 sources and bioavailability. Experimental Biology and Medicine. 2007;232:1266-74.

[18] Degnan PH, Taga ME, Goodman AL. Vitamin b12 as a modulator of gut microbial ecology. Cell Metabolism. 2014;20:769-78.

[19] Allen RH, Stabler SP. Identification and quantitation of cobalamin and cobalamin analogues in human feces. The American Journal of Clinical Nutrition. 2008;87:1324-35.

[20] Alpers DH, Russell-Jones G. Gastric intrinsic factor: The gastric and small intestinal stages of cobalamin absorption. A personal journey. Biochimie. 2013;95:989-94.

[21] Kozyraki R, Cases O. Vitamin b12 absorption: Mammalian physiology and acquired and inherited disorders. Biochimie. 2013;95:1002-7.

[22] Adkins Y, Lönnerdal B. Mechanisms of vitamin b12 absorption in breast-fed infants. Journal of Pediatric Gastroenterology and Nutrition. 2002;35:192-8.

[23] Baik HW, Russell RM. Vitamin b12 deficiency in the elderly. Annual Review of Nutrition. 1999;19:357-77.

[24] Allen LH. How common is vitamin b-12 deficiency? The American Journal of Clinical Nutrition. 2009;89:693S-6S.

[25] Erin M, Benoist B, Lindsay HA. Review of the magnitude of folate and vitamin b12 deficiencies worldwide. Food and Nutrition Bulletin. 2008;29:S38-S51.

[26] Clarke R, Grimley Evans J, Schneede J, Nexo E, Bates C, Fletcher A, et al. Vitamin b12 and folate deficiency in later life. Age and Ageing. 2004;33:34-41.

[27] Clarke R, Sherliker P, Hin H, Nexo E, Hvas AM, Schneede J, et al. Detection of vitamin b12 deficiency in older people by measuring vitamin b12 or the active fraction of vitamin b12, holotranscobalamin. Clinical Chemistry. 2007;53:963-70.

[28] MacFarlane AJ, Greene-Finestone LS, Shi Y. Vitamin b-12 and homocysteine status in a folate-replete population: Results from the canadian health measures survey. The American Journal of Clinical Nutrition. 2011;94:1079-87.

[29] Andrès E, Loukili NH, Noel E, Kaltenbach G, Abdelgheni MB, Perrin AE, et al. Vitamin b12 (cobalamin) deficiency in elderly patients. Canadian Medical Association Journal. 2004;171:251-9.

[30] Hernandez CMR, Oo TH. Advances in mechanisms, diagnosis, and treatment of pernicious anemia. Discovery Medicine. 2015;19:159-68.

[31] Quay SC, Aprile PC, Go ZO, Sileno AP. Cyanocobalamin low viscosity aqueous formulations for intranasal delivery. Google Patents; 2016.

[32] Asselt DZB, Merkus FWHM, Russel FGM, Hoefnagels WHL. Nasal absorption of hydroxocobalamin in healthy elderly adults. British Journal of Clinical Pharmacology. 1998;45:83-6.

[33] Graham ID, Jette N, Tetroe J, Robinson N, Milne S, Mitchell SL. Oral cobalamin remains medicine's best kept secret. Archives of Gerontology and Geriatrics. 2007;44:49-59.

[34] Harde H, Das M, Jain S. Solid lipid nanoparticles: An oral bioavailability enhancer vehicle. Expert Opinion on Drug Delivery. 2011;8:1407-24.

[35] Chen L, Remondetto GE, Subirade M. Food protein-based materials as nutraceutical delivery systems. Trends in Food Science & Technology. 2006;17:272-83.

[36] Arangoa MA, Ponchel G, Orecchioni AM, Renedo MJ, Duchêne D, Irache JM. Bioadhesive potential of gliadin nanoparticulate systems. European Journal of Pharmaceutical Sciences. 2000;11:333-41.

[37] Arbós P, Arangoa MA, Campanero MA, Irache JM. Quantification of the bioadhesive properties of protein-coated pvm/ma nanoparticles. International Journal of Pharmaceutics. 2002;242:129-36.

[38] Rieux A, Fievez V, Garinot M, Schneider YJ, Préat V. Nanoparticles as potential oral delivery systems of proteins and vaccines: A mechanistic approach. Journal of Controlled Release. 2006;116:1-27.

[39] Lee J. Nanoparticle-assisted controlled drug release. Journal of Nanomedicine & Biotherapeutic Discovery. 2014; 4(2): e133.

[40] Ummadi S, Shravani B, Rao NG, Reddy MS, Nayak BS. Overview on controlled release dosage form. 2013; 3: 258-69.

[41] Ritger PL, Peppas NA. A simple equation for description of solute release i. Fickian and non-fickian release from non-swellable devices in the form of slabs, spheres, cylinders or discs. Journal of Controlled Release. 1987;5: 23-36.

[42] Panyam J, Dali MM, Sahoo SK, Ma W, Chakravarthi SS, Amidon GL, et al. Polymer degradation and in vitro release of a model protein from poly(d,l-lactide-co-glycolide) nano- and microparticles. Journal of Controlled Release. 2003;92:173-87.

[43] Panakanti P. Atorvastatin loaded solidlipid nanoparticles: Formulation, optimization, and in vitro characterization. 2012; 2: 23-32.

[44] Li Z, Ha J, Zou T, Gu L. Fabrication of coated bovine serum albumin (bsa)-epigallocatechin gallate (egcg) nanoparticles and their transport across monolayers of human intestinal epithelial caco-2 cells. Food & Function. 2014;5:1278-85.

[45] Yang J, Zhou Y, Chen L. Elaboration and characterization of barley protein nanoparticles as an oral delivery system for lipophilic bioactive compounds. Food & Function. 2014;5:92-101.

[46] Penalva R, Esparza I, Agüeros M, Gonzalez-Navarro CJ, Gonzalez-Ferrero C, Irache JM. Casein nanoparticles as carriers for the oral delivery of folic acid. Food Hydrocolloids. 2015;44:399-406.

[47] Kageyama H, Ueda H, Tezuka T, Ogasawara A, Narita Y, Kageyama T, et al. Differences in the p1′ substrate specificities of pepsin a and chymosin. The Journal of Biochemistry. 2010;147:167-74.

[48] Rawlings ND, Salvesen G. Handbook of proteolytic enzymes. Third Edition ed. London: Academic Press; 2013.

[49] Neves J, Bahia MF, Amiji MM, Sarmento B. Mucoadhesive nanomedicines: Characterization and modulation of mucoadhesion at the nanoscale. Expert Opinion on Drug Delivery. 2011;8:1085-104.

[50] Cone RA. Barrier properties of mucus. Advanced Drug Delivery Reviews. 2009;61:75-85.

[51] Smart JD. The basics and underlying mechanisms of mucoadhesion. Advanced Drug Delivery Reviews. 2005;57:1556-68.

[52] Elzoghby AO, Elgohary MM, Kamel NM. Chapter six - implications of protein- and peptide-based nanoparticles as potential vehicles for anticancer drugs. In: Donev R, editor. Advances in protein chemistry and structural biology: Academic Press; 2015. p. 169-221.

[53] Goldstein IJ, Hughes RC, Monsigny M, Osawa T, Sharon N. What should be called a lectin? Nature. 1980;285:66.

[54] Xiang S, Tong H, Shi Q, Fernandes JC, Jin T, Dai K, et al. Uptake mechanisms of non-viral gene delivery. Journal of Controlled Release. 2012;158:371-8.

[55] McMahon HT, Boucrot E. Molecular mechanism and physiological functions of clathrin-mediated endocytosis. Nature Reviews Molecular Cell Biology. 2011;12:517.

[56] Rejman J, Oberle V, Zuhorn IS, Hoekstra D. Size-dependent internalization of particles via the pathways of clathrin- and caveolae-mediated endocytosis. Biochemical Journal. 2004;377:159-69.

[57] Ma Z, Lim LY. Uptake of chitosan and associated insulin in caco-2 cell monolayers: A comparison between chitosan molecules and chitosan nanoparticles. Pharmaceutical Research. 2003;20:1812-9.

[58] Kiss AL, Botos E. Endocytosis via caveolae: Alternative pathway with distinct cellular compartments to avoid lysosomal degradation? Journal of Cellular and Molecular Medicine. 2009;13:1228-37.

[59] Conner SD, Schmid SL. Regulated portals of entry into the cell. Nature. 2003;422:37-44.

[60] Lim JP, Gleeson PA. Macropinocytosis: An endocytic pathway for internalising large gulps. Immunology And Cell Biology. 2011;89:836.

[61] Yin WK, Feng SS. Effects of particle size and surface coating on cellular uptake of polymeric nanoparticles for oral delivery of anticancer drugs. Biomaterials. 2005;26:2713-22.

[62] Desai MP, Labhasetwar V, Walter E, Levy RJ, Amidon GL. The mechanism of uptake of biodegradable microparticles in caco-2 cells is size dependent. Pharmaceutical Research. 1997;14:1568-73.

[63] Zhang J, Field C, Vine D, Chen L. Intestinal uptake and transport of vitamin b12-loaded soy protein nanoparticles. Pharmaceutical Research. 2014;32:1288–303.

[64] He C, Hu Y, Yin L, Tang C, Yin C. Effects of particle size and surface charge on cellular uptake and biodistribution of polymeric nanoparticles. Biomaterials. 2010;31:3657-66.

[65] Arvizo RR, Miranda OR, Thompson MA, Pabelick CM, Bhattacharya R, Robertson JD, et al. Effect of nanoparticle surface charge at the plasma membrane and beyond. Nano Letters. 2010;10:2543-8.

[66] Banerjee A, Qi J, Gogoi R, Wong J, Mitragotri S. Role of nanoparticle size, shape and surface chemistry in oral drug delivery. Journal of Controlled Release. 2016; 238: 176-85.

[67] Kulkarni SA, Feng SS. Effects of particle size and surface modification on cellular uptake and biodistribution of polymeric nanoparticles for drug delivery. Pharmaceutical Research. 2013;30:2512-22.

[68] Hauck TS, Ghazani AA, Chan WC. Assessing the effect of surface chemistry on gold nanorod uptake, toxicity, and gene expression in mammalian cells. Small. 2008;4:153-9.

[69] Huang X, Teng X, Chen D, Tang F, He J. The effect of the shape of mesoporous silica nanoparticles on cellular uptake and cell function. Biomaterials. 2010;31:438-48.

[70] Chithrani BD, Ghazani AA, Chan WC. Determining the size and shape dependence of gold nanoparticle uptake into mammalian cells. Nano Letters. 2006;6:662-8.

[71] Rougerie P, Miskolci V, Cox D. Generation of membrane structures during phagocytosis and chemotaxis of macrophages: Role and regulation of the actin cytoskeleton. Immunological reviews. 2013;256: 222-39.

[72] Van Kruiningen HJ, West AB, Freda BJ, Holmes KA. Distribution of peyer's patches in the distal ileum. 2002; 8: 180-5.

[73] Snapper CM. Distinct immunologic properties of soluble versus particulate antigens. Frontiers in Immunology. 2018;9:598.

[74] Aramaki Y, Tomizawa H, Hara T, Yachi K, Kikuchi H, Tsuchiya S. Stability of liposomes in vitro and their uptake by rat peyer's patches following oral administration. Pharmaceutical Research. 1993;10:1228-31.

[75] Weber CR. Dynamic properties of the tight junction barrier. Annals of the New York Academy of Sciences. 2012;1257:77-84.

[76] Wang X, Wang N, Yuan L, Li N, Wang J, Yang X. Exploring tight junction alteration using double fluorescent probe combination of lanthanide complex with gold nanoclusters. Scientific Reports. 2016;6:32218.

[77] Bernkop-Schnürch A, Kast CE, Guggi D. Permeation enhancing polymers in oral delivery of hydrophilic macromolecules: Thiomer/gsh systems. Journal of Controlled Release. 2003;93:95-103.

[78] Dave VS, Gupta D, Yu M, Nguyen P, Varghese Gupta S. Current and evolving approaches for improving the oral permeability of bcs class iii or analogous molecules. Drug Development and Industrial Pharmacy. 2017;43:177-89.

[79] Park K. The controlled drug delivery systems: Past forward and future back. Journal of controlled release : official journal of the Controlled Release Society. 2014;190:3-8.

[80] Aditya NP, Espinosa YG, Norton IT. Encapsulation systems for the delivery of hydrophilic nutraceuticals: Food application. Biotechnology Advances. 2017;35:450-7.

[81] Li X, Qi J, Xie Y, Zhang X, Hu S, Xu Y, et al. Nanoemulsions coated with alginate/chitosan as oral insulin delivery systems: Preparation, characterization, and hypoglycemic effect in rats. International Journal of Nanomedicine. 2013;8:23-32.

[82] Matalanis A, Jones OG, McClements DJ. Structured biopolymer-based delivery systems for encapsulation, protection, and release of lipophilic compounds. Food Hydrocolloids. 2011;25:1865-80.

[83] Torchilin VP. Recent advances with liposomes as pharmaceutical carriers. Nature Reviews Drug Discovery. 2005;4:145-60.

[84] Patel Z, Patel S, Patel B, Pardeshi C. Nose to brain targeted drug delivery bypassing the blood-brain barrier: An overview. 2012; 4: 610-5.

[85] Yi J, Lam TI, Yokoyama W, Cheng LW, Zhong F. Beta-carotene encapsulated in food protein nanoparticles reduces peroxyl radical oxidation in caco-2 cells. Food Hydrocolloids. 2015;43:31-40.

[86] Zimet P, Rosenberg D, Livney YD. Re-assembled casein micelles and casein nanoparticles as nano-vehicles for ω-3 polyunsaturated fatty acids. Food Hydrocolloids. 2011;25:1270-6.

[87] Abbasi A, Emam-Djomeh Z, Mousavi MAE, Davoodi D. Stability of vitamin d3 encapsulated in nanoparticles of whey protein isolate. Food Chemistry. 2014;143:379-83.

[88] McClements DJ. Protein-stabilized emulsions. Current Opinion in Colloid & Interface Science. 2004;9:305-13.

[89] Wilde P, Mackie A, Husband F, Gunning P, Morris V. Proteins and emulsifiers at liquid interfaces. Advances in Colloid and Interface Science. 2004;108–109:63-71.

[90] Hoare TR, Kohane DS. Hydrogels in drug delivery: Progress and challenges. Polymer. 2008;49:1993-2007.

[91] Joye IJ, McClements DJ. Production of nanoparticles by anti-solvent precipitation for use in food systems. Trends in Food Science & Technology. 2013;34:109-23.

[92] Xu H, Jiang Q, Reddy N, Yang Y. Hollow nanoparticles from zein for potential medical applications. Journal of Materials Chemistry. 2011;21:18227-35.

[93] Shutava TG, Balkundi SS, Vangala P, Steffan JJ, Bigelow RL, Cardelli JA, et al. Layer-by-layer-coated gelatin nanoparticles as a vehicle for delivery of natural polyphenols. ACS Nano. 2009;3:1877-85.

[94] Gan Z, Zhang T, Liu Y, Wu D. Temperature-triggered enzyme immobilization and release based on cross-linked gelatin nanoparticles. PLoS ONE. 2012;7:e47154.

[95] Yoo HS, Choi HK, Park TG. Protein–fatty acid complex for enhanced loading and stability within biodegradable nanoparticles. Journal of Pharmaceutical Sciences. 2001;90:194-201.

[96] Yang C, Wang Y, Chen L. Fabrication, characterization and controlled release properties of oat protein gels with percolating structure induced by cold gelation. Food Hydrocolloids. 2017;62:21-34.

[97] Zhang J, Liang L, Tian Z, Chen L, Subirade M. Preparation and in vitro evaluation of calcium-induced soy protein isolate nanoparticles and their formation mechanism study. Food Chemistry. 2012;133:390-9.

[98] Shpigelman A, Cohen Y, Livney YD. Thermally-induced β-lactoglobulin–egcg nanovehicles: Loading, stability, sensory and digestive-release study. Food Hydrocolloids. 2012;29:57-67.

[99] Gupta AK, Gupta M, Yarwood SJ, Curtis ASG. Effect of cellular uptake of gelatin nanoparticles on adhesion, morphology and cytoskeleton organisation of human fibroblasts. Journal of Controlled Release. 2004;95:197-207.

[100] Yang L, Cui F, Cun D, Tao A, Shi K, Lin W. Preparation, characterization and biodistribution of the lactone form of 10-hydroxycamptothecin (hcpt)-loaded bovine serum albumin (bsa) nanoparticles. International Journal of Pharmaceutics. 2007;340:163-72.

[101] Sadeghi S, Madadlou A, Yarmand M. Microemulsification–cold gelation of whey proteins for nanoencapsulation of date palm pit extract. Food Hydrocolloids. 2014;35:590-6.

[102] Wu Y, MacKay JA, R. McDaniel J, Chilkoti A, Clark RL. Fabrication of elastin-like polypeptide nanoparticles for drug delivery by electrospraying. Biomacromolecules. 2009;10:19-24.

[103] Gulfam M, Kim JE, Lee JM, Ku B, Chung BH, Chung BG. Anticancer drug-loaded gliadin nanoparticles induce apoptosis in breast cancer cells. Langmuir. 2012;28:8216-23.

[104] Lee SH, Heng D, Ng WK, Chan HK, Tan RBH. Nano spray drying: A novel method for preparing protein nanoparticles for protein therapy. International Journal of Pharmaceutics. 2011;403:192-200.

[105] Elzoghby AO, Samy WM, Elgindy NA. Novel spray-dried genipin-crosslinked casein nanoparticles for prolonged release of alfuzosin hydrochloride. Pharmaceutical Research. 2013;30:512-22.

[106] Weiss J, Kanjanapongkul K, Wongsasulak S, Yoovidhya T. Electrospun fibers: Fabrication, functionalities and potential food industry applications. Nanotechnology in the Food, Beverage and Nutraceutical Industries. 2012; 13: 362-97.

[107] Fu TJ, Abbott UR, Hatzos C. Digestibility of food allergens and nonallergenic proteins in simulated gastric fluid and simulated intestinal fluida comparative study. Journal of Agricultural and Food Chemistry. 2002;50:7154-60.

[108] Elzoghby AO, Samy WM, Elgindy NA. Protein-based nanocarriers as promising drug and gene delivery systems. Journal of Controlled Release. 2012;161:38-49.

[109] Bangham AD, Standish MM, Watkins JC. Diffusion of univalent ions across the lamellae of swollen phospholipids. Journal of Molecular Biology. 1965;13:238-52.

[110] Zhou W, Liu W, Zou L, Liu W, Liu C, Liang R, et al. Storage stability and skin permeation of vitamin c liposomes improved by pectin coating. Colloids and Surfaces B: Biointerfaces. 2014;117:330-7.

[111] Batzri S, Korn ED. Single bilayer liposomes prepared without sonication. Biochimica et Biophysica Acta (BBA) - Biomembranes. 1973;298:1015-9.

[112] Fan MH, Xu SY, Xia SQ, Zhang XM. Preparation of salidroside nano-liposomes by ethanol injection method and in vitro release study. European Food Research and Technology. 2008;227:167-74.

[113] Szoka F, Papahadjopoulos D. Procedure for preparation of liposomes with large internal aqueous space and high capture by reverse-phase evaporation. Proceedings of the National Academy of Sciences. 1978;75:4194-8.

[114] Xia S, Xu S. Ferrous sulfate liposomes: Preparation, stability and application in fluid milk. Food Research International. 2005;38:289-96.

[115] Emami S, Azadmard-Damirchi S, Peighambardoust SH, Valizadeh H, Hesari J. Liposomes as carrier vehicles for functional compounds in food sector. Journal of Experimental Nanoscience. 2016;11:737-59.

[116] Eloy JO, Claro de Souza M, Petrilli R, Barcellos JPA, Lee RJ, Marchetti JM. Liposomes as carriers of hydrophilic small molecule drugs: Strategies to enhance encapsulation and delivery. Colloids and Surfaces B: Biointerfaces. 2014;123:345-63.

[117] Chapman D, Williams RM, Ladbrooke BD. Physical studies of phospholipids. Vi. Thermotropic and lyotropic mesomorphism of some 1,2-diacyl-phosphatidylcholines (lecithins). Chemistry and Physics of Lipids. 1967;1:445-75.

[118] Richards MH, Gardner CR. Effects of bile salts on the structural integrity of liposomes. Biochimica et Biophysica Acta (BBA) - General Subjects. 1978;543:508-22.

[119] Liu W, Ye A, Liu W, Liu C, Han J, Singh H. Behaviour of liposomes loaded with bovine serum albumin during in vitro digestion. Food Chemistry. 2015;175:16-24.

[120] Lowe PJ, Coleman R. Membrane fluidity and bile salt damage. Biochimica et Biophysica Acta (BBA) - Biomembranes. 1981;640:55-65.

[121] Rowland RN, Woodley JF. The stability of liposomes in vitro to ph, bile salts and pancreatic lipase. Biochimica et Biophysica Acta (BBA) - Lipids and Lipid Metabolism. 1980;620:400-9.

[122] Giroux HJ, Constantineau S, Fustier P, Champagne CP, St-Gelais D, Lacroix M, et al. Cheese fortification using water-in-oil-in-water double emulsions as carrier for water soluble nutrients. International Dairy Journal. 2013;29:107-14.

[123] Pimentel-González DJ, Campos-Montiel RG, Lobato-Calleros C, Pedroza-Islas R, Vernon-Carter EJ. Encapsulation of lactobacillus rhamnosus in double emulsions formulated with sweet whey as emulsifier and survival in simulated gastrointestinal conditions. Food Research International. 2009;42:292-7.

[124] Aditya NP, Aditya S, Yang HJ, Kim HW, Park SO, Ko S. Co-delivery of hydrophobic curcumin and hydrophilic catechin by a water-in-oil-in-water double emulsion. 2015; 173: 7-13.

[125] Benichou A, Aserin A, Garti N. Double emulsions stabilized with hybrids of natural polymers for entrapment and slow release of active matters. Advances in Colloid and Interface Science. 2004;108-109:29-41.

[126] Wen J, Zhang Q, Zhu D, Zhang W. Performance study on particle size variables for nano multiple emulsions. Journal of Dispersion Science and Technology. 2017;38:801-6.

[127] Muschiolik G, Dickinson E. Double emulsions relevant to food systems: Preparation, stability, and applications. Comprehensive Reviews in Food Science and Food Safety. 2017;16:532-55.

[128] Ding S, Anton N, Akram S, Er-Rafik M, Anton H, Klymchenko A, et al. A new method for the formulation of double nanoemulsions. Soft Matter. 2017;13:1660-9.

[129] Hanson JA, Chang CB, Graves SM, Li Z, Mason TG, Deming TJ. Nanoscale double emulsions stabilized by single-component block copolypeptides. Nature. 2008;455:85.

[130] Müller RH, Mäder K, Gohla S. Solid lipid nanoparticles (sln) for controlled drug delivery – a review of the state of the art. European Journal of Pharmaceutics and Biopharmaceutics. 2000;50:161-77.

[131] Müller RH, Radtke M, Wissing SA. Solid lipid nanoparticles (sln) and nanostructured lipid carriers (nlc) in cosmetic and dermatological preparations. Advanced Drug Delivery Reviews. 2002;54:S131-S55.

[132] Müller RH, Radtke M, Wissing SA. Nanostructured lipid matrices for improved microencapsulation of drugs. International Journal of Pharmaceutics. 2002;242:121-8.

[133] Das S, Chaudhury A. Recent advances in lipid nanoparticle formulations with solid matrix for oral drug delivery. AAPS PharmSciTech. 2011;12:62-76.

[134] Almeida AJ, Runge S, Müller RH. Peptide-loaded solid lipid nanoparticles (sln): Influence of production parameters. International Journal of Pharmaceutics. 1997;149:255-65.

[135] Saloň I, Hanuš J, Ulbrich P, Štěpánek F. Suspension stability and diffusion properties of yeast glucan microparticles. Food and Bioproducts Processing. 2016;99:128-35.

[136] Casadei MA, Cesa S, Pacelli S, Paolicelli P, Tita B, Vitali F. Dextran-based hydrogel microspheres obtained in w/o emulsion: Preparation, characterisation and in vivo studies. Journal of Microencapsulation. 2014;31:440-7.

[137] Yu YL, Zhang MJ, Xie R, Ju XJ, Wang JY, Pi SW, et al. Thermo-responsive monodisperse core–shell microspheres with pnipam core and biocompatible porous ethyl cellulose shell embedded with pnipam gates. Journal of Colloid and Interface Science. 2012;376:97-106.

[138] Sarti F, Iqbal J, Müller C, Shahnaz G, Rahmat D, Bernkop-Schnürch A. Poly(acrylic acid)–cysteine for oral vitamin b12 delivery. Analytical Biochemistry. 2012;420:13-9.

[139] Abubakr N, Lin SX, Chen XD. Effects of drying methods on the release kinetics of vitamin b12 in calcium alginate beads. Drying Technology. 2009;27:1258-65.

[140] Matsumoto A, Kitazawa T, Murata J, Horikiri Y, Yamahara H. A novel preparation method for plga microspheres using non-halogenated solvents. Journal of Controlled Release. 2008;129:223-7.

[141] Demir S, Ogan A, Kayaman-Apohan N. Intrinsic factor and vitamin b12 complex-loaded poly[lactic-co-(glycolic acid)] microspheres: Preparation, characterization and drug release. Polymer International. 2008;57:372-7.

[142] Sohier J, Dijkhuizen-Radersma R, Groot K, Bezemer JM. Release of small water-soluble drugs from multiblock copolymer microspheres: A feasibility study. European Journal of Pharmaceutics and Biopharmaceutics. 2003;55:221-8.

[143] Muschiolik G, Scherze I, Preissler P, Weiß J, Knoth A, Fechner A. Multiple emulsions - preparation and stability. 13th World Congress of Food Science & Technology. IUFOST 2006: 123-37.

[144] Kukizaki M, Goto M. Preparation and evaluation of uniformly sized solid lipid microcapsules using membrane emulsification. Colloids and Surfaces A: Physicochemical and Engineering Aspects. 2007;293:87-94.

[145] O'Regan J, Mulvihill DM. Sodium caseinate–maltodextrin conjugate stabilized double emulsions: Encapsulation and stability. Food Research International. 2010;43:224-31.

[146] Regan JO, Mulvihill DM. Water soluble inner aqueous phase markers as indicators of the encapsulation properties of water-in-oil-in-water emulsions stabilized with sodium caseinate. Food Hydrocolloids. 2009;23:2339-45.

[147] Fechner A, Knoth A, Scherze I, Muschiolik G. Stability and release properties of double-emulsions stabilised by caseinate–dextran conjugates. Food Hydrocolloids. 2007;21:943-52.

[148] Matos M, Gutiérrez G, Iglesias O, Coca J, Pazos C. Enhancing encapsulation efficiency of food-grade double emulsions containing resveratrol or vitamin b12 by membrane emulsification. Journal of Food Engineering. 2015;166:212-20.

[149] Amsden B, Misra G, Marshall M, Turner N. Synthesis and characterization of biodegradable networks providing saturated-solution prolonged delivery. Journal of Pharmaceutical Sciences. 2008;97:860-74.

[150] Sharifpoor S, Amsden B. In vitro release of a water-soluble agent from low viscosity biodegradable, injectable oligomers. European Journal of Pharmaceutics and Biopharmaceutics. 2007;65:336-45.

[151] Sarti F, Müller C, Iqbal J, Perera G, Laffleur F, Bernkop-Schnürch A. Development and in vivo evaluation of an oral vitamin b12 delivery system. European Journal of Pharmaceutics and Biopharmaceutics. 2013;84:132-7.

[152] Guo B, Gong Q, Wang J, Huang Y, Zhuang D, Liang J. Fabrication of uniform porous cnts/activated carbon composite spheres by oil-drop method in stratified oils and their adsorption of vb12. RSC Advances. 2015;5:46997-7003.

[153] Imshennik VK, Suzdalev IP, Stavinskaya ON, Shklovskaya NI, Schünemann V, Trautwein AX, et al. Preparation and characterization of porous carbon loaded with iron particles: A possible magnetic carrier of medical drugs. Microporous Materials. 1997;10:225-30.

[154] Chen H, Wang B, Gao D, Guan M, Zheng L, Ouyang H, et al. Broad-spectrum antibacterial activity of carbon nanotubes to human gut bacteria. Small. 2013;9:2735-46.

[155] Wang Y, Chen Z, Ba T, Pu J, Chen T, Song Y, et al. Susceptibility of young and adult rats to the oral toxicity of titanium dioxide nanoparticles. Small. 2013;9:1742-52.

[156] Araújo F, Shrestha N, Granja PL, Hirvonen J, Santos HA, Sarmento B. Safety and toxicity concerns of orally delivered nanoparticles as drug carriers. Expert Opinion on Drug Metabolism & Toxicology. 2015;11:381-93.

[157] Zhang J, Tian Z, Liang L, Subirade M, Chen L. Binding interactions of β-conglycinin and glycinin with vitamin b12. The Journal of Physical Chemistry B. 2013;117:14018-28.

[158] Othayoth R, Mathi P, Bheemanapally K, Kakarla L, Botlagunta M. Characterization of vitamin–cisplatin-loaded chitosan nano-particles for chemoprevention and cancer fatigue. Journal of Microencapsulation. 2015;32:578-88.

[159] Britto D, Moura MR, Aouada FA, Pinola FG, Lundstedt LM, Assis OBG, et al. Entrapment characteristics of hydrosoluble vitamins loaded into chitosan and n,n,n-trimethyl chitosan nanoparticles. Macromolecular Research. 2014;22:1261-7.

[160] Britto D, Moura MR, Aouada FA, Mattoso LHC, Assis OBG. N,n,n-trimethyl chitosan nanoparticles as a vitamin carrier system. Food Hydrocolloids. 2012;27:487-93.

[161] Bochicchio S, Barba AA, Grassi G, Lamberti G. Vitamin delivery: Carriers based on nanoliposomes produced via ultrasonic irradiation. LWT - Food Science and Technology. 2016;69:9-16.

[162] Jung SH, Cho YS, Jun SS, Koo JS, Cheon HG, Shin BC. Topical application of liposomal cobalamin hydrogel for atopic dermatitis therapy. Pharmazie. 2011; 66: 430-5.

[163] Ohsawa T, Miura H, Harada K. Improvement of encapsulation efficiency of water-soluble drugs in liposomes formed by the freeze-thawing method. Chemical & Pharmaceutical Bulletin. 1985;33:3945-52.

[164] Costa AP, Xu X, Burgess DJ. Freeze-anneal-thaw cycling of unilamellar liposomes: Effect on encapsulation efficiency. Pharmaceutical Research. 2014;31:97-103.

[165] Genç L, Kutlu HM, Güney G. Vitamin b12-loaded solid lipid nanoparticles as a drug carrier in cancer therapy. Pharmaceutical Development and Technology. 2015;20:337-44.

[166] Yang J, Huang J, Zeng H, Chen L. Surface pressure affects b-hordein network formation at the air–water interface in relation to gastric digestibility. Colloids and Surfaces B: Biointerfaces. 2015;135:784-92.

[167] Wang R, Tian Z, Chen L. A novel process for microencapsulation of fish oil with barley protein. Food Research International. 2011;44:2735-41.

[168] Wang R, Tian Z, Chen L. Nano-encapsulations liberated from barley protein microparticles for oral delivery of bioactive compounds. International Journal of Pharmaceutics. 2011;406:153-62.

[169] Chanput W, Theerakulkait C, Nakai S. Antioxidative properties of partially purified barley hordein, rice bran protein fractions and their hydrolysates. Journal of Cereal Science. 2009;49:422-8.

[170] Kawase SI, Matsumura Y, Murakami H, Mori T. Comparison of antioxidative activity among three types of prolamin subunits. Journal of Cereal Science. 1998;28:33-41.

[171] Simpson DJ. Proteolytic degradation of cereal prolamins—the problem with proline. Plant Science. 2001;161:825-38.

[172] Wang C, Tian Z, Chen L, Temelli F, Liu H, Wang Y. Functionality of barley proteins extracted and fractionated by alkaline and alcohol methods. Cereal Chemistry Journal. 2010;87:597-606.

[173] Parmentier J, Becker MMM, Heintz U, Fricker G. Stability of liposomes containing bio-enhancers and tetraether lipids in simulated gastro-intestinal fluids. International Journal of Pharmaceutics. 2011;405:210-7.

[174] Merrill AL, Watt BK. Energy value of foods: Basis and derivation. Washington DC: Agricultural Research Service, United States Department of Agriculture; 1973.

[175] Zhang LP, Li KX. Fine processing technologies of live stock by-product (in chinese). China Light Industry Press; 2009.

[176] DuBois M, Gilles KA, Hamilton JK, Rebers PA, Smith F. Colorimetric method for determination of sugars and related substances. Analytical Chemistry. 1956;28:350-6.

[177] Cui F, Shi K, Zhang L, Tao A, Kawashima Y. Biodegradable nanoparticles loaded with insulin–phospholipid complex for oral delivery: Preparation, in vitro characterization and in vivo evaluation. Journal of Controlled Release. 2006;114:242-50.

[178] Liu DZ, Chen WY, Tasi LM, Yang SP. Microcalorimetric and shear studies on the effects of cholesterol on the physical stability of lipid vesicles. Colloids and Surfaces A: Physicochemical and Engineering Aspects. 2000;172:57-67.

[179] Quinn PJ. The effect of tocopherol on the structure and permeability of phosphatidylcholine liposomes. Journal of Controlled Release. 2012;160:158-63.

[180] Ganapathy V, Ganapathy ME, Leibach FH. Protein digestion and assimilation. In: Yamada T, editor. Textbook of gastroenterology. Hoboken: Blackwell Publishing Ltd; 2009. p. 464-77.

[181] Appel W. Chymotrypsin: Molecular and catalytic properties. Clinical Biochemistry. 1986;19:317-22.

[182] Qi JC, Chen JX, Wang JM, Wu FB, Cao LP, Zhang GP. Protein and hordein fraction content in barley seeds as affected by sowing date and their relations to malting quality. Journal of Zhejiang University Science B. 2005;6:1069-75.

[183] Olsen JV, Ong SE, Mann M. Trypsin cleaves exclusively c-terminal to arginine and lysine residues. Molecular & Cellular Proteomics. 2004;3:608-14.

[184] Hillaireau H, Couvreur P. Nanocarriers' entry into the cell: Relevance to drug delivery. Cellular and Molecular Life Sciences. 2009;66:2873-96.

[185] Greenspan P, Mayer EP, Fowler SD. Nile red: A selective fluorescent stain for intracellular lipid droplets. The Journal of Cell Biology. 1985;100:965-73.

[186] Allen LH. Bioavailability of vitamin b12. International Journal for Vitamin and Nutrition Research. 2010;80:330-5.

[187] Feeney RE, Whitaker JR. Modification of proteins. In: Feeney RE, Whitaker JR, editors. Food proteins. Washington, DC: American Chemical Society; 1982. p. 420.

[188] Li L, Qiao P, Yang J, Lu L, Tan S, Lu H, et al. Maleic anhydride-modified chicken ovalbumin as an effective and inexpensive anti-hiv microbicide candidate for prevention of hiv sexual transmission. Retrovirology. 2010;7:37.

[189] Thompson LU, Reyes ES. Modification of heat coagulated whey protein concentrates by succinylation. Journal of Dairy Science. 1980;63:715-21.

[190] Franzen KL, Kinsella JE. Functional properties of succinylated and acetylated soy protein. Journal of Agricultural and Food Chemistry. 1976;24:788-95.

[191] El-Adawy TA. Functional properties and nutritional quality of acetylated and succinylated mung bean protein isolate. Food Chemistry. 2000;70:83-91.

[192] Mirmoghtadaie L, Kadivar M, Shahedi M. Effects of succinylation and deamidation on functional properties of oat protein isolate. Food Chemistry. 2009;114:127-31.

[193] Matoba T, Doi E. In vitro digestibility of succinylated protein by pepsin and pancreatic proteases. Journal of Food Science. 1979;44:537-9.

[194] Siu M, Thompson LU. In vitro and in vivo digestibilities of succinylated cheese whey protein concentrates. Journal of Agricultural and Food Chemistry. 1982;30:743-7.

[195] Satake K, Okuyama T, Ohashi M, Shinoda T. The spectrophotometric determination of amine, amino acid and peptide with 2, 4, 6-trinitrobenzene 1-sulfonic acid. The Journal of Biochemistry. 1960;47:654-60.

[196] Sashidhar RB, Capoor AK, Ramana D. Quantitation of ϵ-amino group using amino acids as reference standards by trinitrobenzene sulfonic acid: A simple spectrophotometric method for the estimation of hapten to carrier protein ratio. Journal of Immunological Methods. 1994;167:121-7.

[197] Kato A, Nakai S. Hydrophobicity determined by a fluorescence probe method and its correlation with surface properties of proteins. Biochimica et Biophysica Acta. 1980;624:13-20.

[198] Almutawah A, Barker SA, Belton PS. Hydration of gluten: A dielectric, calorimetric, and fourier transform infrared study. Biomacromolecules. 2007;8:1601-6.

[199] Ullah A, Vasanthan T, Bressler D, Elias AL, Wu J. Bioplastics from feather quill. Biomacromolecules. 2011;12:3826-32.

[200] Zhao CB, Zhang H, Xu X-Y, Cao Y, Zheng M-Z, Liu J-S, et al. Effect of acetylation and succinylation on physicochemical properties and structural characteristics of oat protein isolate. Process Biochemistry. 2017;57:117-23.

[201] Suzuki M, Shimanouchi T. Infrared and raman spectra of succinic acid crystal. Journal of Molecular Spectroscopy. 1968;28:394-410.

[202] Xiang Z, Runge T. Emulsifying properties of succinylated arabinoxylan-protein gum produced from corn ethanol residuals. Food Hydrocolloids. 2016;52:423-30.

[203] Silverstein RM, Webster FX, Kiemle DJ, Bryce DL. Spectrometric identification of organic compounds: John wiley & sons; 2014.

[204] Qi G, Li N, Wang D, Sun XS. Physicochemical properties of soy protein adhesives modified by 2-octen-1-ylsuccinic anhydride. Industrial Crops and Products. 2013;46:165-72.

[205] Yin SW, Tang CH, Wen QB, Yang XQ, Yuan DB. The relationships between physicochemical properties and conformational features of succinylated and acetylated kidney bean (phaseolus vulgaris l.) protein isolates. Food Research International. 2010;43:730-8.

[206] Pons T, Uyeda HT, Medintz IL, Mattoussi H. Hydrodynamic dimensions, electrophoretic mobility, and stability of hydrophilic quantum dots. The Journal of Physical Chemistry B. 2006;110:20308-16.

[207] Selling G, Sessa DJ. Multivalent carboxylic acids to modify the properties of zein. Industrial Crops and Products. 2007;25:63-9.

[208] Khalil AA, Deraz SF, Elrahman SA, El-Fawal G. Enhancement of mechanical properties, microstructure, and antimicrobial activities of zein films cross-linked using succinic anhydride, eugenol, and citric acid. Preparative Biochemistry and Biotechnology. 2015;45:551-67.

[209] Xu H, Shen L, Xu L, Yang Y. Controlled delivery of hollow corn protein nanoparticles via non-toxic crosslinking: In vivo and drug loading study. Biomedical Microdevices. 2015;17:8.

[210] Desai PP, Date AA, Patravale VB. Overcoming poor oral bioavailability using nanoparticle formulations – opportunities and limitations. Drug Discovery Today: Technologies. 2012;9:e87-e95.

[211] Date AA, Hanes J, Ensign LM. Nanoparticles for oral delivery: Design, evaluation and state-of-the-art. Journal of Controlled Release. 2016;240:504-26.

[212] Guzey D, McClements DJ. Impact of electrostatic interactions on formation and stability of emulsions containing oil droplets coated by β-lactoglobulin−pectin complexes. Journal of Agricultural and Food Chemistry. 2007;55:475-85.

[213] Zhao J, Xiang J, Wei T, Yuan F, Gao Y. Influence of environmental stresses on the physicochemical stability of orange oil bilayer emulsions coated by lactoferrin–soybean soluble polysaccharides and lactoferrin–beet pectin. Food Research International. 2014;66:216-27.

[214] Tokle T, Lesmes U, McClements DJ. Impact of electrostatic deposition of anionic polysaccharides on the stability of oil droplets coated by lactoferrin. Journal of Agricultural and Food Chemistry. 2010;58:9825-32.

[215] Xiang J, Liu F, Fan R, Gao Y. Physicochemical stability of citral emulsions stabilized by milk proteins (lactoferrin, α-lactalbumin, β-lactoglobulin) and beet pectin. Colloids and Surfaces A: Physicochemical and Engineering Aspects. 2015;487:104-12.

[216] Dhawan S, Singla AK, Sinha VR. Evaluation of mucoadhesive properties of chitosan microspheres prepared by different methods. AAPS PharmSciTech. 2004;5:122-8.

[217] Cullen RW, Oace SM. Methylmalonic acid and vitamin b12 excretion of rats consuming diets varying in cellulose and pectin. The Journal of Nutrition. 1978;108:640-7.

[218] Luo X, Chen B, Ding L, Tang F, Yao S. Hplc-esi-ms analysis of vitamin b12 in food products and in multivitamins-multimineral tablets. Analytica Chimica Acta. 2006;562:185-9.

[219] Zironi E, Gazzotti T, Barbarossa A, Devicienti C, Scardilli M, Pagliuca G. Technical note: Development and validation of a method using ultra performance liquid chromatography coupled with tandem mass spectrometry for determination of vitamin b12 concentrations in milk and dairy products. Journal of Dairy Science. 2013;96:2832-6.

[220] Szterk A, Roszko M, Małek K, Czerwonka M, Waszkiewicz-Robak B. Application of the spe reversed phase hplc/ms technique to determine vitamin b12 bio-active forms in beef. Meat Science. 2012;91:408-13.

[221] Babidge PJ, Babidge WJ. Determination of methylmalonic acid by high-performance liquid chromatography. Analytical Biochemistry. 1994;216:424-6.

[222] Berardi A, Bisharat L. Nanotechnology systems for oral drug delivery: Challenges and opportunities. In: Massadeh S, editor. Nanotechnology in drug delivery. Cheshire: One Central Press; 2014. p. 53-74.

[223] Ivanov AI. Pharmacological inhibition of endocytic pathways: Is it specific enough to be useful? In: Ivanov AI, editor. Exocytosis and endocytosis. Totowa, NJ: Humana Press; 2008. p. 15-33.

[224] Smith ADM, Ellis H. Absorption of vitamin b12 in the rat. The Lancet. 1965;286:1277-8.

[225] Allen RH, Stabler SP, Savage DG, Lindenbaum J. Diagnosis of cobalamin deficiency i: Usefulness of serum methylmalonic acid and total homocysteine concentrations. American Journal of Hematology. 1990;34:90-8.

[226] Kim J, Gherasim C, Banerjee R. Decyanation of vitamin b12 by a trafficking chaperone. Proceedings of the National Academy of Sciences. 2008;105:14551-4.

[227] National Research Council (U. S. A.). Nutrient requirements of laboratory animals, fourth revised edition, 1995. Washington, DC: The National Academies Press; 1995.

[228] Akbarzadeh A, Rezaei-Sadabady R, Davaran S, Joo SW, Zarghami N, Hanifehpour Y, et al. Liposome: Classification, preparation, and applications. Nanoscale Research Letters. 2013;8:102.

[229] Cremers CM, Knoefler D, Vitvitsky V, Banerjee R, Jakob U. Bile salts act as effective protein-unfolding agents and instigators of disulfide stress in vivo. Proceedings of the National Academy of Sciences. 2014;111:E1610-E9.

[230] Euston SR, Bellstedt U, Schillbach K, Hughes PS. The adsorption and competitive adsorption of bile salts and whey protein at the oil–water interface. Soft Matter. 2011;7:8942-51.

[231] Sun H, Chow ECY, Liu S, Du Y, Pang KS. The caco-2 cell monolayer: Usefulness and limitations. Expert Opinion on Drug Metabolism & Toxicology. 2008;4:395-411.

[232] Dan N, Cutler DF. Transcytosis and processing of intrinsic factor-cobalamin in caco-2 cells. Journal of Biological Chemistry. 1994;269:18849-55.

[233] Russell-Jones GJ, Arthur L, Walker H. Vitamin b12-mediated transport of nanoparticles across caco-2 cells. International Journal of Pharmaceutics. 1999;179:247-55.

[234] El Aidy S, van den Bogert B, Kleerebezem M. The small intestine microbiota, nutritional modulation and relevance for health. Current Opinion in Biotechnology. 2015;32:14-20.

[235] LeBlanc JG, Milani C, de Giori GS, Sesma F, van Sinderen D, Ventura M. Bacteria as vitamin suppliers to their host: A gut microbiota perspective. Current Opinion in Biotechnology. 2013;24:160-8.

[236] Dutton RJ, Turnbaugh PJ. Taking a metagenomic view of human nutrition. Current Opinion in Clinical Nutrition & Metabolic Care. 2012;15:448-54.

[237] U.S. Food and Drug Administration. Redbook 2000: A chronic toxicity studies with rodents https://www.Fda.Gov/food/guidanceregulation/guidancedocumentsregulatoryinformation/ingredientsadditivesgraspackaging/ucm078349.Htm.